

**RMZ**

**MATERIALS and  
GEOENVIRONMENT**

**MATERIALI in GEOOKOLJE**



RMZ – M&G, **Vol. 60**, No. 1  
pp. 1–96 (2013)

Ljubljana, July 2013

## RMZ – Materials and Geoenvironment

### RMZ – Materiali in geokolje

ISSN 1408-7073

#### Old title/Star naslov

Mining and Metallurgy Quarterly/Rudarsko-metalurški zbornik  
ISSN 0035-9645, 1952–1997

Copyright © 2013 RMZ – Materials and Geoenvironment

#### Published by/Izdajatelj

Faculty of Natural Sciences and Engineering, University of Ljubljana/  
Naravoslovnotehniška fakulteta, Univerza v Ljubljani

#### Associated Publisher/Soizdajatelj

Institute for Mining, Geotechnology and Environment, Ljubljana/  
Inštitut za rudarstvo, geotehnologijo in okolje  
Velenje Coal Mine/Premogovnik Velenje

#### Editor-in-Chief/Glavni urednik

Peter Fajfar

#### Editorial Manager/Odgovorni urednik

Jakob Likar

#### Editorial Board/Uredniški odbor

Vlasta Čosovič, Sveučilište u Zagrebu  
Evgen Dervarič, Univerza v Ljubljani  
Meta Dobnikar, Ministrstvo za izobraževanje, znanost in šport  
Jan Falkus, Akademia Górniczo-Hutnicza im. S. Staszica w Krakowie  
Aleksandar Ganić, Univerzitet u Beogradu  
Borut Kosec, Univerza v Ljubljani  
Jakob Likar, Univerza v Ljubljani  
David John Lowe, British Geological Survey  
Ilija Mamuzić, Sveučilište u Zagrebu  
Milan Medved, Premogovnik Velenje  
Peter Moser, Montanuniversität Leoben  
Primož Mrvar, Univerza v Ljubljani  
Heinz Palkowski, Technische Universität Clausthal  
Daniele Peila, Politecnico di Torino  
Sebastiano Pelizza, Politecnico di Torino  
Jože Ratej, Inštitut za rudarstvo, geotehnologijo in okolje v Ljubljani  
Andrej Šmuc, Univerza v Ljubljani  
Milan Terčelj, Univerza v Ljubljani  
Milivoj Vulić, Univerza v Ljubljani  
Nina Zupančič, Univerza v Ljubljani  
Franc Zupančič, Univerza v Mariboru

#### Editorial Office/Uredništvo

Secretary/Tajnica Ines Langerholc  
Technical Editor/Tehnična urednica Helena Buh  
Editor of website/Urednik spletne strani Timotej Verbovšek

#### Editorial Address/Naslov uredništva

RMZ – Materials and Geoenvironment  
Aškerčeva cesta 12, p. p. 312  
1001 Ljubljana, Slovenija  
Tel.: +386 (0)1 470 45 00  
Fax.: +386 (0)1 470 45 60  
E-mail: rmz-mg@ntf.uni-lj.si

#### Linguistic Advisor/Lektor

Jože Gasperič

#### Design and DTP/Oblikovanje, prelom in priprava za tisk

ideJA? za ITGTO NTF

#### Print/Tisk

Birografika BORI, d. o. o.  
Printed in 300 copies./Naklada 300 izvodov.

#### Published/Izhajanje

4 issues per year./4 številke letno.

Partly funded by Ministry of Education, Science and Sport of Republic of Slovenia./Pri financiranju revije sodeluje Ministrstvo za izobraževanje, znanost in šport Republike Slovenije.

Articles published in Journal "RMZ M&G" are indexed in international secondary periodicals and databases: Članki objavljeni v periodični publikaciji „RMZ M&G“ so indeksirani v mednarodnih sekundarnih virih: Civil Engineering Abstracts, CA SEARCH® – Chemical Abstracts® (1967–present), Materials Business File, Inside Conferences, ANTE: Abstract in New Technologies and Engineering, METADEX®, GeoRef, CSA Aerospace & High Technology Database, Aluminium Industry Abstracts, Computer and Information Systems, Mechanical & Transportation Engineering Abstracts, Corrosion Abstracts, Earthquake Engineering Abstracts, Solid State and Superconductivity Abstracts, Electronics and Communications Abstracts.

The authors themselves are liable for the contents of the papers./Za mnenja in podatke v posameznih sestavkih so odgovorni avtorji.

Annual subscription for individuals in Slovenia: 16.69 EUR, for institutions: 22.38 EUR. Annual subscription for the rest of the world: 20 EUR, for institutions: 40 EUR/Letna naročnina za posameznike v Sloveniji: 16,69 EUR, za inštitucije: 33,38 EUR. Letna naročnina za tujino: 20 EUR, inštitucije: 40 EUR.

Current account/Tekoči račun

Nova ljubljanska banka, d. d. Ljubljana: UJP 01100-6030708186

VAT identification number/Davčna številka

24405388

#### Online Journal/Elektronska revija

www.rmz-mg.com

# Table of Contents

## Kazalo

### *Original scientific papers*

#### *Izvirni znanstveni članki*

- The impact of strain rate on sheet metal formability at room temperature** 3  
Vpliv hitrosti deformacije na preoblikovalnost pločevine v hladnem stanju  
Tomaž Pepelnjak, Sanja Smoljanič
- Genetic programming and artificial neural network modeling of PM10 emission close to a steel plant** 9  
Modeliranje emisij PM10 ob železarni z genetskim programiranjem in nevronskimi mrežami  
Miha Kovačič, Sandra Senčič, Uroš Župerl
- Palynostratigraphic and palaeoecological studies of the Cretaceous strata in the Bornu Basin, northeastern Nigeria** 17  
Palinostratigrafske in paleoekološke študije krednih skladov iz kadunje Bornu v severovzhodni Nigeriji  
Olugbenga Ademola Boboye
- Textural and bitumen saturation analyses of tar sand deposits in Southwestern Nigeria** 31  
Analiza teksture in nasičenosti z bitumnom v nahajališčih naftnega peska v jugozahodni Nigeriji  
A. Akinmosin, A. O. Adelaja
- Geochemical evaluation of the Pan-African pegmatites from parts of Oban massif, southeast Nigeria** 39  
Geokemična preiskava panafriških pegmatitov iz delov Obanskega masiva v jugovzhodni Nigeriji  
M. I. Oden, E. E. Igonor, E. E. Ukwang
- Sedimentological characteristics, provenance and hydrocarbon potential of post-santonian sediments in Anambra Basin, Southeastern Nigeria** 47  
Sedimentološke značilnosti, izvor in potencial ogljikovodikov postsantonijških sedimentov v Kadunji Anambra v Jugovzhodni Nigeriji  
Matthew E. Nton, Shereef A. Bankole

### *Review papers*

#### *Pregledni članki*

- Life cycle assessment of an intermodal steel building unit** 67  
Ocena trajnostnega cikla intermodulne jeklene gradbene enote  
Darko Milanović, Branislav Milanović, Boris Agarski, Milana Ilić, Branislava Crnobrnja, Aleš Nagode, Borut Kosec, Igor Budak

### *Professional papers*

#### *Strokovni članki*

- Mineralogical and chemical characterization of major basement rocks in Ekiti State, SW-Nigeria** 73  
Mineraloške in kemične značilnosti glavnih kamnin podlage v državi Ekiti v JZ Nigeriji  
Abel O. Talabi

### *Event notes*

#### *Novice*

- Students from the Department of Materials and Metallurgy became World Champions of the 7th Virtual Steelmaking Challenge** 87  
Študenta Oddelka za materiale in metalurgijo sta postala svetovna prvaka v virtualni izdelavi jekla  
Matjaž Knap

## Historical Review

More than 90 years have passed since the University Ljubljana in Slovenia was founded in 1919. Technical fields were united in the School of Engineering that included the Geologic and Mining Division, while the Metallurgy Division was established only in 1939. Today, the Departments of Geology, Mining and Geotechnology, Materials and Metallurgy are all part of the Faculty of Natural Sciences and Engineering, University of Ljubljana.

Before World War II, the members of the Mining Section together with the Association of Yugoslav Mining and Metallurgy Engineers began to publish the summaries of their research and studies in their technical periodical Rudarski zbornik (Mining Proceedings). Three volumes of Rudarski zbornik (1937, 1938 and 1939) were published. The War interrupted the publication and it was not until 1952 that the first issue of the new journal Rudarsko-metalurški zbornik – RMZ (Mining and Metallurgy Quarterly) was published by the Division of Mining and Metallurgy, University of Ljubljana. Today, the journal is regularly published quarterly. RMZ – M&G is co-issued and co-financed by the Faculty of Natural Sciences and Engineering Ljubljana, the Institute for Mining, Geotechnology and Environment Ljubljana, and the Velenje Coal Mine. In addition, it is partly funded by the Ministry of Education, Science and Sport of Slovenia.

During the meeting of the Advisory and the Editorial Board on May 22, 1998, Rudarsko-metalurški zbornik was renamed into “RMZ – Materials and Geoenvironment (RMZ – Materials in Geookolje)” or shortly RMZ – M&G. RMZ – M&G is managed by an advisory and international editorial board and is exchanged with other world-known periodicals. All the papers submitted to the RMZ – M&G undergoes the course of the peer-review process.

RMZ – M&G is the only scientific and professional periodical in Slovenia which has been published in the same form for 60 years. It incorporates the scientific and professional topics on geology, mining, geotechnology, materials and metallurgy. In the year 2013, the Editorial Board decided to modernize the journal’s format.

A wide range of topics on geosciences are welcome to be published in the RMZ – Materials and Geoenvironment. Research results in geology, hydrogeology, mining, geotechnology, materials, metallurgy, natural and anthropogenic pollution of environment, biogeochemistry are the proposed fields of work which the journal will handle.

Editor-in-Chief

## Zgodovinski pregled

Že več kot 90 let je minilo od ustanovitve Univerze v Ljubljani leta 1919. Tehnične stroke so se združile v tehniški visoki šoli, ki sta jo sestavljala oddelka za geologijo in rudarstvo, medtem ko je bil oddelek za metalurgijo ustanovljen leta 1939. Danes oddelki za geologijo, rudarstvo in geotehnologijo ter materiale in metalurgijo delujejo v sklopu Naravoslovnotehniške fakultete Univerze v Ljubljani.

Pred 2. svetovno vojno so člani rudarske sekcije skupaj z Združenjem jugoslovanskih inženirjev rudarstva in metalurgije začeli izdajanje povzetkov njihovega raziskovalnega dela v Rudarskem zborniku. Izšli so trije letniki zbornika (1937, 1938 in 1939). Vojna je prekinila izdajanje zbornika vse do leta 1952, ko je izšel prvi letnik nove revije Rudarsko-metalurški zbornik – RMZ v izdaji odsekov za rudarstvo in metalurgijo Univerze v Ljubljani. Danes revija izhaja štirikrat letno. RMZ – M&G izdajajo in financirajo Naravoslovnotehniška fakulteta v Ljubljani, Inštitut za rudarstvo, geotehnologijo in okolje ter Premogovnik Velenje. Prav tako izdajo revije financira Ministrstvo za izobraževanje, znanost in šport.

Na seji izdajateljskega sveta in uredniškega odbora je bilo 22. maja 1998 sklenjeno, da se Rudarsko-metalurški zbornik preimenuje v RMZ – Materiali in geookolje (RMZ – Materials and Geoenvironment) ali skrajšano RMZ – M&G. Revija RMZ – M&G upravlja izdajateljski svet in mednarodni uredniški odbor. Revija je v vključena v mednarodno izmenjavo svetovno znanih publikacij. Vsi članke so podvrženi recenzijem postopku.

RMZ – M&G je edina strokovno-znanstvena revija v Sloveniji, ki izhaja v nespremenjeni obliki že 60 let. Združuje področja geologije, rudarstva, geotehnologije, materialov in metalurgije. Uredniški odbor je leta 2013 sklenil, da posodobi obliko revije.

Za objavo v reviji RMZ – Materiali in geookolje so dobrodošli tudi prispevki s širokega področja geoznanosti, kot so: geologija, hidrologija, rudarstvo, geotehnologija, materiali, metalurgija, onesnaževanje okolja in biokemija.

Glavni urednik

# The impact of strain rate on sheet metal formability at room temperature

## Vpliv hitrosti deformacije na preoblikovalnost pločevine v hladnem stanju

**Tomaž Pepelnjak<sup>1,\*</sup>, Sanja Smoljanič<sup>2</sup>**

<sup>1</sup> University of Ljubljana, Faculty of Mechanical Engineering, Aškerčeva 6, SI-1000 Ljubljana, Slovenia

<sup>2</sup> University of Novi Sad, Faculty of Technical Sciences, Trg Dositeja Obradovica 6, YU-21000 Novi Sad, Serbia

\*Corresponding author. E-mail: tomaz.pepelnjak@fs.uni-lj.si

### Abstract

It is known that in warm and hot forming the forming speed and with it combined strain rate has immense role on material flow in bulk and sheet metal operations. In contrast, the influence of the strain rate on the flow curve is only rarely analyzed at room temperature. Presented work analyzes the influence of strain rate on flow curve of DC04 deep drawing material obtained by the uni-axial tensile test. After the evaluation of the flow curves as a function of strain rate the deep drawing of box-shaped test specimen was performed with two drawing speeds. The influence of the forming speed on the forming force and onset of necking was analyzed.

**Key words:** sheet metal forming, deep drawing, strain rate, room temperature forming

### Izvleček

Hitrost deformacije je pri preoblikovanju v toplem in vročem stanju ključni parameter procesa tako pri preoblikovanju pločevine kot tudi pri masivnem preoblikovanju. Nasprotno od tega je vpliv hitrosti preoblikovanja le redko analiziran za preoblikovanje v hladnem. V članku je analiziran vpliv hitrosti deformacije na krivuljo plastičnosti jekla za globoki vlek kakovosti DC04, pridobljeno z enoosnim nateznim preizkusom. Po ovrednotenju krivulj plastičnosti v odvisnosti od hitrosti deformacije smo z dvema hitrostima izvedli tudi globoki vlek preizkusne pravokotne škatle. Opazovali smo potek preoblikovalne sile in lokalizacijo materiala v odvisnosti od preoblikovalne hitrosti.

**Ključne besede:** preoblikovanje pločevine, globoki vlek, hitrost deformacije, hladno preoblikovanje

## Introduction

In the last century many researchers have analysed forming velocity and with it connected strain rate effect on plastic deformation and flow curves of various materials. Rao & Do-  
raivelu<sup>[1]</sup> in 1980 made comparison of earlier researches and conclude that different materials can be successfully processed with different speeds having different limits of the highest attainable strain rate. As a highest attainable was declared the strain rate where the material was still deformable without fast tearing. For example, steel and some aluminium alloys can be deformed in strain rate range from  $2 \times 10^{-3} \text{ s}^{-1}$  to  $3 \times 10 \text{ s}^{-1}$ , copper and brass in range from  $10^{-3} \text{ s}^{-1}$  to  $10^{-2} \text{ s}^{-1}$ , steel at high temperature from  $10 \text{ s}^{-1}$  to  $103 \text{ s}^{-1}$ , stainless steel in rate range from  $5 \times 10^{-6} \text{ s}^{-1}$  to  $3 \times 10^{-2} \text{ s}^{-1}$ . Bailey, Haas & Shah<sup>[2]</sup> in 1971 made a research about velocity and temperature effect on flow curve of aluminium alloys. Obtained results have shown that required stress in tension necessary to obtain particular deformation is getting higher with increase of a strain rate at a constant temperature, and getting lower with increase of a temperature at a constant strain rate. Velocity effect of a deformation is getting more pronounced with increasing of temperature. Rao, Prasad & Hawbolt<sup>[3]</sup> in 1996 made a research on low carbon steel. On the basis of their results it can be concluded that with enhancement of strain rate and reduction of temperature, tensile strength is increasing and entire flow curve of material increase its level. Lee & Yeh<sup>[4]</sup> in 1997 made some experiments to determine dynamic relation between yield strength and deformation of steel alloy. Obtained results showed that yield strength is magnifying with increasing of strain rate or with decrease of the temperature. Odeshi, Al-Ameeri & Bassim<sup>[5]</sup> in 2005 investigated velocity effect of projectile impact on deformation speed of material and its flow curve. On the basis of experiments they determined that speed of projectile impact has an effect on the strain rate of the observed material. When the speed of projectile impact and also strain rate are higher, the higher is yield strength maximum. Tsao, Wu, Leong & Fang<sup>[6]</sup> observed flow curve behaviour of commercially pure titanium during the hot tensile

deformation. In this case, level of flow curve is again increasing with increasing of strain rate and decreasing with changing of temperature. In order to obtain reliable data of the materials used in automotive industry Kim & Huh<sup>[7]</sup> have analysed deformability of two steels common used in body-in-white production. They have selected CQ (commercial quality) steel and dual phase ferrite-martensite steel DP590. The common tensile test, used for analysis of the flow curve was not applicable for their research due to the large testing length of 80 mm or 50 mm. Since the strain rate is calculated from the deformation speed and the length of the specimen as

$$\varphi = \frac{d\varphi}{dt} = \frac{v}{l} \quad [\text{s}^{-1}] \quad (1)$$

the total deformed length should be as small as possible. In Equation 1 the  $\varphi$  represents logarithmic strain,  $v$  the deformation speed and the length of a specimen. For this purpose Kim & Huh have selected miniaturized tensile specimens – Figure 1. Good clamping of the specimen necessary to minimise dynamic responses of the entire testing system was assured by screwing of the specimen into the clamping head. They diminish with such clamping system also the sliding danger which may appear at high testing velocities.

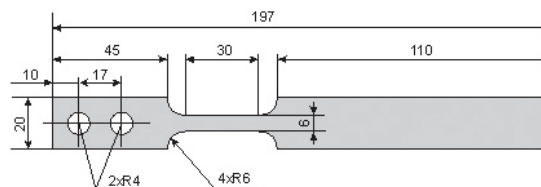
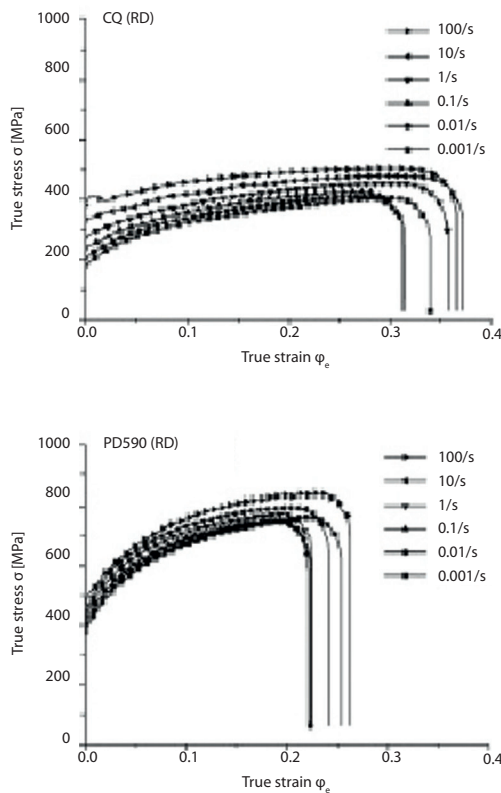


Figure 1: Specimen for testing at high strain rates<sup>[7]</sup>.

The selected steels CQ and DP590 have shown that also at room temperature the flow curves are increasing with the increase of the strain rate. The authors have selected large testing range of the strain rates from  $0.001 \text{ s}^{-1}$  to  $100 \text{ s}^{-1}$  with an increment of one decade. The obtained flow curves for the rolling direction (RD) are presented on Figure 2.

For both steels it can be observed that the yield stress and the level of the flow curve increases with the strain rate. Considering the CQ steel,

this phenomenon is more emphasized at lower strains up to the  $\varphi_e = 0.1$  while at DP590 steel quality the increase of the flow curve is more emphasised at strains above  $\varphi_e = 0.1$ . On the other hand the behaviour regarding the total elongation is similar: it is increased from 0.1–100  $s^{-1}$  while at quasi-static strain conditions below strain rate of 0.1  $s^{-1}$  the total elongation is smaller and the material rupture at lower equivalent strains. Kim & Huh have analysed also the forming limit diagram under quasi-static loading at strain rate of 0.001  $s^{-1}$  to 0.0018  $s^{-1}$  and at strain rate of 60–120  $s^{-1}$ . For both materials, there is no significant decrease in the forming limit curve (FLC) and only minor difference between the static and dynamic loading. The difference between both strain rates ranges is to observe only at the range between bottom and upper FLC line determining the reliability band of the FLD. The narrowing of this bend is more emphasized in the case of the dual phase steel DP590 – Figure 3.



**Figure 2:** Flow curves of CQ and DP590 steel at various strain rates [7].

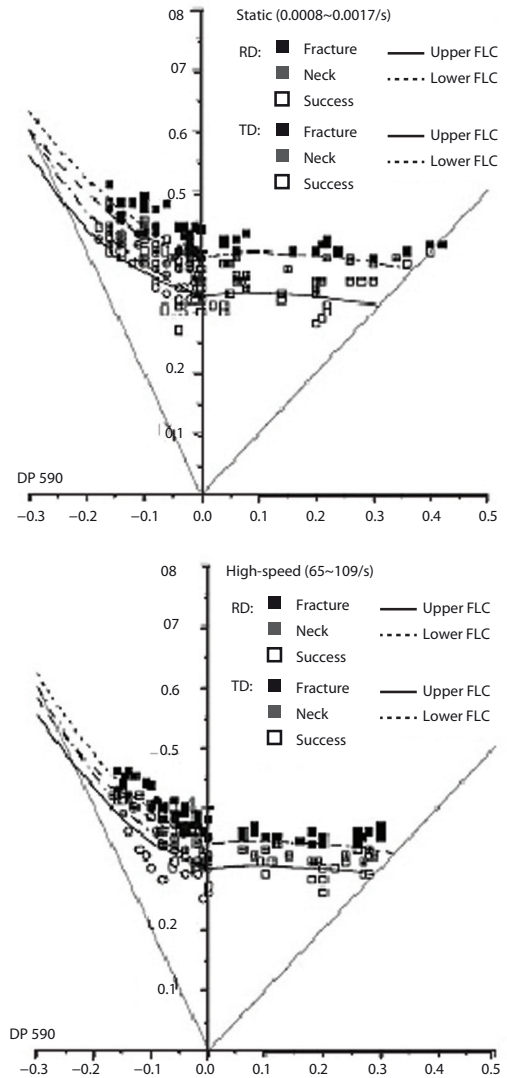


**Figure 3:** Forming limit curves of DP590 at different strain rates [7].

Jie et al.<sup>[8]</sup> have analysed the influence of strain rate on aluminium killed steel (AKDQ). They have also selected downscaled specimen with similar dimensions as Kim & Huh, however they have used for experiments the multipurpose Interlaken servo press with 260 kN nominal force. They have found out that with the increase of the strain rate the flow curve and yield point of the material are also increased. The forming analyses of magnesium alloy AZ31 done by Lee et al.<sup>[9]</sup> at elevated temperatures between 250 °C and 400 °C has shown that the increase of the strain rate also here increase the level of the flow curve but on the other hand the forming limit curve decreases at higher strain rates. While Lee et al. made forming analyses of

sheet metal Kobold et al.<sup>[10]</sup> analysed the AZ80 bulk material in compression stress state. Similar to Lee et al. they also observed increase of yield stress with increase of the strain rate.

## Material properties of deep drawing steel DC04

The household appliance industry, some applications of automotive sector as well as other industrial sectors implement various grades of common DC deep drawing steel qualities, mostly suitable for painting after the forming. Since the companies are also in this sector forced to shorten the production times the analyses of the material DC04 on various strain rates were performed. Two speeds of the tensile testing machine were selected resulting in a strain rate of  $0.0025 \text{ s}^{-1}$  and  $0.02 \text{ s}^{-1}$ . In order to improve the accuracy of the measurements of the uni-axial tensile test the standardized  $80 \text{ mm} \times 20 \text{ mm}$  specimens were selected despite lower attainable strain rates. The selection of the forming velocity at testing machine was adapted to the performances of the hydraulic press Litostroj HUO-2-250-400 with punch speed of  $0.02 \text{ m/s}$  where the deep drawing tests of box-like specimens were performed. The formability of the material was analysed in three directions regarding the rolling direction: longitudinal, transverse and at  $45^\circ$ . The thickness of analysed sheet metal was  $0.6 \text{ mm}$ . The flow curves at both analysed strain rates for all three directions are presented on Figure 4. Five experiments were performed in each direction. Figure 4 represents the average values of flow curves for the analysed material in various directions regarding the rolling direction. Differences between the flow curves obtained at both strain rates are clearly visible. The highest increase of the flow curve can be observed perpendicular to the rolling direction where material expresses also the highest elongation at fracture. The material of DC04 quality expresses at observed strain rates only minor decrease of the total elongation at strain rate 10 times higher as the standardised one.

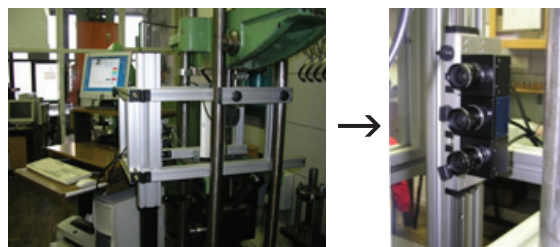
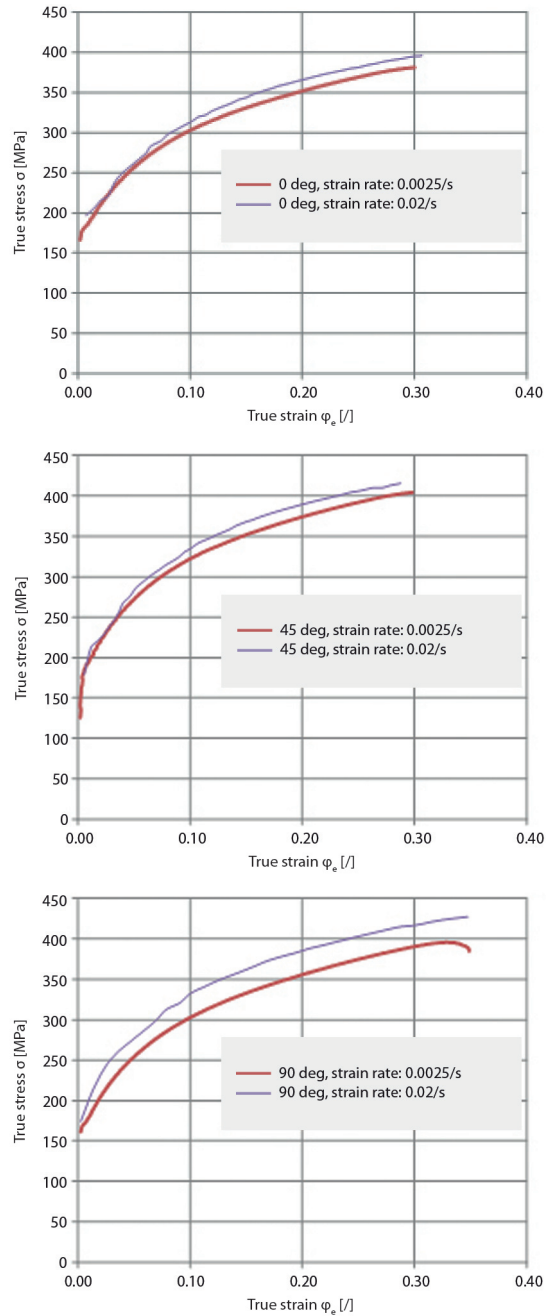


**Figure 4:** Comparative flow curves for different directions regarding the rolling direction of the sheet metal (top and bottom left) and measurement equipment for acquisition of the tensile test (bottom right).

## Analyses of deep drawing of a rectangular box

The forming of a rectangular box has served for comparative determination of necking and tearing limit for analysed material DC04 at two different strain rates. The forming speed was set to quasi-static forming with punch speed of 5 mm/s and at 4-times higher speed of 20 mm/s being the press maximal speed. The blank has dimensions of 165 mm × 145 mm with 20 mm trimmed corners while the drawn box has dimensions of 70 mm × 100 mm with radii of 5 mm, 8 mm, 11 mm and 15 mm on its circumference, bottom radius of 5 mm and a flange radius of 7 mm – Figure 5. Different drawing depths ranging from 24 mm to 31 mm were selected in order to determine the necking and fracture limit of the drawn box. The drawing depth was incremental increased from 24 mm by 1 mm until the onset of necking or tearing was observed. The onset of necking followed by corner tearing appears at the smallest box corner. Since the flow curves of the DC04 material have shown the sensitivity on the strain rate it was to expect that the forming force should be also higher at higher forming speeds. The acquisition of force versus punch travel diagram did not prove this assumption. The course of the forming force was almost identical for both forming speeds.

Onset of necking appears at punch speed of 4 mm/s at the drawing depth of 25.3 mm while the fracture of the smallest corner appears at drawing depth of 27.7 mm. On the other hand, the necking range of the smallest corner at drawing speed of 20 mm/s is wider having a spread from drawing depth of 27 mm to 34 mm and the box tearing appears at drawing depths above 34 mm.

## Conclusions

The strain rate and temperature have immense influence on flow curves and forming limit diagrams at warm and hot forming. At room temperature the strain rate influence is less emphasised and therefore less known in industrial practice. With drastically decrease of production times in stamping operations

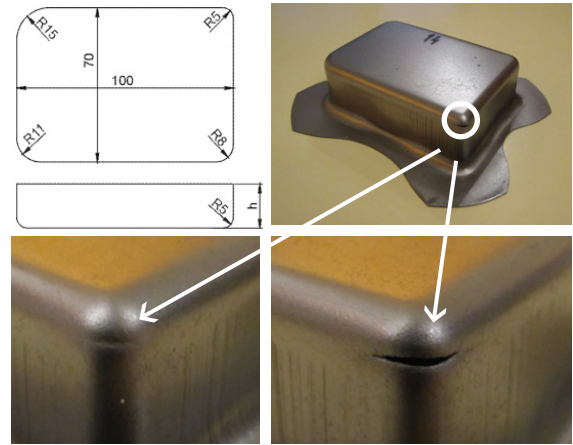


**Figure 5:** Specimen geometry (left) and specimen formability limit with tearing (bottom left) and necking (bottom right).

the strain rate influence cannot be neglected. Recent works have shown that in some cases also at room temperature the increase of the yield stress and flow curves is observed with increase of the strain rate. The flow curves of DC04 material were analysed at two strain rates; 0.002 5 s<sup>-1</sup> and 0.02 s<sup>-1</sup>. The first strain rate is prescribed by the standard for uniaxial tensile test while the second one was calculated according to the maximal punch speed of the press used for deep drawing experiments. Flow curves in three main directions according to the rolling direction have shown increase of the flow curve level at a higher strain rate without any decrease of the total elongation at fracture. The deep drawing test on the other hand has shown interesting phenomenon where the localisation on the critical corner of the specimen appear earlier at small forming speed of 4 mm/s as at five times higher forming speed of 20 mm/s.

With further research work the FLD need to be determined for both forming speeds to gain deeper overview of the DC04 material behavior at various strain rates. Finally, with gained material and formability data the FEM simulations of the deep drawing of the test box need to be performed.

## Acknowledgements

This paper is part of research work within the Eureka project E! 5783 - ECO-CAN entitled INNOVATIVE ECO-FRIENDLY PROCESSING OF

VOLUMETRIC SHEET METAL COMPONENTS financed by the Slovene Ministry of Education, Science, Culture and Sport. The authors are very grateful for the financial support.

The authors thank the CEEPUS programme for making them possible to be mobile within the network CII-HR-0108.

## References

- [1] Rao, K. P., Doraivelu, S. M. (1982): Flow curve and deformation of materials at different temperatures and strain rates. *Journal of mechanical working technology*; Vol. 6, pp. 63–88.
- [2] Bailey, J. A., Haas, S. L., Shah, M. K. (1972): Effect of strain rate and temperature on the resistance to torsional deformation of several aluminium alloys. *International Journal of Mechanical Sciences*; Vol. 44, pp. 735–754.
- [3] Rao, K. P., Prasad, Y. K. D. V., Hawbolt, E. B. (1996): Hot deformation studies on a low – carbon steel: Part I – Flow curves and the constitutive relationship. *Journal of materials processing technology*; Vol. 56, pp. 897–907.
- [4] Lee, W. – S., Yeh, G. – W. (1997): The plastic deformation behaviour of AISI 4340 alloy steel subjected to high temperature and high strain rate loading conditions. *Journal of materials processing technology*; Vol. 71, pp. 224–234.
- [5] Odeshi, A. G., AL – Ameer, S., Bassim, M. N. (2005): Effect of high strain rate on plastic deformation of a low alloy steel subjected to ballistic impact. *Journal of materials processing technology*; Vol. 162–163, pp. 385–391.
- [6] Tsao, L. C., Wu, H. Y., Leong, J. C., Fang, C. J. (2012): Flow stress behaviour commercial pure titanium sheet during warm tensile deformation. *Materials and Design*; Vol. 34, pp. 179–184.
- [7] Kim, S. B., Huh, H., Bok, H. H., Moon, M. B. (2011): Forming limit diagram of auto-body steel sheets for high-speed sheet metal forming. *Journal of Materials Processing Technology*; Vol. 211, pp. 851–862.
- [8] Jie, M., Cheng, C. H., Chan, L. C., Chow, C. L. (2009): Forming limit diagrams of strain-rate-dependent sheet metals. *International Journal of Mechanical Sciences*; Vol. 51, No. 4, pp. 269–275.
- [9] Lee, Y. S., Kwon, Y. N., Kang, S. H., Kim, S. W., Lee, J. H. (2008): Forming limit of AZ31 alloy sheet and strain rate on warm sheet metal forming. *Journal of Materials Processing Technology*; Vol. 201, pp. 431–435.
- [10] Kobold, D., Pepelnjak, T., Gantar, G., Kuzman, K. (2010): Analysis of deformation characteristics of magnesium AZ80 wrought alloy under hot conditions. *Strojniški vestnik*; Vol. 56, No. 12, ISSN 0039-2480, pp. 823–832.

# Genetic programming and artificial neural network modeling of PM10 emission close to a steel plant

## Modeliranje emisij PM10 ob železarni z genetskim programiranjem in nevronskimi mrežami

Miha Kovačič<sup>1,\*</sup>, Sandra Senčič<sup>2</sup>, Uroš Župerl<sup>3</sup>

<sup>1</sup>Štore Steel, d.o.o., Železarska cesta 3, SI-3220 Štore, Slovenia

<sup>2</sup>Kova, d.o.o., Teharska cesta 4, SI-3000 Celje, Slovenia

<sup>3</sup>University of Maribor, Faculty of Mechanical Engineering, Smetanova ulica 17, SI-2000 Maribor, Slovenia

\*Corresponding author. E-mail: miha.kovacic@store-steel.si

### Abstract

To implement sound air quality policies, regulatory agencies require tools to evaluate the outcomes and costs associated with various emission reduction strategies. The applicability of such tools can also remain uncertain. It is furthermore known that source-receptor models cannot be implemented through deterministic modeling. The article presents an attempt of PM10 emission modeling carried close to a steel production area with the genetic programming and artificial neural network method. The daily PM10 concentrations, daily rolling mill and steel plant production, meteorological data (wind speed and direction – hourly average, air temperature – hourly average and rainfall – daily average), weekday and month number were used for modeling during a monitoring campaign of almost half a year (23. 6. 2010 to 12. 12. 2010). The genetic programming modeling results show superior agreement with measured daily PM10 concentrations.

**Key words:** steel plant, PM10 concentrations, modeling, genetic programming, artificial neural network

### Izvleček

Za implementacijo politike kakovosti zraka so od regulativnih agencij zahtevana orodja za ovrednotenje rezultatov in stroškov, povezanih s strategijami za zmanjšanje emisij. Uporaba takšnih orodij ostaja negotova. Velja, da za modele tipa vir-prejemnik težko uporabljamo deterministično modeliranje. V članku je predstavljen poskus modeliranja emisij delcev PM10 v bližini jeklarne z genetskim programiranjem in nevronskimi mrežami. Pri skoraj polletni merilni kampanji (od 23. 6. 2010 do 12. 12. 2010) smo zbirali podatke o dnevni koncentracijah delcev PM10, dnevni proizvodnji valjarne in jeklarne, meteorološke podatke (urno povprečje smeri in hitrosti vetra ter temperature, dnevne padavine), o zaporednem številu dni v tednu in mesecu v letu. Rezultati, dobljeni z genetskim programiranjem, kažejo izjemno dobro ujemanje z izmerjenimi koncentracijami PM10.

**Ključne besede:** železarna, koncentracije PM 10, modeliranje, genetsko programiranje, nevronske mreže

## Introduction

Particulate matter (PM) pollution is, especially in residential areas near industrial areas, a problem of great concern. This is not only because of the adverse health effects but also because of reduced visibility.<sup>[1-3]</sup>

To reduce PM levels in the air a deep knowledge of the contributing sources, background emissions, the influence of the meteorological conditions, as well as of PM<sub>10</sub> formation and transport processes is needed.

However, current state-of-the-art PM<sub>10</sub> modeling does not allow us to quantitatively model the whole range of emissions behavior, which is why the dispersion modeling is thus increasingly connected with intelligent algorithms such as artificial neural networks<sup>[4-9]</sup> and evolutionary computation.<sup>[9]</sup>

The objective of this work was to model PM<sub>10</sub> emissions close to a steel plant area in Slovenia by means of a genetic programming and artificial network method. Genetic programming and neural network method have been proven to be an effective optimization tool for multicriterial and multiparametrical problems.<sup>[10-13]</sup>

In paper is organized that the basic terms and experimental setup are stated in the beginning. Afterwards the idea of the proposed concept is presented. In the conclusion the main contributions of the performed research are summarized, while guidelines for further research are provided.

## Experimental setup

### Sampling sites

Figure 1 shows the locations of the sampling sites, rolling mill, steel plant and residential areas. Influencing PM<sub>10</sub> sources are rolling mill and steel plant, combustion and non-combustion traffic and urban background.

### Sampling

Samples for this study were collected between 23. 6. 2010 and 12. 12. 2010. Sampling was performed 1.5 m above the ground. PM<sub>10</sub> samples were collected for 24 h on Mondays using low-volume samplers equipped with EPA-equiva-

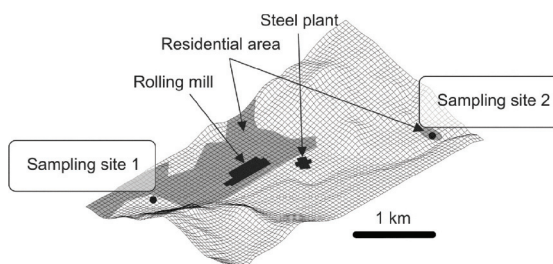


Figure 1: Topographic view of the study area.

lent size-selective inlets. Particles with diameter 10  $\mu\text{m}$  (PM<sub>10</sub>) were collected on cellulose esters membranes with high collection efficiencies (99 %). In total 172 PM<sub>10</sub> samples for each sampling site were available.

Before and after the samplings were made the filters were exposed for 24–48 h on open but dust-protected sieve-trays in an air-conditioned weighing room. The gravimetric determination of the mass was carried out using an analytical microbalance (precision 1  $\mu\text{g}$ ) located in the weighing room. In order to remove static electricity from filters the balance is equipped with a special kit in a Faraday shield.

The limit value of the EU directive – i.e. a daily mean PM<sub>10</sub> concentration – is 50  $\mu\text{g}/\text{m}^3$ . At the sampling site 1 and 2 the measured PM<sub>10</sub> concentration exceeded limit value four times and five times, respectively.

Figure 2 shows the measured PM<sub>10</sub> concentrations during the study period for the sampling sites.

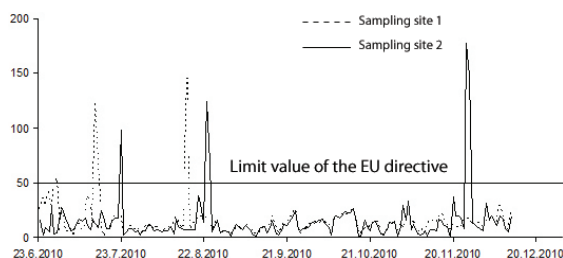
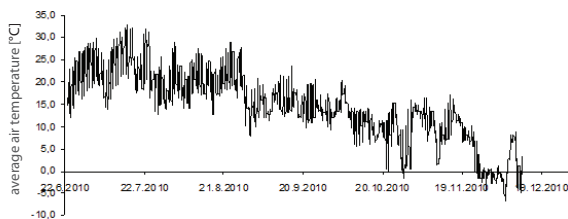


Figure 2: The measured PM<sub>10</sub> concentrations during the study period for the sampling sites.

### Meteorological data

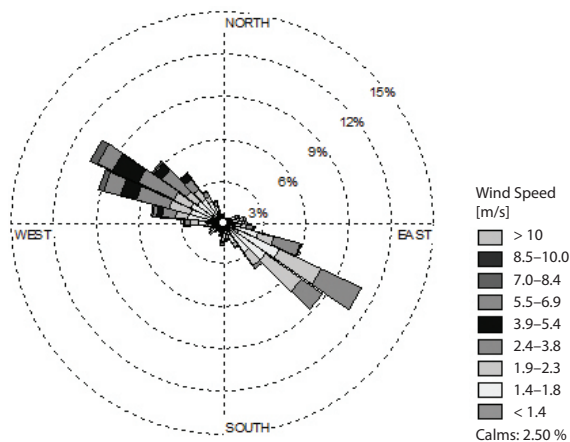
Hourly average air temperature, wind speed and direction and daily rainfall data were made available to the authors by the Slovenian Environment Agency.

Figure 3 shows the hourly average temperatures during the study period.



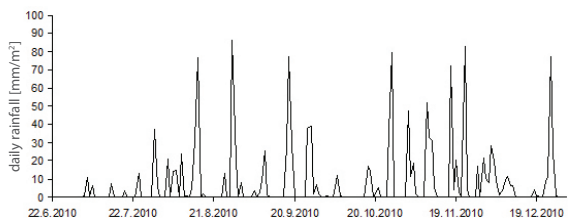
**Figure 3:** The hourly average temperatures during the study period.

Figure 4 shows the frequency distribution of wind direction and wind speed obtained based on wind direction and speed data measured every hour during the study period.



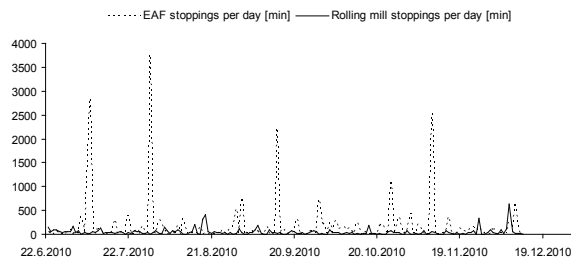
**Figure 4:** Frequency distribution of wind direction and wind speed.

Figure 5 shows the daily rainfall during the period of the study.



**Figure 5:** Daily rainfall during the study period.

The hourly data based on electric arc and rolling mill production was collected during the study period. During the study period, the electric arc furnace was stopped for 28 465 min and the rolling mill was stopped for 8 213 min. Figure 6 shows the minutes of stopping per day for the electric arc furnace and rolling mill during the study period.



**Figure 6:** Minutes of stopping per day for the electric arc furnace and rolling mill during the study period.

### Genetic programming modeling

Genetic programming is probably the most general evolutionary optimization method.<sup>[14]</sup> The organisms that undergo adaptation are in fact mathematical expressions (models) for the PM10 concentrations prediction in the present work. The concentration prediction is based on the available function genes (i.e., basic arithmetical functions) and terminal genes (i.e., independent input parameters, and random floating-point constants). In the present case the models consist of the following function genes: addition (+), subtraction (-), multiplication (\*) and division (/), and the following terminal genes: weekday (*WEEKDAY*) and month number (*MONTH*), wind speed [m/s] (*SPEED*), wind direction [°] (*DIRECTION*), air temperature [°C] (*TEMP*), rainfall [ml] (*RAIN*), electro arc furnace efficiency [min/hour] (*EAF*), rolling mill efficiency [min/hour] (*ROLLING*). In order to ascertain the influence of seasons and traffic during workday hours the weekday and month number were also added as terminal genes. One of the randomly generated mathematical models

$$\left(\frac{TEMP}{RAIN} + 2\right) \cdot \frac{EAF}{5.1} \quad (1)$$

is schematically represented in Figure 7 as a program tree with included function genes (\*, +, /) and terminal genes (*TEMP*, *RAIN*, *EAF* and a real number constants 2 and 5.1). Random computer programs of various forms and lengths are generated by means of the selected genes at the beginning of the simulated evolution. The varying of the computer programs is performed by means of the genetic operations during several iterations, known as generations. After the completion of the variation of the computer programs a new genera-

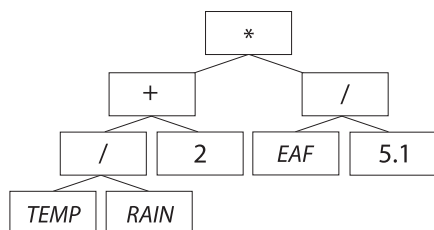


**Figure 7:** Randomly generated mathematical model for the PM10 concentrations prediction, represented in program tree form.

tion is obtained. Each generation is compared with the experimental data. The process of changing and evaluating organisms is repeated until the termination criterion of the process is fulfilled. The maximum number of generations is chosen as a termination criterion in the present algorithm.

The following evolutionary parameters were selected for the process of simulated evolutions: 500 for the size of the population of organisms, 100 for the maximum number of generations, 0.4 for the reproduction probability, 0.6 for the crossover probability, 6 for the maximum permissible depth in the creation of the population, 10 for the maximum permissible depth after the operation of crossover of two organisms, and 2 for the smallest permissible depth of organisms in generating new organisms. Genetic operations of reproduction and crossover were used. For selection of organisms the tournament method with tournament size 7 was used. 100 independent civilizations of mathematical models for prediction of the PM10 concentration were developed. The best evolution sequence of 100 generations was computed in 8 h and 41 min on 2.39 GHz processor and 2 GB of RAM by an AutoLISP based in-house coded computer program.

The model fitness  $f$  has been defined as:

$$f = \sum_{i=1}^n (P_i - M_i) + N \cdot 10\,000 \quad (2)$$

where  $n$  is the size of sample data and,  $P_i$  is predicted PM10 concentration,  $M_i$  is measured PM10 concentration and  $N$  is the number of all cases when:

$$P_i < 50 \wedge M_i > 50 \vee M_i < 50 \wedge P_i > 50$$

The limit value of the EU directive, i.e. a daily mean PM10 concentration, is  $50 \mu\text{g}/\text{m}^3$ . The

number  $N$  tells us when the prediction is above that limit value, when in order to assure PM10 concentration exceedance prediction by developed predictive model it should in fact be below the limit, and also when prediction by developed predictive model should be above the limit.

The simulated evolution in one run of the genetic programming system (out of 100) produced the following best model for prediction of PM10 concentration for sampling site 1 (cf. equation 3) with fitness of 1 019.95, number  $N = 0$  and average deviation of  $5.96 \mu\text{g}/\text{m}^3$ .

The best evolutionary developed model (out of 100) for prediction of PM10 concentration for sampling site 1 (cf. equation 4) with fitness of 11 124.67, number  $N = 1$  (on the 30. 6. 2010 the measured PM10 concentrations were  $53.6 \mu\text{g}/\text{m}^3$  and predicted  $21.41 \mu\text{g}/\text{m}^3$ ), and average deviation of  $6.54 \mu\text{g}/\text{m}^3$ .

Figures 8 and 9 show measured and predicted PM10 concentrations for sampling sites 1 and 2, respectively.

## Artificial neural network modeling

Artificial neural networks consist of a large number of processing elements, called neurons that operate in parallel. Computing with neural networks is non-algorithmic. They are trained through examples rather than programmed by software. The Multi-Layer BP network is a supervised, continuous valued, multi-input and multi-output feedforward multi-layer network that follows a gradient descent method. [14]

The gradient descent method alters the weight by an amount proportional to the partial derivative of the error with respect to the weight in question. The backpropagation phase of the neural network alters the weights  $w_{ji}$  so that the error of the network is minimized. This is achieved by taking a pair of input/output vectors and feeding the input vector into the net. The net generates an output vector and than the output vector is compared to the output vector supplied. The comparison gives us the error value. The error is then passed back through the network (backpropagation process), modifying the weights due to this error using the

$$\begin{aligned}
& \left( DIRECTION + \left( DIRECTION + MONTH - WEEKDAY + \frac{SPEED (-1.99563 + 3WEEKDAY + 4MONTH WEEKDAY)}{MONTH - WEEKDAY} + \right. \right. \\
& \left. \left. + \frac{WEEKDAY (-1.99563 + MONTH WEEKDAY)}{MONTH - \frac{1}{2} + MONTH WEEKDAY} \right) \right) / \left( \frac{-1.99563 + MONTH WEEKDAY}{MONTH + WEEKDAY - \frac{-1.99563 + MONTH WEEKDAY}{MONTH - \frac{WEEKDAY}{SPEED}}} + \right. \\
& \left. + \left( (-1.99563 + MONTH WEEKDAY) (-MONTH + (DIRECTION - WEEKDAY)) / (DIRECTION + WEEKDAY + \right. \right. \\
& \left. \left. + MONTH WEEKDAY - \frac{MONTH SPEED (-1.99563 + MONTH WEEKDAY)}{-DIRECTION + MONTH + WEEKDAY} - \frac{MONTH^2 (-1.99563 + MONTH WEEKDAY)}{MONTH - \frac{WEEKDAY}{DIRECTION}} \right) \right) / \\
& \left( \frac{MONTH - 2WEEKDAY + MONTH WEEKDAY}{DIRECTION WEEKDAY} \right) / \left( DIRECTION - RAIN + \left( MONTH - \frac{MONTH - WEEKDAY}{WEEKDAY} \right) + \right. \\
& \left. + MONTH WEEKDAY - \left( -MONTH + \left( MONTH - \frac{MONTH - WEEKDAY}{SPEED} \right) \right) (-1.99563 + MONTH WEEKDAY) \right) \quad (3)
\end{aligned}$$

$$\begin{aligned}
& \left( -5.76596 + MONTH + \frac{TEMP}{DIRECTION} \right) \left( \frac{-\frac{SPEED}{TEMP} + \frac{1 - \frac{SPEED}{TEMP}}{WEEKDAY}}{MONTH} + \frac{\left( EAF + \frac{MONTH + \frac{TEMP}{DIRECTION} - WEEKDAY}{SPEED} + \frac{TEMP}{DIRECTION TEMP} + \frac{TEMP}{EAF} \right) WEEKDAY}{EAF + \frac{SPEED}{DIRECTION TEMP} + \frac{TEMP}{EAF}} \right) \\
& \left( \frac{-\frac{SPEED}{TEMP} + \frac{1 - \frac{SPEED}{TEMP}}{WEEKDAY}}{TEMP} \left( TEMP + \frac{-\frac{SPEED}{TEMP} + \frac{1 - \frac{SPEED}{TEMP}}{WEEKDAY}}{DIRECTION} + \frac{EAF RAIN SPEED}{TEMP (-TEMP + \frac{TEMP}{WEEKDAY})} WEEKDAY \right) \right) \\
& \left. \right) / DIRECTION WEEKDAY + \\
& \frac{MONTH - \frac{WEEKDAY^2}{TEMP} + \frac{SPEED TEMP^2}{WEEKDAY \left( DIRECTION + \frac{TEMP - (TEMP + WEEKDAY)}{DIRECTION} \right)}}{DIRECTION + \frac{MONTH - WEEKDAY + \frac{TEMP + \frac{EAF WEEKDAY}{SPEED TEMP} - \frac{-TEMP + WEEKDAY}{DIRECTION}}{EAF + \frac{EAF RAIN}{TEMP WEEKDAY} + \frac{-TEMP + WEEKDAY + \frac{-TEMP + WEEKDAY}{DIRECTION}}{DIRECTION}}}{DIRECTION}} + 0.30872 \quad (4)
\end{aligned}$$

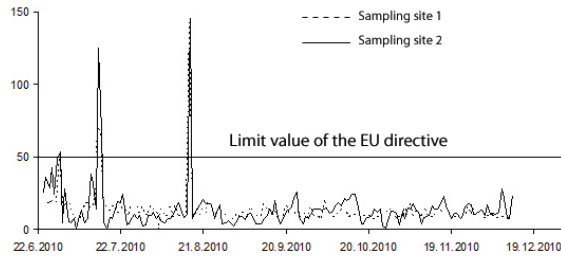


**Figure 8:** Measured and predicted PM10 concentrations [ $\mu\text{g}/\text{m}^3$ ] for sampling site 1.

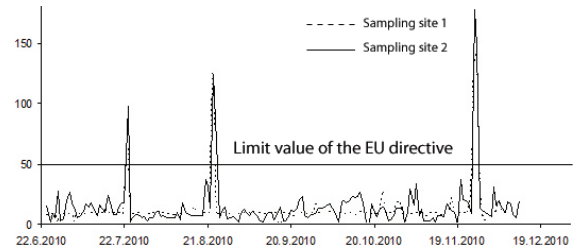


**Figure 9:** Measured and predicted PM10 concentrations [ $\mu\text{g}/\text{m}^3$ ] for sampling site 2.

equations. Hence, if the same set of input/output vectors are presented to the network, the error would be smaller than previously found. For modeling the PM10 emission, three-layer feed-forward neural networks were used (Figure 10). They contained 9 neurons in the input layer, and 1 in the output layer. The number of

neurons in the hidden layer was varied in different experiments.

The detailed topology of the used ANN with optimal training parameters and mathematical principle of the neuron is shown on Figure 3. The ANN were trained with the following parameters: weekday (*WEEKDAY*) and month

number (*MONTH*), wind speed [m/s] (*SPEED*), wind direction [°] (*DIRECTION*), air temperature [°C] (*TEMP*), rainfall [ml] (*RAIN*), electro arc furnace efficiency [min/h] (*EAF*), rolling mill efficiency [min/h] (*ROLLING*).

The ANN registers the input data only in the numerical form therefore the information about the inputs must be transformed into numerical code. The learning method is error backpropagation. Signals passed through the neurons in the hidden and output layers are transformed on the basis of an Tangent (nonlinear) function which allows the identification of the nonlinear system. The data is automatically normalized in order to make the training process faster. This was done by mapping each term to a value between 0 and 1 using the Max Min method. This normalized data was utilized as the inputs and outputs to train the ANN. In other words, two vectors are formed in order to train the neural network: Input vector is [*WEEKDAY*, *MONTH*, *SPEED*, *DIRECTION*, *TEMP*, *RAIN*, *EAF*, *ROLLING*, *HOURL*]. The output vector is [PM10 concentration].

Training of the ANN is finished when the testing error is less than the tolerance limit. This tolerance limit is defined to 4 % at the beginning of the training. On average, the networks needed 63 iterations to achieve this goal. Approximately 8 min of training during machin-

ing are needed to set up the full prediction performance of ANN. After the neural network had been trained it was applied to 50 examples that did not take part in the training process. This time the solutions of the examples (PM10 concentration) were not supplied, so that the network had to estimate them.

To evaluate the individual effects of network topology and training parameters on the performance of neural network 40 different networks were trained, tested and analyzed. From the results the following conclusions can be drawn:

- LWrs.
- To minimize the estimation errors, momentum rates between 0.001 and 0.005 are good.
- It is found that there is an optimum number of hidden nodes beyond there is no significant change in the error prediction. In this instance, the optimum number of hidden layer nodes is 3.
- Networks trained with the tanh transfer function in all their processing elements give the least prediction errors, while those employing sigmoid and sine give the highest and next highest prediction errors respectively.
- By using a multi-layer perceptron with backpropagation training method, the neural network is trained to an accuracy of  $\pm 3\%$  error.

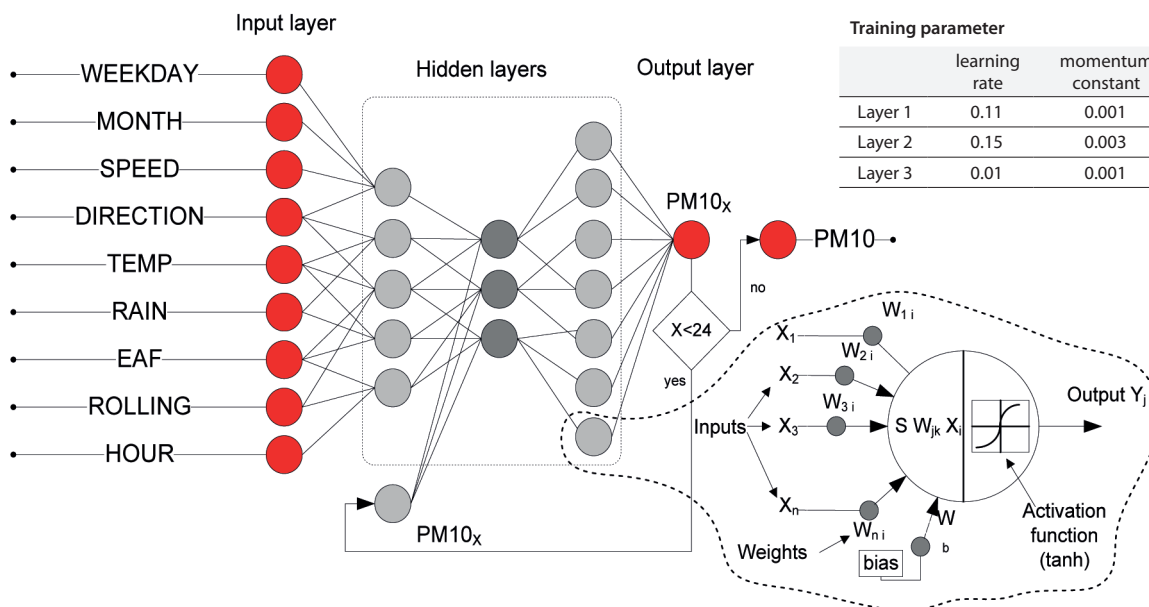
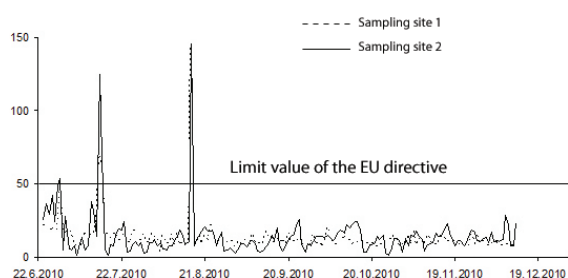


Figure 10: Predictive force model topology.

In testing the model, the PM10 concentrations for sampling site 1 and 2 were predicted with average deviation of  $9.47 \mu\text{g}/\text{m}^3$  and  $11.92 \mu\text{g}/\text{m}^3$ , respectively. The number of cases  $N$  when the prediction is above the EU directive limit value, when in order to assure PM10 concentration exceedance prediction by developed predictive model it should in fact be below the limit, and also when prediction by developed predictive model should be above the limit is for both sampling sites 6.

Figures 11 and 12 show measured and predicted PM10 concentrations for sampling sites 1 and 2, respectively.



**Figure 11:** Measured and predicted PM10 concentrations [ $\mu\text{g}/\text{m}^3$ ] for sampling site 1.

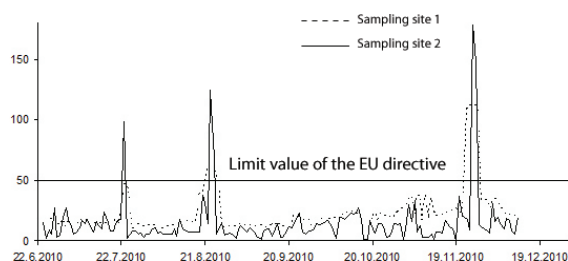


**Figure 12:** Measured and predicted PM10 concentrations [ $\mu\text{g}/\text{m}^3$ ] for sampling site 2.

The distribution of concentrations deviation of training, test and verification data is presented in the Table 1.

**Table 1:** Distribution of concentrations deviation of training, test and verification data.

	Sampling site 1			Sampling site 2		
	Training data	Testing data	All data	Training data	Testing data	All Data
<b>N</b>	121	50	171	121	50	171
<b>Average [<math>\mu\text{g}/\text{m}^3</math>]</b>	5.85	18.23	9.47	3.41	14.23	6.58
<b>St. dev. [<math>\mu\text{g}/\text{m}^3</math>]</b>	4.53	14.63	10.39	3.17	9.72	7.66

## Conclusions

This paper presented the possibility of the PM10 concentration prediction close to a steel plant area with genetic programming and artificial networks. The daily PM10 concentrations, daily rolling mill and steel plant production, meteorological data (wind speed and direction – hourly average, air temperature – hourly average and rainfall – daily average), weekday and month number were used for modeling during a monitoring campaign of almost half a year (23. 6. 2010 to 12. 12. 2010). The special fitness function for genetic programming system was designed in order to assure also PM10 limit value exceedance prediction. For each sampling site the best models for PM10 prediction were obtained from 100 runs of the genetic programming system. The model for sampling sites 1 and 2 predicts concentrations within an average error range of  $5.96 \mu\text{g}/\text{m}^3$  and  $6.54 \mu\text{g}/\text{m}^3$ , respectively. All exceedances of the EU directive limit value ( $50 \mu\text{g}/\text{m}^3$ ) were administered at sampling site 1, but only 4 out of 5 of these occurred at sampling site 2. In general it is also important to know how many times the prediction is above EU directive limit value when it should in fact (measured values) be below the limit and otherwise. The number of such cases at sampling site 1 and 2 are 0 and 2, respectively. Also the special artificial neural network topology adjustments were used. 40 different neural networks were trained, tested and analyzed. The best artificial neural network for sampling sites 1 and 2 predicts concentrations within an average error range of  $9.47 \mu\text{g}/\text{m}^3$  and  $11.92 \mu\text{g}/\text{m}^3$ , respectively. 2 out of 4 EU directive limit value ( $50 \mu\text{g}/\text{m}^3$ ) exceedances were administered at sampling site 1 and only 4 out of 5 of these occurred at

sampling site 2. The number, when the prediction is above that limit value, when in order to assure PM10 concentration exceedance prediction by developed predictive model it should in fact be below the limit, and also when prediction by developed predictive model should be above the limit, was 6 at both sampling sites. In the future we will carry out genetic programming based dispersion modeling according to the calculated wind field, air temperature, humidity and rainfall in a 3D Cartesian coordinate system. The prospects for arriving at a robust and faster alternative to the well-known Lagrangian and Gaussian dispersion models are optimistic.

## References

- [1] Marcazzan, G. M., Ceriani, M., Valli, G., Vecchi, R. (2003): Source apportionment of PM10 and PM2.5 in Milan (Italy) using receptor modeling. *The Science of the Total Environment*, 317, 137–147.
- [2] Watson, J. G. (2002): Visibility: science and regulation. *Journal of the Air and Waste Management Association*, 52, 628–713.
- [3] Vrins, E., Schofield, N. (2000): Fugitive dust emission by an ironmaking site. *Journal of Aerosol Science*, 31, 524–525.
- [4] Kukkonena, J., Partanena, L., Karppinen, A., Ruuskanen, J., Junninen, H., Kolehmainen, M., Niska, H., Dorling, S., Chatterton, T., Foxall, R., Cawley, G. (2003): Extensive evaluation of neural network models for the prediction of NO<sub>2</sub> and PM10 concentrations, compared with a deterministic modelling system and measurements in central Helsinki, *Atmospheric Environment*, 37, 4539–4550.
- [5] Zhou, H., Cen, K., Fan, J. (2004): Modeling and optimization of the NO<sub>x</sub> emission, characteristics of a tangentially fired boiler with artificial neural networks. *Energy*, 29, 167–183.
- [6] Hooyberghsa, J., Mensink, C., Dumont, G., Fierens, F., Brasseur, O. (2005): A neural network forecast for daily average PM10 concentrations in Belgium. *Atmospheric Environment*, 39, 3279–3289.
- [7] Perez, P., Reyes, J. (2006): An integrated neural network model for PM10 forecasting. *Atmospheric Environment*, 40, 2845–2851.
- [8] Grivas, G., Chaloulakou, A. (2006): Artificial neural network models for prediction of PM10 hourly concentrations, in the Greater Area of Athens, Greece. *Atmospheric Environment*, 40, 1216–1229.
- [9] Kovačič, M., Uratnik, P., Brezočnik, M., Turk, R. (2007): Prediction of the bending capability of rolled metal sheet by genetic programming. *Materials and Manufacturing Processes*, 22, 634–640.
- [10] Kovačič, M., Šarler, B. (2009): Application of the genetic programming for increasing the soft annealing productivity in steel industry. *Materials and Manufacturing Processes*, 24(3), 369–374.
- [11] Kovačič, M. (2009): Genetic programming and Jominy test modeling. *Materials and Manufacturing Processes*, 24(7), 806–808.
- [12] Kovačič, M., Senčič, S. (2010): Critical inclusion size in spring steel and genetic programming. *RMZ - Materials and Geoenvironment*, 57(1), 17–23.
- [13] Koza, J. R. (1999): Genetic Programming III. Morgan Kaufmann, San Francisco, 3–16.
- [14] Župerl, U., Čuš, F., Kiker, E. (2009): Adaptive network based inference system for estimation of flank wear in end-milling. *Journal of Materials Processing Technology*, 209(3), 1504–1511.

# Palynostratigraphic and palaeoecological studies of the Cretaceous strata in the Bornu Basin, northeastern Nigeria

## Palinostratigrafske in paleoekološke študije krednih skladov iz kadunje Bornu v severovzhodni Nigeriji

**Olugbenga Ademola Boboye**

University of Ibadan, Department of Geology, Ibadan-Nigeria

Corresponding author. E-mail: oa.boboye@mail.ui.edu.ng

### Abstract

The palynological and palaeoecological studies have been carried out on one hundred and forty samples retrieved from an exploratory well (Murshe-1) to evaluate the palaeoenvironment, palaeoclimatic conditions, palynofacies zonations and the possible connection of the basin to the Paleo-Tethys Ocean.

The well recorded fairly rich occurrence of microfossils dominated by land derived forms. The pervasiveness of igneous intrusive encountered in the well suggests a high thermal gradient which could have resulted into the "cooking-up" of the deposited marine shale. It was observed that freshwater environment had influenced only on the Campanian-Maastrichtian sediments which suggests the influence of lagoonal and estuarine environment on the sediments by which possibly might have been deposited. The occurrence of *Araucariacites australis* from late Cenomanian-Turonian sediments suggests drought to less humid climate. The prevalent species in the humid conditions were rare and/or absent in the late Cenomanian to Santonian sediments, however they were found in abundance in the Campanian-Paleocene sediments suggesting a prevalence of humid climate in the Campanian-Maastrichtian which prevailed into the Paleocene period. The palynological data supported the concepts that Nigeria belong to the West African-South American (WASA) phytogeographic Province and the Palmae Province during the Maastrichtian.

**Key words:** palynofacies, palaeoenvironment, palaeoclimate, thermal gradient, phytogeographic Province

### Izvleček

Predmet palinološke in paleoekološke raziskave je bil preučiti na podlagi sto štiridesetih vzorcev iz raziskovalne vrtine Murshe-1 paleookolje, paleopodnebne razmere, palinofacialno zonalnost in mogočo zvezo kadunje Bornu s paleotetidnim oceanom.

Z vrtino so razkrili precej bogato najdišče mikrofosilov, med katerimi prevladujejo kopenske oblike. Navrtali so tudi magmatsko predornino, katere značilnosti nakazujejo visok toplotni gradient, ki je očitno povzročil „segretje“ okoljskega morskega laporja. Ugotovljajo, da se je sladkovodno okolje uveljavilo samo v kampanijsko-maastrichtijskih sedimentih, sicer pa prevladuje lagunsko in delno okolje. Najdba fosila *Araucariacites australis* iz poznih cenomanijsko-turonijskih plasti priča o suhem do nizkovlažnem podnebju. Prevladujoče vrste iz vlažnega podnebja so postale redke ali jih ni v poznocenomanijsko-turonijskih plasteh, medtem ko so njihove najdbe spet obilne v kampanijsko-paleocenskih usedlinah, kar priča o ponovni prevladi vlažnih podnebnih razmer v kampanij-maastrichtiju, kar se nadaljuje vse do paleocenske dobe. Palinološki podatki podpirajo zamisel, da je pripadala Nigerija v maastrichtiju zahodnoafriško-južnoameriški fitogeografski provinci (WASA) in provinci Palmae.

**Ključne besede:** palinološki facies, paleookolje, paleopodnebje, toplotni gradient, fitogeografska provinca

## Introduction

The studied well is located in the Bornu Basin NE Eastern Nigeria. It lies within longitude 12° E to 14°20' E and latitude 13°00' N to 12°00' N (Figures 1a and b). The drainage (Figure 1c) shows that the major rivers from Chad Basin flows in a northeast direction with and empties itself into Lake Chad. A lot of work has been done in Bornu Basin by various workers like Burke (1976), Petters (1981), Fairhead (1986), Genik (1992, 1993), Carter et al. (1963), Barber (1965), Cratchley & Jones (1965), Miller et al., (1968) Okosun (1995) and Cratchley et al., (1984) amongst others.

Reyment & Taita (1972) and Boboye (2008) carried out palaeontological and palynological studies of the Bornu Basin. Reyment (1965) correlated the ammonite biostratigraphy of the Benue Trough and Chad Basin. Petters (1982) recognized eleven concurrent – range zones of varying geochronological durations after studying the Albian-Pliocene benthic foraminifera from six Central West African sedimentary Basins. Boboye (2008) revealed that the palynomorphs' assemblages in this basin are moderately rich but poorly preserved. It is also established that the sediments in this basin are moderately poorly sorted to well sorted, the grains are angular to sub-rounded. The

fine modal are mainly quartz and k-feldspar with subordinate grains of plagioclase microcline, polycrystalline quartz. The sediments are mineralogically and texturally matured in which the argillaceous sandstone, terrigenous mudstone and subordinate igneous intrusive rocks compositionally dominate. Olugbemiro (1997) revealed that foraminiferal assemblages are low in diversity and medium to high in abundance in Bornu Basin. His work indicated that the Fika Shale Formation was deposited under oxic-suboxic shallow epicontinental sea conditions, the Gongila Formation deposited in marine environment, and the Bima sandstone Formation may not be wholly continental as suggested by previous workers because occurrences of planktonic foraminifera at the top of the formation.

The application of palynological data in palaeoenvironmental reconstruction has been attempted by several authors (Batten, 1973, 1982; Vajda-Santivanez, 1998). Also, Ojo & Akande (2004) have used relative abundance of terrestrially derived pollen and marine derived dinoflagellates to interpret the depositional environment of the Cenomanian to Coniacian sediments in three boreholes penetrated in Gongila and Yola Basins. They showed that pollen and spore percentages decreases down-hole which corroborated with this study, as

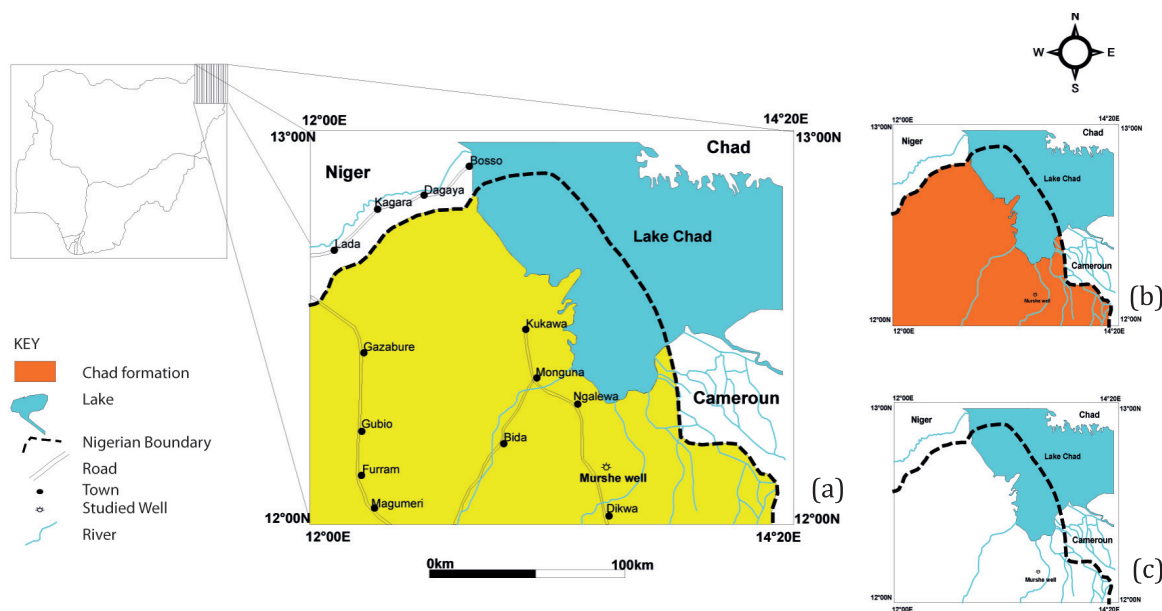


**Figure 1:** Location map of the study area indicating the position of Murshel 1 well (a); The geological map of Chad basin indicating Chad formation (b); The drainage map of study area showing the upward movement of rivers into lake Chad (c).

interpreted in Yolde Formation. This fact contradicts earlier works which show that Yolde Formation reflect nearshore marine but is in line with the proposition that continental condition prevailed during this time so it does not suggest a paralic shallow marine environment due to prevalence of drought to humid pollen species. The purpose of this paper is to determine the age, palynomorphs distribution, palaeoenvironment and palaeoclimate conditions as well as the palynofacies zonation. The biostratigraphic study involved the analysis of pollen, spores, dinoflagellates and algae for chronostratigraphic biozonation.

## Geology of the study area

The Bornu Basin is a Nigerian sector of Chad Basin which is a broad intracratonic depression in Central West Africa containing buried rifts in the Niger Republic. The sedimentation of the Bornu Basin commenced with the deposition of continental, poorly sorted, sparsely fossiliferous, medium to coarse grained, sandstone (Bima Formation) lying directly on the basement. This study revealed that the formation is composed of intercalation of shale (heterolith) and sandstones, as reported by some authors (Carter et al., 1963, Avbovbo et al., 1986 and Boboye 2008). Overlying the Bima Formation is the Gongila Formation that is composed of sandstones and bluish black shale (calcareous) deposited in a shallow marine environment (Carter et al., 1963, Avbovbo et al., 1986). These deposits mark the onset of marine incursion into this basin. This transgression reached its maximum in the Turonian, (during which the Fika Shale Formation was deposited in an open marine environment) and continue into Senonian after which a regressive phase of deposition occurred (Carter et al., 1963, Avbovbo et al., 1986). In the Maastrichtian, estuarine and/or deltaic environment prevailed which led to the deposition of the Gombe Sandstone in some part of the northeastern Nigeria (Carter et al., 1963, Avbovbo et al., 1986). The formation constitutes intercalated shale, siltstones and ironstones.

An extensional deformation occurred in the Maastrichtian which was later restructured

into an elongate NE-SW graben system. The sub basins developed in response to rifting and created space for the emplacement of the Tertiary Kerri-kerri Formation, which overlies unconformably, the Cretaceous sediments (Carter et al., 1963). In the Pleistocene, the continental Chad Formation was unconformably laid down over Kerri-Kerri and/or Gombe Sandstone Formations (Carter et al., 1963, Avbovbo et al., 1986). However towards the end of the Tertiary up to Recent, there are widespread of volcanic activity occurrences in the southern and central part of the basin (Burke, 1976). The lithostratigraphic successions observed in the studied well and the sampled intervals are shown in Figure 2.

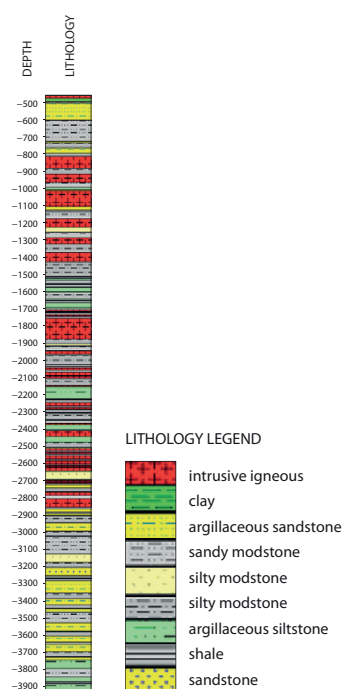


Figure 2: Lithostratigraphy of the studied well.

## Material and methods

One hundred and forty cutting samples were used for this study and the sampling of the well was done at 5 m interval. The samples were separated into two parts; a part was logged in the sedimentological laboratory while the other part was thoroughly washed with distilled water through 5 µm polyester sieve. This size was used for the preparation in this work. The mesh sizes often used are 10 µm and 20 µm.

The 10 µm gauzes being fine enough to catch all, but if the smallest spores is known to be present, 5 µm mesh size may be used. This was to remove drilling mud contaminants and then dried for 24 hours at 50 °C for palynological analysis. Ten grams of each sample were digested with 30 ml of 10 % HCl to remove CaCO<sub>3</sub>. It was then digested with 30 ml of 40 % HF for 24 h to remove silica. The content was sieve with water and later oxidized in Schulze solution (mixture of nitric acid and potassium chlorate) for 30 min, washed with 10 % potassium hydroxide and centrifuged. The aliquotus was dispersed with polyvinyl alcohol, dried and then mounted on DPX. The distribution charts for the recovered palynomorphs are presented (Figure 4).

Detailed description was used in the generation of the litho-log and for biostratigraphic interpretation of the well (Figures 2 and 3). Fresh sample of clay, sandy mudstone, silty mudstone and shale from this log were selected for routing palynological processing and the details are discussed.

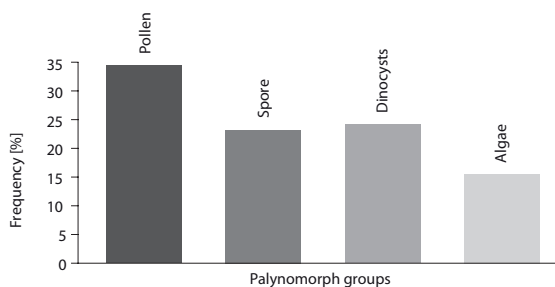


Figure 4a: Histogram of frequency (%) of palynomorph distribution in the studied well.

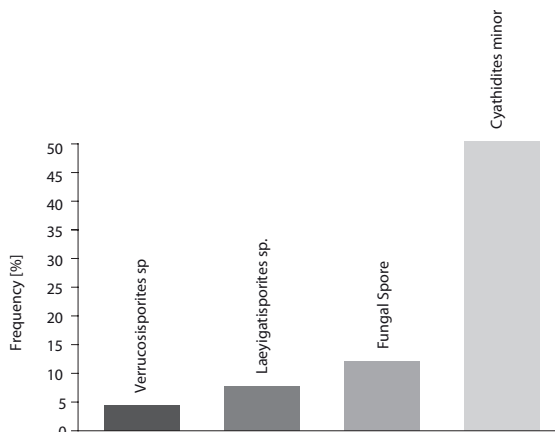


Figure 4b: Frequency (%) distribution of sporomorph groups in the studied well.

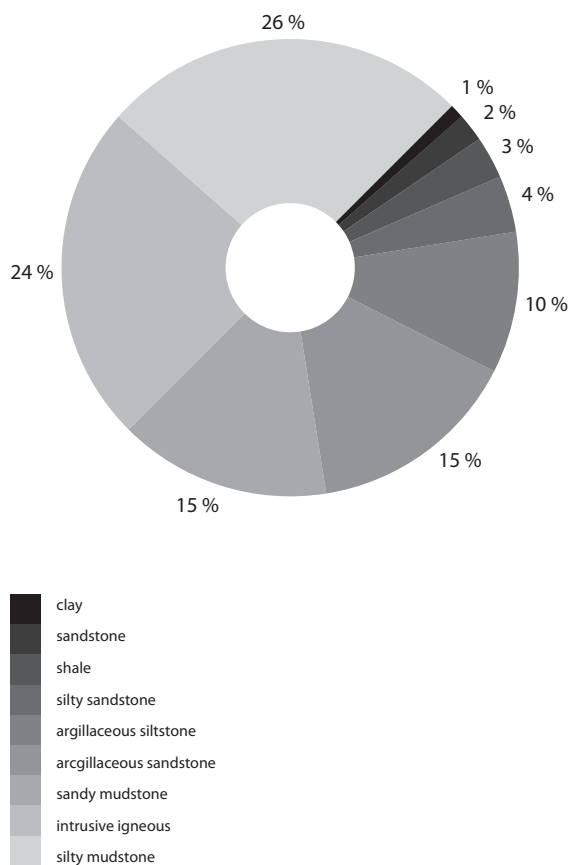


Figure 3: Lithofacies distribution within the studied well.

Clay constitute the upper section of the well with a thickness of about 20 m while shale formed an intercalation ranging from 2 m to 30 m occupying an overall thickness of 95 m in the entire section. Sandy mudstone also formed an intercalation and ranged in thickness from 15 m to 120 m with an overall thickness of 495 m. Finally, the silty mudstone which contained most of the analyzed sample ranges from 35 m to 90 m and it occupies an overall thickness of 869 m in logged section. Argillaceous sandstone range from 3 m to 50 m with a total thickness of 343 m in the log section. Silty Sandstone ranges from 10 m to 50 m with a thickness of 140 m in the log. Also sandstone ranges from 2 m to 50 m occurring in three intervals with a total thickness of 72 m while igneous intrusive occurred throughout the well covering a total thickness of about 797 m.

The chart for the lithofacies shows that 26 % is silty mudstone, intrusive igneous 24 %, sandy mudstone 15 %, argillaceous sandstone 15 %, argillaceous siltstone 10 %, silty sandstone 4 %, sandstone 2 %, shale 3 % and clay 1 % (Figure 3).

## Results and Discussion

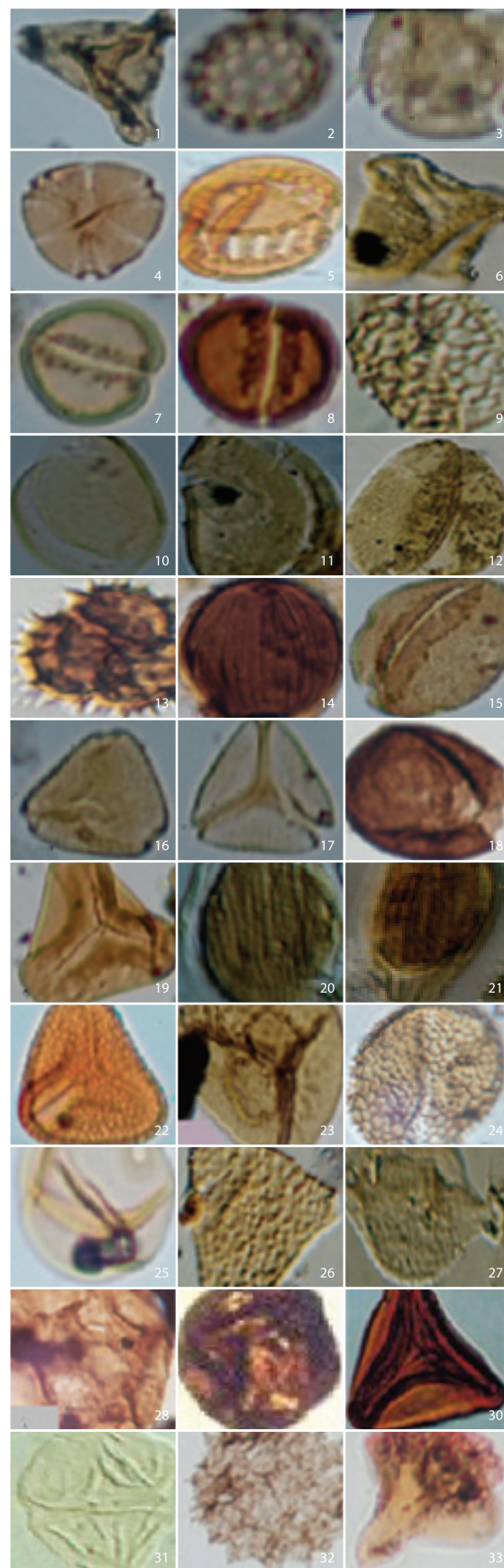
### *Palynomorph distribution*

A total of one hundred and seven species of pollen, spores, dinoflagellate, algae and other palynomorphs were recorded from the Murshe -1 well (Figure 4) and some of the key species are well represented (Figures 4 and 5).

A total of fortyfive species of pollen include; *Afropollis jordanus*, *Alnipollenites venus*, *Aquilapollenites minimus*, *Araucariacites australis*, *Cicatricosisporites* sp., *Cretacaeiporites mulleri*, *Cretacaeiporites scabratus*, *Cretacaeiporites* sp., *Droseridites senonicus*, *Echitricolporites trianguliformis*, *Ephedripites ambiguus*, *Ephedripites multicostatus*, *Ephedripites* spp., *Ericipites* sp., *Gemmate pollen*, *Gemmazonocolpites cingulatus*, *Gleicheniidites senonicus*, *Gleicheniidites* sp., *Graminidites* sp., *Auriculiidites reticulatus*, *Inaperturopollenites* sp., *Leptolepidites major*, *Longapertites chlonovae*, *Longapertites marginatus*, *Longapertites microfoveolatus*, *Monocolpites marginatus*, *Monocolpites* sp., *Monocolpopollenites sphaeroidites*, *Pollen indeterminate*,

**Figure 5:** Some of the palynomorphs' species recovered from the studied well.

1. *Aquilapollenites* sp., × 800
2. *Chenopodipollis* sp., × 800
3. *Cretacaeiporites mulleri*, Herngreen, 1973, × 800
4. *Tricolporites* sp., × 800
5. *Tubistephanocolpites cylindricus*, Salami, 1984, × 800
6. *Aquilapollenites minimus*, Jardiné & Magloire, 1965, × 800
7. *Monocolpopollenites* sp., × 800
8. *Monocolpopollenites sphaeroidites*, Jardiné & Magloire, 1965, × 800
9. *Dichastopollenites* sp., May, 1975, × 800
10. *Longapertites chlonovae*, Jardiné & Magloire, 1965, × 400
11. *Longapertites microfoveolatus*, Jan du Chêne & Adegoko, 1978, × 400
12. *Longapertites marginatus*, Van Hoeken-Klinkenberg, 1964, × 400
13. *Droseridites senonicus*, Jardiné & Magloire, 1965, × 800
14. *Ephedripites multicostatus*, Brenner, 1963, × 400
15. *Monocolpites marginatus*, Van Der Hammen, 1954, × 800
16. *Triorites africaensis*, Jardiné & Magloire, 1965, × 800
17. *Syncolporites* sp., × 800
18. *Araucariacites australis*, Cookson, 1947 ex Couper, 1953, × 400
19. *Gleicheniidites senonicus*, Ross, 1949, × 800
20. *Ephedripites* sp., × 400
21. *Ephedripites ambiguus*, Azema & Boltenhagen, 1974, × 800
22. *Foveotriletes margaritae*, (Van Der Hammen) G. H. M., 1968, × 800
23. *Zlvisporis blanensis*, Pacltová, 1961, × 800
24. *Retimonocolpites* sp., × 800
25. *Graminidites* sp., × 800
26. *Proteacidites sigalii*, Boltenhagen, 1978, × 800
27. *Auriculiidites reticulatus*, Elsik, 1964, × 800
28. *Cretacaeiporites* sp., × 800
29. *Cretacaeiporites scabratus*, Herngreen, 1973, × 800
30. *Gleicheniidites* sp., × 800
31. *Dinogymnium euclaense*, Cookson and Eisenack, 1970, × 800
32. *Pediastrum* sp., × 800
33. *Botryococcus braunii*, Kutzing, 1987, × 800



*Proteacidites sigalii*, *Proteacidites* sp., *Chenopodipollis* sp., *Psilamonocolpites* sp., *Psilatricolporites* sp., *Chenopodipollis* sp., *Retimonocolpites* sp., *Steevesipollenites* sp., *Syncolpites* spp., *Syncolporites* spp., *Tricolpites* sp., Tricolporate forms, *Tricolporites* sp., *Tricolporopollenites* sp., *Triorites africaensis*, *Triorites* sp., *Tubistephano-colpites cylindricus*, and *Monosulcites* sp.

A palynoflora contains thirty diverse spore assemblages including the *Cingulatisporites ornatus*, *Concavissimisporites* sp., *Cyathidites australis*, *Cyathidites minor*, *Cyathidites* sp., *Deltoidospora* sp., *Dictyophyllidites harrissi*, *Distaverrusporites simplex*, *Zlavisporis blanensis*, *Foraminisporites daiiyl*, *Foveotriletes margaritae*, Fungal spore, Gemmate spore, Incertae sedis, *Laevigatosporites* sp., *Lycopodiumsporites* sp., *Polypodiaceasporites* sp., *Liliacidites* sp., *Psilatritetes radiatus*, *Psilatritporites* sp., *Rugulatisporites caperatus*, *Rugulatisporites* sp., *Spore indeterminate*, Trilete spores sp., *Verrucatosporites* sp., *Verrucosisporites* sp.

A total of 32 species of dinoflagellate cysts include; *Achomosphaera* sp., *Andalusiella* sp., *Batiacasphaera* sp., *Chlamydothorella albertii*, *Cometodinium* sp., *Cribroperidinium edwardsii*, *Cyclonephelium* sp., *Dinogymnium euclaensis*, *Exochosphaeridium phragmites*, *Florentinia* sp., *Foram wall lining*, *Gardodinium cf. elongatum*, *Gonyaulacysta* sp., *Isabelidinium* sp., *Leiosphaeridia* sp., *Leptodinium* sp., *Nelsoniella aceras*, *Odontochitina costata*, *Oligosphaeridium complex*, *Palaeocystodinium* sp., *Polysphaeridium* spp., *Protoperidinium* sp., *Senegalinium bicaevatum*, *Senegalinium* sp., *Spinidinium* sp., *Spiniferites ramosus*, *Spiniferites* sp., *Subtilisphaera pirnaensis*, *Subtilisphaera pontis-mariae*, *Subtilisphaera* sp., *Trichodinium delicatum*, *Trichodinium* sp.

Fresh water algae include only one species of *Pediastrum*, *Botryococcus braunii* and other palynomorphs are *Areoligera* sp., hyphae, fungal fruit body and foraminiferal linings.

### **Palynostratigraphy**

The well yielded fairly rich and diverse abundance of palynomorphs, although some of them have been highly carbonized due to volcanism that characterized the region towards the end of Tertiary to Recent (Burke, 1976) which has

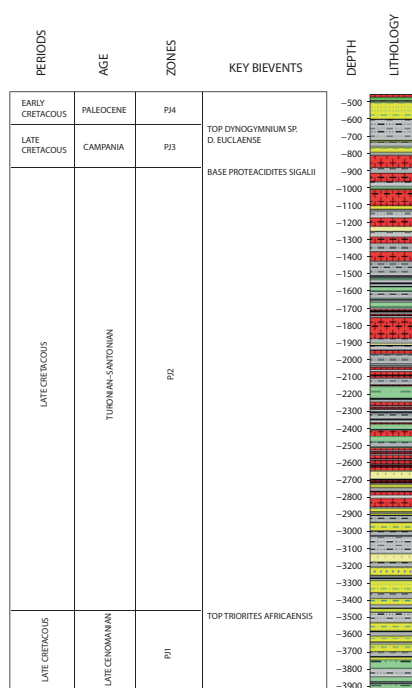
affected their preservation. There is a significant decrease in the abundance of microfossils at the basal section (1 910–3 928 m) of the well. The middle part (630–1 910 m) recorded fairly rich occurrence of microfossil dominated by land derived species such as *Zlavisporis blanensis*, *Araucariacites australis*, *Proteacidites sigalii*, *Tricolporopollenites* spp., *Cyathidites minor* and *Monocolpites* sp. while the uppermost section (120–630 m) recorded scanty occurrence of microfossil.

Moderately rich and diverse occurrence of dinoflagellate cysts such as *Dinogymnium* spp., *Subtilisphaera* spp., *Cribroperidinium* spp., *Odontochitina costata* and *Oligosphaeridium complex* were recorded at several horizons within the studied section, with common records of fresh water to slightly brackish algae (*Botryococcus braunii* and *Pediastrum* sp.) which suggests a shallow marine environment with frequent freshwater incursion. Few rare species are restricted to each zone. It is worth mentioning here the occurrence of rare to spot records of Albian/Cenomanian markers such as *Afropollis jardinus* and *Cretacaeiporites scabratus*. They usually show single occurrences in isolated samples and this can be assumed to be reworked from older sediments into younger horizons. The Cretaceous/Tertiary (K/T) boundary is placed at 630 m which is defined by the top/extinction of *Dinogymnium* sp. recorded at that horizon.

Four microflora zones have been established for the Murshe-1 well based on the stratigraphic distribution of diagnostic palynological markers (Figure 6). This has been correlated with palyno-zones of Salard Cheboldaef (1990), Lawal and Moullade (1986), Muller et al. (1987), Jan du Chêne et al., (1978 and Boboye, 2008).

### **PJ1 Microflora Zone (late Cenomanian)**

This zone is marked with the rare occurrence of microflora. It is characterized by the presence of several taxa including *Araucariacites australis*, *Cretacaeiporites scabratus*, *Ephedripites* sp., *Graminidites* sp., *Inaperturopollenites* sp., *Monocolpites marginatus*, *Proteacidites sigalii*, *Tricolporites*, *Triorites africaensis*, *Triorites* sp., *Deltoidospora* sp., *Incertae sedis*, *Lyc-*



LITHOLOGY LEGEND

	intrusive igneous
	clay
	argillaceous sandstone
	sandy modstone
	silty modstone
	silty modstone
	argillaceous siltstone
	shale
	sandstone

**Figure 6:** Palynostratigraphic zonation of the studied well.

*podiumsporites* sp., *Polypodiaceosporites* sp., Spore indeterminate, *Araucariacites australis*, *Zlivisporis blanensis*, *Pediastrum* sp., fungal spore and foraminiferal linings.

This is the oldest zone recorded in the studied well section. The top of this interval is defined by the last occurrence of *Triorites africaensis*, while the base is stratigraphically deeper than the last sample encountered. The interval records a decrease in the abundance and diversity of palynomorphs with few occurrences of freshwater algae. This zone correlates with the *Classopollis* spp. Zone of Jan du Chêne et al., (1978).

### **PJ2 Microflora Zone (Turonian-Santonian)**

This zone is rich in well preserved palynomorph; it is marked with the absence of *Cicatricosisporites* sp., *Droseridites senonicus*,

*Gemmazonocolpites angulatus*, *Psilatricolpites* spp., *Psilatricolporites* sp., *Retimonocolpites* sp., *Steevesipollenites* sp., *Tricolporites*, *Triorites* sp., *Concavissimisporites* sp., *Polypodiaceosporites* sp.

The top of this broad zone is defined by the first occurrence of *Proteacidites sigalii* recorded at 890 m, while the last occurrence of *Triorites africaensis* recorded at 3 450 m defines the base of this zone. Also characterized with this zone is *Cretacaeiporites scabratus* which could be reworked from older sediments into younger horizons. The Turonian-Coniacian and the Coniacian-Santonian boundaries could not be established due to poor recovery and stratigraphic distribution of the marker species that define these ages. The zone records a decrease in abundance and diversity of palynomorphs. This zone correlates with *Droseridites senonicus*-*Cretacaeiporites scabratus* Zone of Salard Cheboldaëff (1990) and Boboye (2008).

### **PJ3 Microflora Zone (Campanian-Maastrichtian)**

This zone is defined by the last appearance of *Dinogymnium* sp. (*D. euclaense*). It is marked by abundance of microflora fossils with the absence of some which includes; *Alnipollenites verus*, *Aquilapollenites minimus*, *Droseridites senonicus*, *Echitricolporites trianguliformis*, *Ephedripites ambiguus*, *Ephedripites* sp., *Ericipites* sp., *Gemmazonocolpites cingulatus*, *Gleicheniidites* sp., *Leptolepidites major*, *Syncolpites* spp., *Syncolporites* sp., *Tricolporites* spp., *Triorites africaensis*, *Cyathidites australis*. Gemmate spore, *Incertae sedis*, *Cycopodisporites* spp., *Monosulcites* sp., *Polypodiaceosporites* spp., *Achomosphaera* sp., *Andalusiella* sp., *Batiacasphaera* sp., *Laevigatosporites* sp., *Chlamydophorella albertii*, *Cometodinium* sp., *Cribroperidinium edwardsii*, *Cyclonephelium* sp., *Exochosphaeridium phragmites*, *Florentinia* sp., *Gardodinium cf. elongatum*, *Gonyaulacysta* sp., *Isabelidinium* sp., *Nelsoniella aceras*, *Odontochitima costata*, *Oligosphaeridium complex*, *Palaeocystodinium* spp., *Protoperidinium* sp., *Senegalinium bicavatum*, *Spinidinium* sp., *Spiniferites ramosus*, *Spiniferites* sp., *Subtilisphaera pirnaensis*, *Subtilisphaera pontis-mariae*, *Trichodinium* sp., *Areoligaera* sp., fungal spore, fungal fruit body, foraminiferal linings, *Cre-*

*tacaeiporites scabratus*, *Cretaceaporites* sp. The occurrence of *Cretaceaporites scabratus* within this zone is assumed to have been reworked from older sediments. The base is marked by the first occurrence of *Proteacidites sigalii*.

The top of this zone is marked by the last occurrence of *Dinogymnium* spp., while appearance is tentatively placed at 890 m, coinciding with the first occurrence of *Proteacidites sigalii*. Among other microflora encountered include *Auriculiidites reticulatus*, *Foveotriletes margaritae*, *Cyathidites* sp., *Dictyophyllidites harrissi*, *Concavissimisporites* sp. and *Cicatricosisporites* sp. There is a marked increase in the abundance and diversity of palynomorphs within this interval. Significant occurrences of dinoflagellate cysts are also recorded. This zone correlates with the *Dinogymnium* spp.–*Proteacidites sigalii* Zone of Jan du Chêne et al., (1978).

#### **PJ4 Microflora Zone (Paleocene and younger)**

This zone is defined by the basal occurrence of *Dinogymnium* sp. (*D. euclaense*). It is marked by rare and/or absence of microflora. Among the few encountered include *Graminidites* sp., *Inaperturopollenites* sp., indeterminate pollen, *Psilamonolcolpites* sp., *Psilatricolporites* sp., *Tricolpites* sp., *Tricolporites*, *Rugulatisporites caperatus*, *Pediastrum* sp., fungal spores and hyphae. There is high abundance of *Dinogymnium* sp. (*D. euclaense*), fungal spore and hyphae. The top of this zone is stratigraphically higher than the first sample analyzed and as such was not encountered in the well section. The base is defined by the last occurrence of *Dinogymnium* spp. recorded at 630 m. Sparse records of palynomorphs were recorded within this interval. This zone correlates with *Spinizonolcolpites baculatus* Zone of Muller et al., (1987) and Boboye (2008).

#### **Palaeoecology and Palaeoenvironments**

Changing climate over the period of 93.9 Ma to 56 Ma has been the driving force for the gradual disappearance of drought and humid elements and the appearance of palmae and brackish elements in the palynofloras of north-eastern Nigeria. Spores, dinoflagellates and algae were used for the palaeoenvironment inferences (Figure 7). Fern and allied spores are

generally dominant throughout the whole section. (Figure 4). Pollen and fungal spores show low values (36 % and 23.6 %). Dominant and less abundant elements show little variations throughout the section. Characteristics of the zones are the mangrove element, *Psilatricolporites* sp., the marine representatives (foraminiferal linings) and fresh water algae *Botryococcus braunii*, indicating sedimentation in coastal and shallow marine environments, close to mangrove vegetation. *Botryococcus*, although more typical of fresh water environments, can also occur in slightly brackish water, due to its tolerance to salinity variations (Rull, 1997). Other elements that characterize the study section are fern spores (*Laevigatosporites* sp., *Verrucatosporites*, *Cyathidites minor*), together with *Retimonolcolpites* sp. and the fresh water algae, *Pediastrum*.

*Laevigatosporites* sp. and *Verrucatosporites* has been reported in fresh water swamps, while dinoflagellates, *Andalusiella* sp. and *Dinogymnium euclaense* are near shore marine environment (Vadja-Santinavez, 1998, Awad, 1994, May, 1977). The occurrence of chorate dinocysts such as *Florentinia* sp., *Leioshaeridia* sp., *Oligosphaeridium complex*, *Subtilisphaera* sp. and foraminifera lining are prevalent in open marine environment (Ojo & Akande, 2004, Okosun, 1995, Reymont & Dingle, 1987 and Peters, 1978), while the presence of *Spiniferites ramoscus* and *Spiniferites* sp. suggests oceanic to neritic environment (Vadja-Santinavez, 1998, Awad, 1994, May, 1977). The fungal spores, *Psilamonolcolpites* sp., *Laevigatosporites* sp. and *Verrucatosporites* assemblages could be considered to be a mangrove assemblage deposited in shallow brackish water. The assemblages recovered in this study are composed of palms (*Psilamonolcolpites* sp.), ferns (*Laevigatosporites* sp. and *Verrucatosporites*), and fungal spores, representing coastal swamps (palm/fern swamps) common in the Neotropics.

The succession of these assemblages through time shows dominant pollen signal from palm/fern to mangrove swamps with little changes and the replacement of mangrove swamps. This is also evident in the lithofacies that characterized this section which is controlled by the climate (Boboye, 2010). Indeed during the deposition of the sequence, pollen sedi-

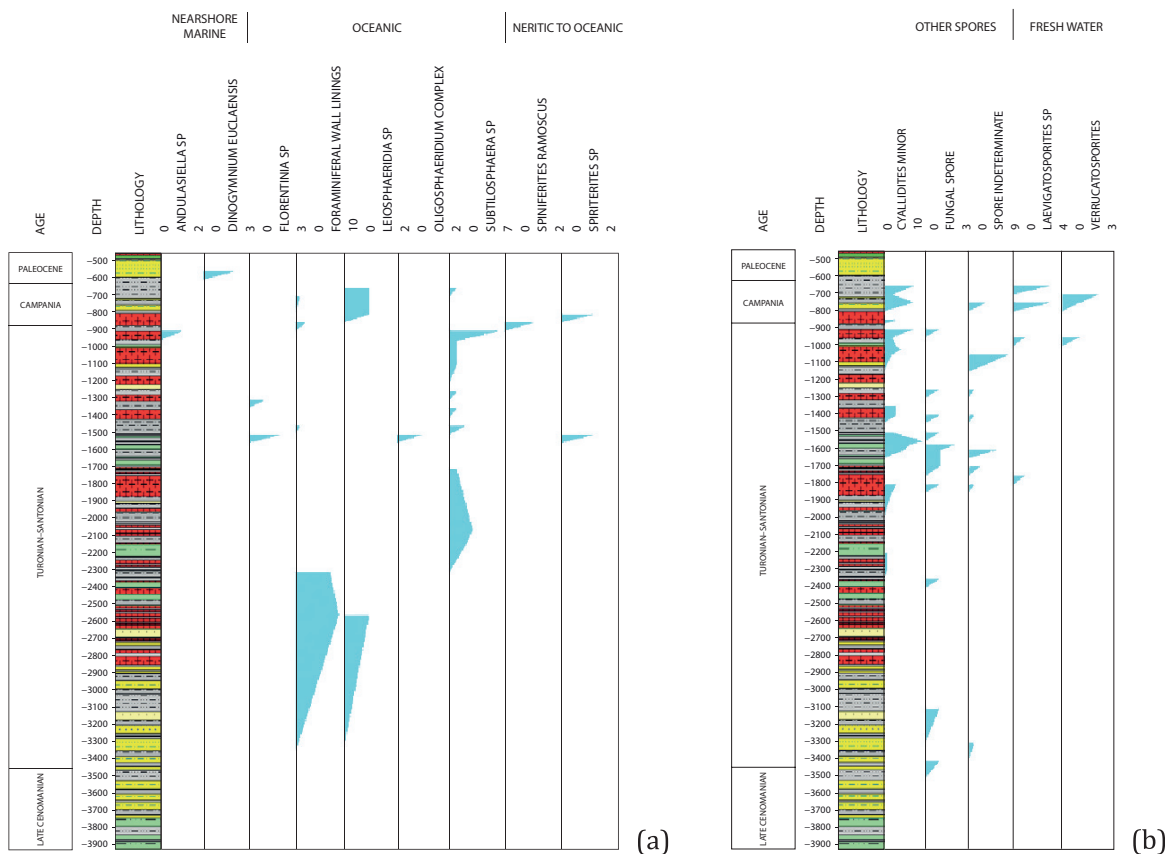


**Figure 7:** The palaeoenvironmental reconstruction based on: (a) Dinoflagellates (b) Spores and (c) Algae.

mentation was mainly composed of palm/fern swamp sporomorphs and pollen deposited under oceanic to fresh water environment. During deposition of the formations in this section (PJ1 to PJ4 Zones), although sporomorphs from palm/fern swamps continue to dominate, sporomorphs from herbaceous swamps increased, and the mangrove pollen was substantially reduced to very few species of fresh to brackish water algae probably transported landward by wind. Therefore the replacement of dinoflagellate assemblages (neritic to oceanic) by fungi spore and algae assemblages (fresh to slightly brackish water) across the zones (Figures 4 and 7) can be interpreted as a regressive trend from shallow shelf to mangrove environments of deposition.

It was observed that fresh water environment had influence only during the Campanian-Maastrichtian to the earliest part of late Cenomanian suggesting that the sediments had lagoonal and estuarine influence on the environment of deposited.

Figure 8 shows that *Ephedripites ambiguus*, *Ephedripites multicostatus*, *Ephedripites* sp.,

and *Ericipites* sp. are more dominant in drought conditions while the occurrences of *Araucariacites australis* is more common during times of drought and less abundant in humid climate. *Gleicheniidites* sp., *Gleicheniidites senonicus*, *Tricolpites* sp., and tricolporates species are humid forms which thrive with reasonable rainfall. The result in this study shows that between the intervals of 1 400 m to 1 500 m, the silty mudstone that was deposited contained pollen that found during the drought periods which indicated that dry climate had prevailed at a time in the Turonian to Santonian. However, the occurrence of *Araucariacites australis* in the late Cenomanian to Santonian suggests a drought to less humid climate which was not observed in Campanian to Maastrichtian. However, the species that were prevalent in humid condition were absent in the late Cenomanian to Santonian while they were found in abundance in the Campanian to Pale-

ocene sediments. This suggests a prevalence of humid climate during this period. The basal section of Turonian to Santonian sediments (Gongila Formation) also shows paucity of sporomorphs. The middle and upper units' exhibits higher content of terrestrial and marine species. The marine dinoflagellates were more abundant in the upper section compared with the terrestrially derived (Turonian to Paleocene) species. This is corroborated with the presence of fresh water pollen (*Laevigatosporites* sp. and *Verrucatosporites* sp.) and the algae, *Pediastrum* sp. Ojo and Akande, (2004) reported a maximum marine transgression in Pindiga Formation and this is reflected in the results (upper section of Turonian to Santonian sediments), which is marked by common chlorate dinoflagellate cysts which include the genera *Spiniferites*, *Florentina* and *Oligosphaeridium* (Schrack, 1991). The fact that the typically open marine dinocyst genera, such

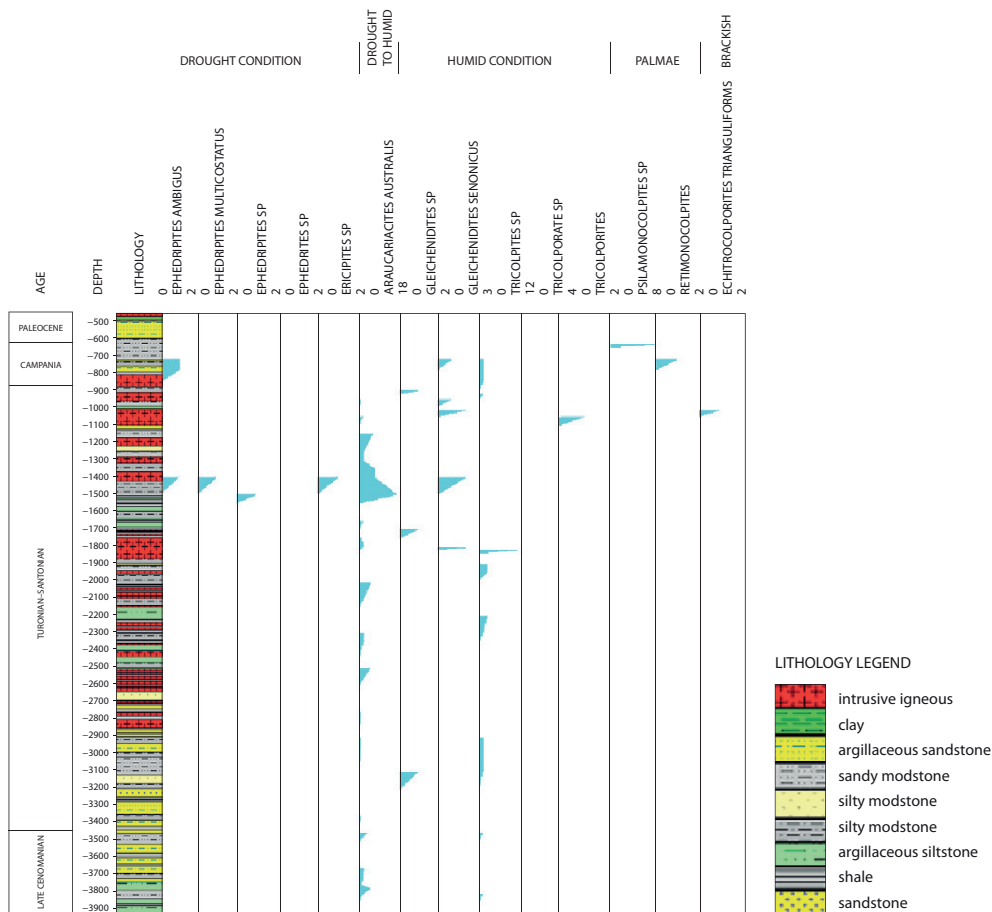


Figure 8: The palaeoclimatic reconstruction of the studied well.

as Florentina, Oligosphaeridium and Subtilisphaera which are cosmopolitan and have Tethyan affinities (Dave & Verdier, 1973, 1976, Below 1982; Batten & Uwins, 1985) present in Turonian to Maastrichtian intervals of the well, lends more credence to possible connection of the Tethys Sea in the north and south to the south Atlantic Ocean (Petters, 1978; Kogbe, 1976; Reyment & Dingle, 1987; Okosun, 1995). All the palynological data supported that Nigeria belong to the West African-South American Phyto-geographic Province and the Palmae Province during the Maastrichtian.

Variations in the vegetation are directly related to fluctuation in climatic conditions during the Cenomanian to Paleocene period. (Awad, 1994; Mauseth, 1991; Crane, 1987).

All through the Cenomanian to Paleocene, palynological assemblage of higher gymnosperm content were deposited, this include Araucariaceae, the producer of *Araucariacities*. A less humid (relatively dry) or even arid condition is assumed by the presence of xerophytic elements. This drought condition is corroborated by the presence of some ephedroids, which can tolerate relatively dry habitat conditions. This is observed from 1 400 m to 1 500 m depths with the association of pteridophyte families, such as Gleicheniaceae which indicate tropical humid environment. A simultaneous subtropical condition and dry phase probably occurred during the Turonian and Santonian (Ojo & Akande, 2004), as inferred by the relatively high diversity of angiosperm pollen such as tricolpate, tricolporate, indicating some reasonable rainfall and local occurrences of xerophytes and ephedroids.

## Conclusions

A total of one hundred and forty cutting samples were analyzed and used in the generation of the litho log and for biostratigraphic interpretations. Argillaceous sandstone ranges from 3 m to 50 m with a total thickness of 343 m in the log section. Silty sandstone has an average thickness of 140 m, the sandstone is 72 m, while the igneous intrusive occurred throughout the well with a total range thickness of 797 m.

A total of one hundred and four species of pollen, spores, dinoflagellates, algae and others were recorded in the well. Diagnostic species identified (*Triorites scabratus*, *Proteacidites sigalii*, *Dinogymnium* sp. (*D. euclaense*)) were used for the age determination and palynostratigraphic zonation of the study area. These are the late Cenomanian (PJ1 Zone, the Turonian-Santonian (PJ2 Zone), the Campanian-Maastrichtian (PJ3 Zone) and Paleocene and younger (PJ4 Zone) ages.

The well yielded fairly rich and diverse abundance of palynomorphs. The uppermost section (120–630 m) recorded scanty occurrence of microflora, while the middle part (630–1 910 m) recorded fairly rich occurrences of microflora dominated by land derived species, such as *Zlivisporis blanensis*, *Araucariacites australis*, *Proteacidites sigalii*, *Tricolporopollenites* spp., *Cyathidites minor* and *Monocolpites* sp. There was significant decrease in the abundance of microflora at the basal section (1 910–3 928 m) of the well.

It is evident that the fresh water environment had influence on the sediment only during the Campano-Maastrichtian to the earlier part of the late Cenomanian. This suggests that the sediments had lagoonal and estuarine influence during emplacement. The results show that the sediments between 1 400 m to 1 500 m depths (silty mudstone) is characterized by drought climate pollen during the Turonian to Santonian period. However, *Araucariacites australis* occurred only from late Cenomanian up to Turonian and Santonian sediments which suggests that a drought to less humid climate existed during these periods.

The species that are prevalent in humid condition were absent in the Santonian and lower - middle part of Turonian periods and also in the late Cenomanian sediments. However, it was found in abundance in the Campano-Maastrichtian and Paleocene sediments, which indicate that humid climate, prevailed into the Paleocene period in the study area. This study has shown the pervasiveness of igneous intrusive in the well which implies a high thermal gradient during the course of deposition which could have led to the “cooking up” of the marine shale (Boboye, 2008).

## References

- Avbovbo, A. A., Ayoola, E. O. & Osahon, G. A. (1986): Depositional and structural styles in Chad Basin of north-eastern Nigeria. *American Association of Petroleum Geoscientists Bulletin*, 70, pp. 1787–1798.
- Awad, M. Z. (1994): Stratigraphic, palynological and paleoecological studies in the East-Central Sudan (Khartoum and Kosti Basins), Late Jurassic to Mid Tertiary: *Berliner Geowissenschaftlich Abhandlungen A*, 161, pp. 1–163.
- Batten, D. J. (1973): Use of palynologic assemblage types in Wealden correlation. *Palaeontology*, 16, pp. 1–40.
- Batten, D. J. (1982): Palynofacies, palaeoenvironments and petroleum, *Journal of Micropalaeontology*, 1, pp. 107–114.
- Batten, D. J. & Uwins, P. J. R. (1985): Early-Late Cretaceous (Aptian-Cenomanian) palynomorphs, *Journal of Micropalaeontology*, 4, pp. 151–168.
- Barber, W. (1965): Pressure water in the Chad Formation of Bornu and Dikwa Emirates, north-eastern Nigeria. *Bulletin Geological Survey of Nigeria*, 35, pp. 1–138.
- Below, R. (1982): Scolochoreate Zysten der Gonyaulacaceae (Dinophyceae) aus der Unterkreieide Marokkos. *Palaeontographica B*, 182, pp. 1–15.
- Boyo, O. A. (2008): Palyno-geochemical characterization of late Albian – early Paleocene lithofacies of the SW Chad Basin. Ph. D. Thesis, (Unpublished) *University of Ibadan, Ibadan, Nigeria*. 220 p.
- Boyo, O. A. & Akaegbobi, I. M. (2010): Sedimentological and Palyno-environmental appraisal of the late Quaternary Sediments northeastern, Bornu Basin. *Quaternary International Journal, Elsevier*, 262, 14–19.
- Burke, K. (1976): The Chad Basin: An active intra-continental basin. *Tectonophysics*, 36, pp. 197–206.
- Carter, J. D., Barber, W., Tait, E. A. & Jones, G. P. (1963): The geology of parts of Adamawa, Bauchi and Bornu provinces in northeastern Nigeria, *Bulletin Geological Survey Nigeria*, 30, pp. 1–109.
- Crane, P. R. (1987): Vegetational consequences of the angiosperm diversification. In: E. M. Friis, W. G. Chaloner and P. R. Crane (eds.). *The origins of angiosperms and their biological consequences*, Cambridge University Press, pp. 107–144.
- Cratchley, C. R. & Jones, J. P. (1965): An interpretation of the geology and gravity anomalies of the Benue Trough Nigeria. *Geophysics Paper, British Oversea Geological Survey*, 1, pp. 126.
- Cratchley, C. R., Louis, P. & Ajakaiye, D. E. (1984): Geophysical and geological evidence for the Benue-Chad Basin, Cretaceous rift valley system and its tectonic implications. *Journal of African Earth Sciences*, 2, pp. 141–150.
- Davey, R. J. & Verdier, J. P. (1973): An investigation of microplankton assemblages from latest Albian (Vraconian) sediments. *Revista Española de Micropalaeontología* 5, pp. 173–212.
- Davey, R. J. & Verdier, J. P. (1976): A review of certain non-tabulate Cretaceous hystrichospherid dinocysts. *Review of Palaeobotany and Palynology*, 22, pp. 307–335.
- Fairhead, J. D. (1986): Geophysical controls on sedimentation with the African Rift Systems. In: L. E. Frostick et al. (Eds.), *Sedimentation in the African Rifts. Geological Society Special Publication*, 25, pp. 19–27.
- Genik, G. J. (1992): Regional framework, structural and petroleum aspects of rift basins in Niger, Chad and the Central African Republic (C.A.R.). *Tectonophysics*, 213, pp. 169–185.
- Genik, G. J. (1993): Petroleum Geology of Cretaceous-Tertiary rift basins in Niger, Chad and Central African Republic. *American Association of Petroleum Geoscientists, Bulletin*, 77, pp. 1405–1434.
- Jan du Chêne, R. E., De Klasz, I. & Archibong, E. E. (1978): Biostratigraphic study of the borehole Ojo-1, S. W. Nigeria, with special emphasis on the Cretaceous microflora. *Revue de Micropaléontologie*, 21, pp. 123–139.
- Lawal, O. & Moullade, E. (1986): Biostratigraphy of Cretaceous sediments in the Upper Benue Basin, N. E. Nigeria. *Revue de Micropaléontologie*, 29, 61–83.
- May, F. E. (1977): Functional morphology, paleoecology and systematic of Dinogymnium tests: *Palynology*, 1, pp. 103–121.
- Mauseth, J. D. (1991): Botany: An introduction to plant biology, *Saunders College Publishing, Philadelphia, Pennsylvania*, 800 p.
- Miller, R. E., Johnston, R. H., Olowu, J. A. I. & Uzoma, J. U. (1968): Groundwater hydrology of the Chad Basin in Bornu and Dikwa emirates, northeastern Nigeria, with special emphasis on the flow life of the artesian system. *Geological Survey, Water Supply Paper*, 1757, pp. 1–48.
- Muller, J., Digiaco, E., & Van Erve, A. W. (1987): A palynological zonation of the Cretaceous, Tertiary and Quaternary of northern South America. *American Association of Stratigraphic Palynologists, Contributions Series*, 19, pp. 91–77.

- Ojo, O. J. & Akande, S. O. (2004): Palynological and palaeoenvironmental analyses of selected samples from Dukul and Jessu formations, Yola Basin, Nigeria. *Nigerian Association of Petroleum Explorationists*, 17/1, pp. 70–76.
- Okosun, E. A. (1995): Review of the Geology of Bornu Basin. *Journal of Mining and Geology*, 31(2), pp. 113–122.
- Olugbemiro, R. O. (1997): Hydrocarbon Potential, maturation and paleoenvironments of the Cretaceous series in Bornu Basin, NE Nigeria. Ph.D. Thesis (Unpublished) *Institut und Museum für Geologie und Paläontologie der Universität Tübingen*, Germany, 14, 150 p.
- Petters, S. W. (1978a): Mid-Cretaceous paleoenvironment and biostratigraphy of the Benue Trough, Nigeria. *Geological Society of America Bulletin*, 89, pp. 151–154.
- Petters, S. W. (1978b): Stratigraphic evolution of the Benue Trough and its implications for the Upper Cretaceous palaeogeography of West Africa. *The Journal of Geology*, 8, 6, pp. 311–322.
- Petters, S. W. (1978c): Foraminifera palaeoecology of the southeastern part of the Maastrichtian-Palaeocene Saharan Epeiric Sea. *Journal of Foraminiferal Research*, 8 (4), pp. 303–313.
- Petters, S. W. (1981): Stratigraphy of Chad and Iullemmeden Basins. *Eclogae Geologicae Helvetia*, 74 (1), pp. 139–159.
- Petters, S. W. (1982): Central West African Cretaceous-Tertiary benthic foraminifera and stratigraphy. *Palaeontographica Abt. A*, 179, pp. 1–104.
- Reyment, R. A. & Dingle, R. V., (1987): Paleogeography of Africa during Cretaceous period: *Palaeogeography, Palaeoclimatology and Palaeoecology*, 59, pp. 93–116.
- Reyment, R. A. & Tait, E. A. (1972): Biostratigraphical dating of the early history of the South Atlantic Ocean. *Philosophical Transactions of the Royal Society of London. Series B, Biological Sciences*. 858), pp. 55–95.
- Rull, V. (1997). Oligo-Miocene Palynology of the Rio Chama sequence (Western Venezuela), with comments on fossil algae as paleoenvironmental indicators, *Palynology*, 21, pp. 213–229.
- Salard-Cheboldaeff, M. (1990): Intertropical African palynostratigraphy from Cretaceous to Late Quaternary times. *Journal of African Earth Sciences*, 11, pp. 1–24.
- Schrank, E. (1991): Mesozoic palynology and continental sediments in NE Africa (Egypt and Sudan): A review. *Journal of African Earth Sciences*, 12, pp. 363–373.
- Vadjda-Santivanez, V. (1998): Cretaceous palynofloras from Southern Scandinavia: *Lund Publications in Geology*, 1, 35, pp. 1–24.



# Textural and bitumen saturation analyses of tar sand deposits in Southwestern Nigeria

## Analiza teksture in nasičenosti z bitumnom v nahajališčih naftnega peska v jugozahodni Nigeriji

A. Akinmosin<sup>1,\*</sup>, A. O. Adelaja<sup>2</sup>

<sup>1</sup>University of Lagos, Geosciences Department, Nigeria

<sup>2</sup>Olabisi Onabanjo University, Department of Earth Sciences, Ago-Iwoye, Nigeria

\*Corresponding author. E-mail: waleakinmosin2001@yahoo.com

### Abstract

The sedimentological properties of tar sand deposits in Idiobilayo and Ajegunle areas of Southwestern Nigeria were studied with the aim of determining the sub-surface occurrence and reservoir properties of tar sand horizons. Altogether, twenty seven tar sand samples were for textural and bitumen saturation analyses.

Results of the textural analysis showed that the sub-surface tar samples are mainly very coarse grained, angular to sub-angular and poorly sorted, which shows that the sediments have not been transported far from the source. The surface samples are medium-grained sands, sub-angular to sub-rounded, and are moderately sorted implying that the sands have undergone a fairly long transportation history.

The textural and morphological characteristics of the surface sands show that they have been transported and deposited by currents of moderate energy, probably streams.

Results of bitumen saturation analysis revealed that the average percentage weight of bitumen in the deeper horizons is 25 %, while that of the shallow horizon is 22 %.

The medium-grained and moderately sorted characteristics of analysed tar sands together with low fine particles.

**Key words:** Bitumen, saturation, textural, reservoir, surface and subsurface.

### Izveleček

Namen preučevanja sedimentoloških značilnosti nahajališč naftnega peska na področjih Idiobilayo in Ajegunle v jugozahodni Nigeriji je bil opredeliti podzemno razširjenost in rezervoarne lastnosti horizontov tega peska. V raziskavo teksture in nasičenosti z bitumnom je bilo zajetih 27 vzorcev naftnega peska.

Rezultati teksturne analize kažejo, da so globlje ležeči peski večinoma zelo debelozrnati, zrna so oglata do zmerno oglata in slabo sortirana, kar nakazuje kratek transport sedimenta od izvirnega področja. Vzorci s površine pripadajo srednjezrnatim peskom s fragmenti, ki so zmerno oglati do zmerno zaobljeni in zmerno sortirani, kar priča o dokaj dolgem transportu.

Teksturne in morfološke značilnosti površinskih peskov nakazujejo transport in sedimentacijo iz vodnih tokov srednje energije, najbrž rek.

Rezultati analize nasičenosti z bitumnom kažejo v globljih nivojih povprečno 25 % in v plitvejših 22 % bitumna.

**Ključne besede:** bitumen, nasičenost, tekstura, rezervoar, površina in globina

## Introduction

Asphalt impregnated sandstones, otherwise referred to as oil sand (tar sand) and active oil seepages occur in southwestern Nigeria within the Eastern Dahomey (Benin) basin, a marginal pull apart (Klemme, 1975) or marginal sag (Kingston et al., 1983) basin. The oil sand outcrops in an E-W belt, approximately 120 km long and 4–6 km wide, extending from Edo/Ondo-Ogun States (Enu, 1985).

Occurrence of the seepage and tar sand deposit over the Okitipupa ridge in the Dahomey basin provided the initial impetus for oil exploration in Nigeria. From the turn of the century to date, no less than fifteen groups comprising public and private ventures have shown varying degrees of interest. Arising from these, a total of one hundred and fifteen (115) boreholes have been drilled across the basin and have confirmed the presence of oil sands and heavy oil. An intense investigation by Ako et al., (1980) was conducted over an area of 17 km<sup>2</sup>, just north of Agbabu village and this particular study has provided a vast amount of information on the oil sand deposits.

The physico-chemical characteristics of the tar sands from outcrops and drillholes in the Agbabu/Ore areas in Ondo state have been extensively reported. The salient aspects of the comprehensive information published within the last two decades covering sedimentological properties, oil saturation, bitumen ultimate analysis, stock-tank properties, calorific values, etc have been published by Adegoke et al. (1980), Oshinowo et al. (1982), Oluwole et al. (1985), Ekweozor & Nwachukwu (1989); Akinmosin et al. (2005 and 2006).

Studies carried out on the series of outcrop sections, cores and drilled cuttings obtained from the various exploration campaigns at the northwestern flank of the belt have shown presence of two horizon-bearing sediments designed as horizons "X" and "Y" (Figure 1). "The X-horizon", being the shallower of the two, constitutes a prominent outcropping unit in most areas, though significantly eroded in the north western part of the basin. The thickness varies from 9 m to about 22 m, with an average of 15 m.

The Y-horizon is a prominent outcropping sequence in the northwestern part of the basin

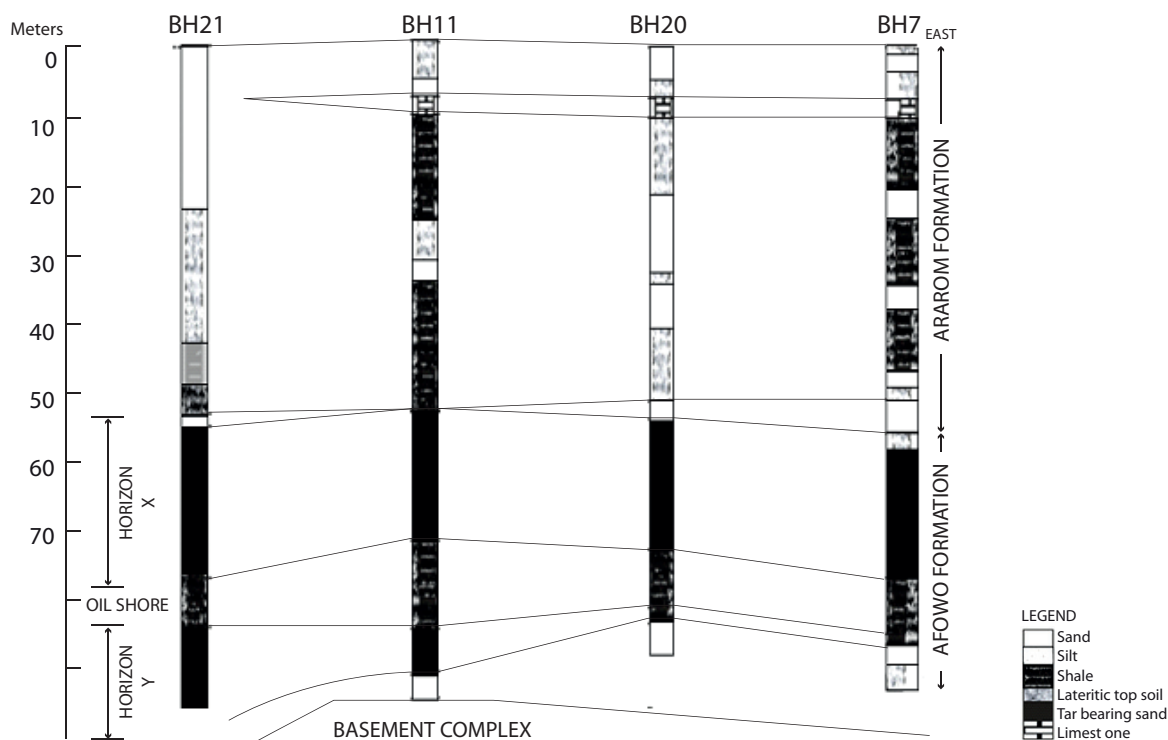


**Figure 1:** Schematic geological east-west cross-section based on drillholes showing the stratigraphic position of horizon containing tar sands horizons in some boreholes (modified from Ekweozor and Nwachukwu, 1989).

where “X horizon” has been largely eroded. Thickness of Y-horizon varies from 3 m in the east to 22.6 m in the west with an average of about 12 m.

For better understanding of the properties of the Nigerian tar sands, the present work focused on the north eastern flank of the belt to evaluate the textural properties of both surface and subsurface deposits. There are four core holes used for this study, these are coded as A4, A14, A15 and A16.

## Geology of the dahomey basin

The study area lies within longitude 004°33' E to 004°35' E and latitude 06°37' N to 06°39' N, Figure 2.

The Benin (Dahomey) Basin is a part of the system of the West African peri-cratonic (margin sag) basin (Klemme, 1975; Kingston et al., 1983) developed during the commencement of rifting, associated with the opening of the Gulf of Guinea, in the Late Jurassic to the Early Cretaceous (Burke et al., 1971; Whiteman, 1982). The crustal separation, typically preceded by

crustal thinning, was accompanied by an extended period of thermally induced basin subsidence through the Middle – Upper Cretaceous to Tertiary times as the South American and the African plates entered a drift phase to accommodate the emerging Atlantic Ocean (Storey, 1995; Mpanda, 1997).

The Ghana Ridge, presumably an offset extension of the Romanche Fracture Zone, confines the basin in the west while the Benin Hinge Line, a Basement escarpment which separates the Okitipupa Structure from the Niger Delta basin, confines it in the east.

The onshore part of the basin covers a broad arc-shaped profile of about 600 km<sup>2</sup> in extent. The onshore section of the basin attains a maximum width, along its N-S axis, around 130 km in the proximity of the border between Nigeria – Republic of Benin. The basin narrows to about 50 km on the eastern side where the basement assumes a convex upwards outline with concomitant thinning of sediments. The lithostratigraphic units of the Cretaceous to Tertiary sedimentary succession of the eastern margin of Dahomey basin according to Idowu et al. (1993), are summarized in Table 1.

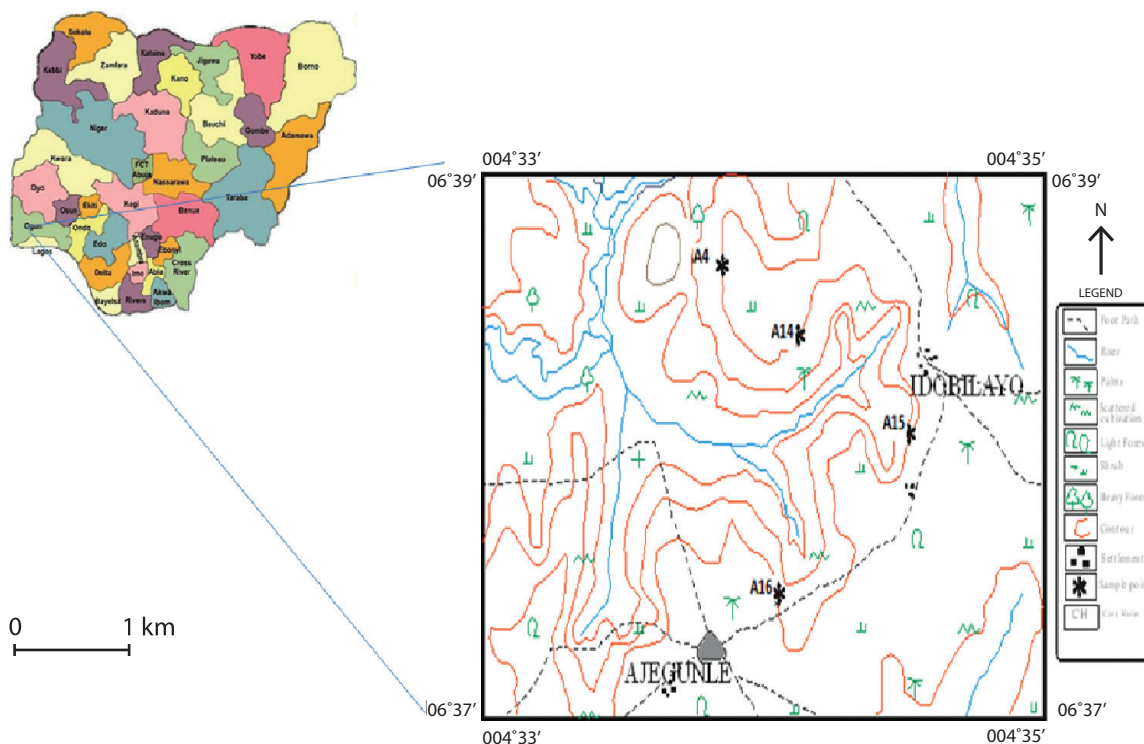


**Figure 2:** Topographical map of the study area showing sampling points.

**Table 1:** Overview of Cretaceous and Tertiary Formations of the Eastern Dahomey Basin (After Idowu et al., 1993)

Age		Formation		Lithology	
		Ako et al., 1980	Omatsola & Adegoke, 1981		
Tertiary	Eocene	Ilaro Formation	Ilaro Formation	Sandstone	
	Paleocene	Oshosun Formation	Oshosun Formation	Shale	
		Ewekoro Formation	Ewekoro Formation	Limestone	
Cretaceous	Maastrichtian		Abeokuta Group	Araromi Formation	Shale
	Turonian			Afowo Formation	Sandstone/shale
	Berremian			Ise Formation	Sandstone

## Materials and Methods

### Description of tar horizons from the drillcores

- Core hole A4: two 9 m and 6 m tar horizons were identified from core logging analysis at the depths of 75.10–84.10 m and 87.10–93.10 m. They are thick respectively. Samples within the tar horizons were taken every 1.5 m. Ten samples were collected altogether.
- Core hole A14: a 6 m thick tar horizon was identified at a depth of 27 m to 33 m. Four samples at interval of 1.5 m were collected.
- Core hole A15: similar to the drillcore A4, two tar horizons were identified at the depths of 18–21 m and 27–30 m, each of them being 3 m thick. Four samples at 1.5 m interval were collected.
- Core hole A16: 3 m thick tar horizon was identified at a depth of 9–12 m. Two samples were collected 1.5 m apart from each other.

Twenty-seven samples of Tar sand (twenty drillcore samples and seven shallow samples) were collected and used for this study around Ajegunle and Idiopopo areas of Southwestern Nigeria (Figure 2).

### Preparation of samples for textural and bitumen saturation analyses

For textural analysis, after cleaning and drying, 100 g were dry-seived using vibrating sieving machine for 15 min with sieves of the following mesh sizes 2.00 mm, 0.180 mm, 0.125 mm, 0.075 mm which are equivalent to (1.00, 1–25, 2.50, 3.00 and 3.75) mm phi values respectively.

The individual and cumulative weights, with their percentages were determined. These data were used to plot histogram and cumulative frequency curve for individual sample on arithmetic and semi-log graphs.

The parameters were computed by using moment statements mean, mode, standard deviation, kurtosis, and skewness (using formulae by Folk & Ward, 1957).

For bitumen saturation analysis, ten grams of each sample were put into a measuring cylinder with toluene for about 180 min. The samples were afterwards washed and decanted, and the procedure was repeated until the samples were clean of bitumen. The washed samples were air dried and re-weighed. The new weights were noted, recorded and subtracted from the initial weights. The difference in weight were converted to percentage and recorded.

Figures 3, 4, 5, 6 are showing lithologies of the respective drill holes.

## Results and Discussion

### Bitumen saturation

The analysis carried out on both the subsurface and surface samples revealed that the weight percentage of bitumen in the subsurface samples ranged between 12 % and 47 % with an average bitumen saturation of 27.14 % while that of The weight percentage of bitumen in surface samples lower, with a range between 16 % and 29 % and an average saturation of 22 % (Table 2). This is a little low compared to the Athasbasca oil – sands in Canada (41 %)

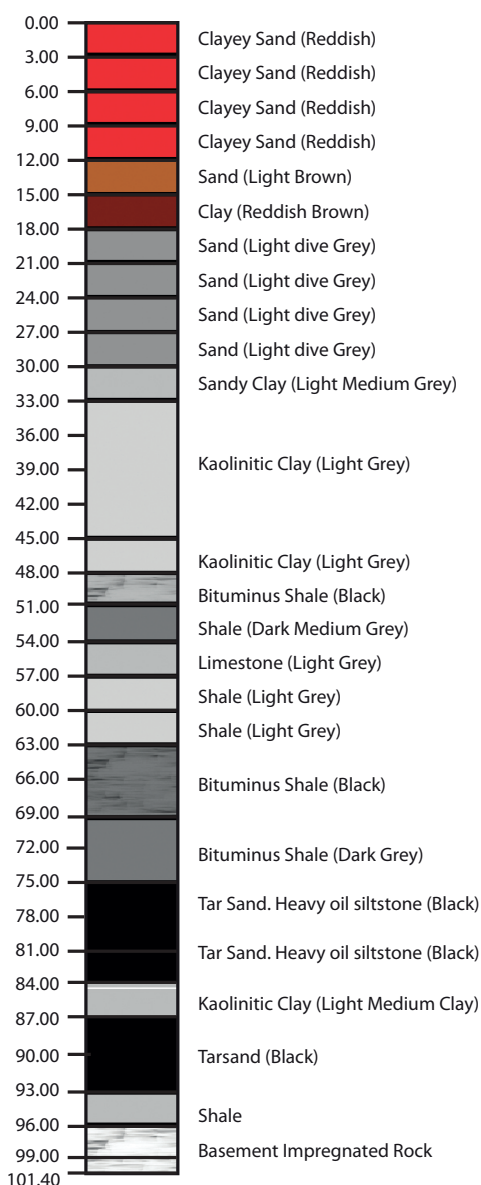


Figure 3: Lithological units of the drill hole A4.

and the Eastern Venezuela deposit (48 %; Tissot and Weite, 1984). According to Coker, (1988), tar sands with bitumen saturation above mass fraction 10 % (or above volume fraction 19.2 %) is classified as bitumen-rich sands. Based on analyses of both, surface and sub-surface deposits of the Nigerian tar sands can be categorized as rich in bitumen.

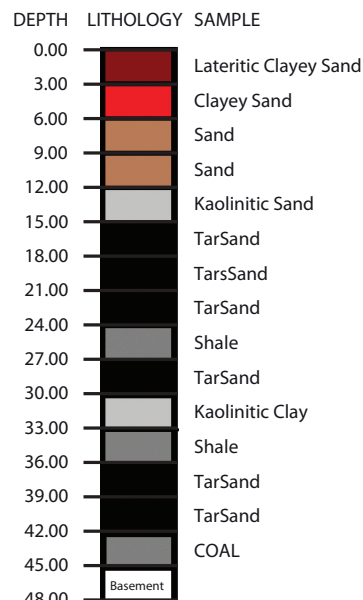


Figure 4: Lithological units of the drill hole A14.

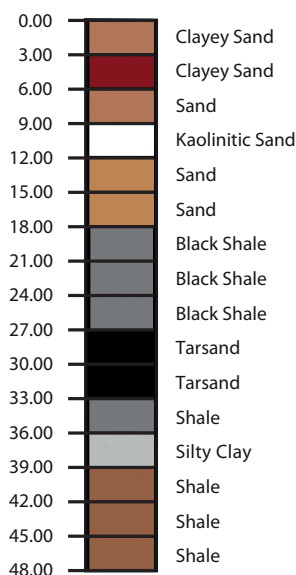


Figure 5: Lithological units of the drill hole A15.

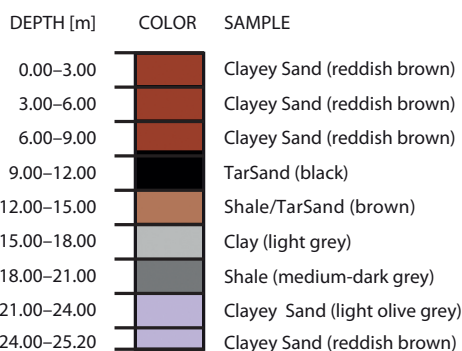


Figure 6: Lithological units of the drill hole A16.

### Textural analysis

Mean results for textural analysis carried out on the twenty (20) subsurface samples and seven (7) surface samples are shown in Tables 3 and 4.

Average bitumen saturation for subsurface samples is (24.83 %) with a ranges between 12 % and 41 %, while average bitumen saturation for surface samples is (22 %) with a ranges between 16 % and 29 %.

**Table 2:** Bitumen saturation

Subsurface Sample Code/ Depth (m):	Number of samples	Mass fraction of tar (w/%)	Surface Sample	Number of samples	Mass fraction of tar (w/%)
A4: 75.10–84.10	6	12	A1	1	22
A4: 87.10–93.10	4	31	B2	1	21
A14: 27–33	4	41	E1	1	29
A15: 18–21	2	26	F4	1	16
A15: 27–30	2	25	M1	1	20
A16: 9–12	2	14	O5	1	21
			P3	1	25

**Table 3:** Summary of textural analysis result for both surface and subsurface tar sand samples

Sample Description: Subsurface Samples Code/ Depth (m):	Mean	Skewness	Kurtosis	Standard Deviation
A4: 75.10–84.10	-0.7	-0.174	1.087	1.920 8
A4: 87.10–93.10	0.783	0.289	0.947	2.654 2
A14: 27–33	0.08	0.258	1.238	0.970 8
A15: 18–21	-0.737	-0.412	0.912	2.275 0
A15: 27–30	-0.26	-0.342	1.022	2.317 0
A16: 9–12	0.23	0.100	0.810	2.858 0
<b>Average:</b>	<b>-0.199</b>	<b>-0.0814</b>	<b>1.002</b>	<b>2.186</b>
Surface Samples:				
A1	0.76	-0.11	1.04	-0.78
B2	1.99	0.55	1.01	0.50
E1	1.43	-0.03	1.05	1.03
F4	1.48	-0.09	1.20	0.54
M1	0.55	0.01	1.15	0.71
O5	0.42	-0.07	2.26	1.1
P3	1.27	0.10	0.91	1.46
<b>Average:</b>	<b>1.13</b>	<b>0.05</b>	<b>1.23</b>	<b>0.65</b>

**Table 4:** Interpretation of statistical parameters of both surface and subsurface tar sand samples

Sample Description: Subsurface Samples Code/ Depth (m):	Bitumen Saturation	Mean	Skewness	Kurtosis	Standard Deviation
A4: 75.10–84.10	12 %	Very Coarse Grained sands	Coarse Skewed	Very Leptokurtic	Poorly sorted
A4: 87.10–93.10	31 %	Coarse grained sands	Fine Skewed	Mesokurtic	Very Poorly sorted
A14: 27–33	41 %	Coarse grained sands	Fine Skewed	Leptokurtic	Moderately sorted
A15: 18–21	26 %	Very Coarse Grained Sand	Strongly Skewed	Mesokurtic	Very poorly sorted
A15: 27–30	25 %	Very Coarse Grained Sand	Strongly Skewed	Mesokurtic	Very poorly sorted
A16: 9–12	14 %	Coarse Grained Sand	Fine Skewed	Platykurtic	Very poorly sorted
<b>Average:</b>	<b>24.83 %</b>	<b>Very Coarse Grained sands</b>	<b>Near Symmetrical</b>	<b>Mesokurtic</b>	<b>Very poorly sorted</b>
<b>Surface Samples:</b>					
A1	22	Medium Grained Sand	Near Symmetrical	Mesokurtic	Moderately sorted
B2	21	Fine Grained Sand	Near Symmetrical	Mesokurtic	Very well sorted
E1	29	Fine Grained Sand	Near Symmetrical	Mesokurtic	Moderately sorted
F4	16	Fine Grained Sand	Near Symmetrical	Leptokurtic	Moderately sorted
M1	20	Medium Grained Sand	Near Symmetrical	Leptokurtic	Moderately sorted
O5	21	Medium Grained Sand	Near Symmetrical	Very Leptokurtic	Poorly sorted
P3	25	Fine Grained Sand	Fine Skewed	Mesokurtic	Poorly sorted
<b>Average:</b>	<b>22</b>	<b>Medium Grained Sand</b>	<b>Near Symmetrical</b>	<b>Leptokurtic</b>	<b>Moderately well sorted</b>

## Conclusions

The bitumen saturation and textural analyses show that subsurface samples contain coarse-grained sand and surface samples medium-grained sand. The textural and morphological characteristics of the subsurface sands indicate transportation and deposition by currents of moderate energy, probably streams. Histogram distribution plots and frequency distribution curves indicate a unimodal source for sediments

of the surface samples. Medium grain-size of surface samples, their moderate sorting, and low content of fine grains suggest that Afowo oil sands reservoir will be of good quality. The percentage weight of bitumen in the subsurface sample ranges between 12 % and 41 %, with an average saturation of 25 % while that of the surface sample ranges between 16 % and 29 %, with an average saturation of 22 %. Bitumen saturation of analysed sands is lower in comparison to the Athasbasca oil-sands deposits in

Canada (mass fraction 41 %) and the Eastern Venezuela deposit (mass fraction 48 %; Tissot & Weite, 1984). Nevertheless, according to the classification of Coker (1988), this saturation however, the Nigerian tar sands can still be classified as tar-rich sands.

## References

- Adegoke, O. S., Ako, B. D., Enu, E. I. (1980): Geotechnical Investigations of the Ondo State bituminous sands. *Geology and Reserves Estimate*, Unpub. Rept., Geological Consultancy Unit, Department of Geology, University of Ile-Ife, Vol. 1, pp. 257.
- Akinmosin, A., Olabode, O. T. & Bassey, C. E. (2005): Provenance study of Bituminous sands in Eastern Dahomey Basin, Southwestern Nigeria, Based on Heavy mineral and Quartz varieties. *Ife Journal of Science*; Vol. 7, No. 1.
- Akinmosin, A., Oreddein, O. S. & Odewande, A. A. (2006): Sedimentological And Reservoir Description of Afowo Oil Sand Deposits, Southwestern Nigeria. *Ife Journal of Science*, Vol. 8, No. 1.
- Ako, B. D., Adegoke, O. S. & Peter, S. W. (1980): Stratigraphy of the Oshosun Formation in Southwestern Nigeria. *Jour. Min. Geol.*; Vol. 17, pp. 9–106.
- Bilman, H. G. (1992): Offshore Stratigraphy and Paleontology of the Dahomey (Benin) Embayment, West Africa. *NAPE Bull.*, Vol. 7, No. 2 pp. 121–130.
- Burke, K. C. B., Dessauvagine, T. F. J., Whiteman, A. J. (1971): The opening of the Gulf of Guinea and Geological History of the Benue Depression and Niger Delta. *Nature Phys. Sci.*, 233 (38), 51–55.
- Coker, S. J. L. (1988): Some Aspects of the Geology of the Bituminous Sands of Parts of the Benin Basin. *Nig. Min. and Geosc. Soc.*, 19, pp. 121.
- Ekweozor, C. M. (1986): Characteristic of the non-asphaltene products of mild chemical degradation of asphaltenes. *Org. Geochem.*, 10, 1053–1058.
- Ekweozor, C. M. & Nwachukwu, J. L. (1989): The origin of tar sands of SouthWestern Nigeria. *N.A.P.E. Bull.*, Vol. 4, No. 2, pp. 82–84.
- Enu, E. I. (1985): Textural characteristic of the Nigerian Tar Sands. *Sedimentary Geology*. Vol. 44, pp. 65–81.
- Folk, R. L. & Ward, W. C. (1959): Bravo River Bar: A Study of the Significant of Grain Size Parameter. *Journ. Sed. Petrol.* 41, 45–1058.
- Idowu, J. O., Ajiboye, S. A., Ilesanmi, M. A. & Tanimola, A., (1993): Origin and significance of organic matter of Oshosun Formation, Southwestern Nigeria. *Jour. Min. Geol.* Vol. 29, pp. 9–17.
- Kingston, D. R., Dishroon, C. P. & Williams, P. A. (1983): Global Basin Classification System. *AAPG. Bull.*, Vol. 67, pp. 2175–2193.
- Klemme, H. D. (1975): Geothermal Gradients, Heatflow and Hydrocarbon Recovery. In: A.G. Fischer and S. Judson (eds), *Petroleum and Global Tectonics*. Princeton, New Jersey, Princeton Univ. Press, pp. 251–304.
- Mpanda, S. (1997): Geological development of east African coastal basin of Tanzania. *Acta Universities, Stockholmiensis*; Vol. 45, pp. 121.
- Oluwole, A. F., Adegoke, O. S., Kehinde, L. O., Nwachukwu, J. I., Coker, S. J. L., Wallace, D., Asubiojo, O. I. & Ogunsola, O. (1985): Nigerian Tar Sands. In: *Proceedings of 3rd Intern. California*, Chap. 33, pp. 373–379.
- Omatsola, M. A. & Adegoke, O. S. (1981): Tectonic evolution and Cretaceous stratigraphy of the Dahomey Basin. *J. min. Geol.*; Vol. 18, No. 1, pp. 130–137.
- Oshinowo, T., Ademodi, B. & Adeniran, S. A. (1982): Bituminous Tar Sands Of Nigeria: Analysis of Oils – Parts I. *Journal of the Nigerian Soc. Of Chemical Engineers*; Vol., No. 1, pp. 44–46.
- Storey, B. C. (1995): The role of mantle plumes in continental break-up, case history from Gondwanaland nature V. 377, pp. 301–308.
- Tissot, B. P. & Welte, D. H. (1984): *Petroleum Formation and Occurrence*. Second Ed. Springer – Verlag, Berlin.
- Whiteman, A. J. (1982): *Nigeria: Its Petroleum Geology, Resources and Potential*, Vol. 2, Graham and Trontman, London.

# Geochemical evaluation of the Pan-African pegmatites from parts of Oban massif, Southeast Nigeria

## Geokemična preiskava panafriških pegmatitov iz delov Obanskega masiva v jugovzhodni Nigeriji

M. I. Oden<sup>1,\*</sup>, E. E. Igonor<sup>2</sup>, E. E. Ukwang<sup>1</sup>

<sup>1</sup>Department of Geology, University of Calabar, Nigeria

<sup>2</sup>Petra Prospectors Limited, Nigeria

\*Corresponding author. E-mail: odenmi@yahoo.com

### Abstract

About 40 pegmatites exposures hosted by the metamorphic (schists and gneisses) and igneous rock unit (porphyritic and non-porphyritic granodiorites), which characterize the area were investigated and representative samples analyzed for geochemical characterization. Macroscopic study shows large crystals of schorls, albite, plagioclase and quartz. Geochemical analysis carried out at the Activation Laboratory – Canada, shows the pegmatites to be peraluminous from estimated Aluminium Saturation Index (ASI) which is greater than one (1). Variation plot of  $\text{Na}_2\text{O} + \text{K}_2\text{O}$  vs.  $\text{SiO}_2$  classifies the rocks as alkali to sub-alkalic types.  $\text{SiO}_2$  and  $\text{Al}_2\text{O}_3$  values which averages at 67.74 % and 14.49 % respectively are lower when compared to pegmatites from similar fields in other parts of the country. But they are richer in  $\text{Fe}_2\text{O}_3$  with an average value of 4.16 %. Trace elements such as Ba, Sr, Zr, Rb, Ta, and Nb have average concentrations of (71.15, 27.50, 16.61, 344.70, 18.14, and 71.70) ppm respectively. While the ratios K/Ba, and K/Cs have very high average values of 430.43 and 1291.30 respectively. These extremely high values suggest that these pegmatites are barren and un-mineralized. Further discrimination using various standard ratios and variation plots for rare-metal mineralization indicates a poor level of mineralization for the Iwurupegmatites, while those of Igbofia and Akwa-Ibami shows very low degree of mineralization especially with respect to Ta-Nb.

**Key words:** Mineralization, Rare-metal, Southeastern Nigeria

### Izvleček

Za geokemično opredelitev smo preiskali kakih 40 izdankov pegmatitov iz metamorfnih (kristalni skrilačci in gnajsi) in magmatskih (porfiritski in neporfiritski granodioriti) kamninskih enot, značilnih za to območje, in analizirali reprezentativne vzorce. Makroskopsko so opazni veliki kristali šorlitov, albite, plagioklaza in kremenca. Geokemične analize, ki so jih opravili v Activation Laboratory v Kanadi, pričajo o peraluminjskem značaju pegmatitov, kar kaže ugotovljena vrednost indeksa nasičenosti aluminija (ASI), ki je večja od enote <sup>(1)</sup>. Variacijski diagram  $\text{Na}_2\text{O} + \text{K}_2\text{O}$  glede na  $\text{SiO}_2$  uvršča kamnine med alkalijske do subalkalijske tipe. Vsebnosti  $\text{SiO}_2$  in  $\text{Al}_2\text{O}_3$  s povprečjema 67,74 % in 14,49 % so nižje v primerjavi s tistimi za pegmatite podobnih območij iz drugih delov države. Vsebujejo pa več  $\text{Fe}_2\text{O}_3$  s povprečjem 4,16 %. Sledne prvine kot Ba, Sr, Zr, Rb, Ta in Nb imajo po vrsti naslednje povprečne koncentracije: (7,15, 27,50, 16,61, 344,70, 18,14 in 70) ppm. Razmerji K/Ba in K/Cs imata zelo visoki povprečji, in sicer 430,43 in 1291,30. Te izjemno visoke vrednosti pričajo o tem, da so pegmatiti jalovi, neorudeni. Nadaljnje razvrščanje na osnovi raznih standardnih razmerij in variacijskih diagramov orudenja z redkimi kovinami nakazuje nizko raven orudenja za pegmatite območja Iwuru in zelo nizko raven orudenja za pegmatite območij Igbofia in Akwa-Ibami, zlasti kar zadeva Ta-Nb.

**Ključne besede:** orudenje, redke kovine, jugovzhodna Nigerija



ies in Nigeria from which he recognized and defined 7 broad fields of the Precambrian rare-metals pegmatites of Nigeria. This study aims at evaluating and classifying the pegmatites of the study area, and their economic importance based on geo-chemical characteristics.

The pegmatites found within the metamorphic terrain have undergone a high degree of weathering, but the granodiorites and the pegmatites intruding the metamorphic rocks, which are the host rocks, were not deformed. The pegmatites of southeast Nigeria, which originate either from the cooling of the granodiorites or from the metamorphism and anatexis of country rocks, has been dated as rocks formed between 600 ma and 530 ma (Matheis and Caen-Vanchete, 1983). Ekwueme, (1989), further showed that they were emplaced as syn-collisional and volcanic arc granites. From hand specimen, the general mineralogy of the pegmatites can be summed up as quartz + feldspar (orthoclase and albite) + biotite + muscovite + tourmaline and other accessory minerals. Books of muscovite and graphic growth of quartz plus feldspar are mostly seen in samples of Iwuru area, while the Akwa-Ibami area is dominated by random crystals of schorls which could be as much as 30–40 % in the mode. Associated minerals such as tin, tourmaline, and beryl have been reported by the locals to have been mined in the past from both areas. Petrographic studies have been detailed in Raeburn, (1927), and Igonor, et al., (2010). Ekwueme and Matheis (1995) have shown with strong evidence that the pegmatites and older granites of southeast Nigeria are closely related, that in fact the pegmatites are derived from the cooling of the granodiorites and hence both rock types have a common petrogenetic origin. Similarly, the pegmatites of the metamorphic rock unit were suggested to have been formed from facies metamorphism and anatexis of country rock (Ekwueme, 1990).

## Materials and methods

The area of study (Igbofia-Akwa-Ibami-Iwuru) is located between latitudes 5°20' N to 5°27' N and longitudes 8°09' E to 8°18' E, in the western region of the Oban massif, southeastern Nigeria

(Figure 1). This area is characterized by thick forestation, highly undulating topography, with several stream channels. All these make accessibility remote and difficult.

Geologic mapping was undertaken to study the various lithological units of the study area (Oban massif) with special interest in the pegmatite veins occurring in the area. The structural orientation and physical characteristics of the veins were observed. These pegmatite occurrences, which cover an area extent of approximately 230 km<sup>2</sup> exceeds about 50 outcrop bodies, out of which about 40 were sampled and representative samples collected for further studies and geochemical analyses. 12 composite samples, which are representative of the pegmatites and their host rocks were taken for further geochemical analysis. Pulverized whole rock samples and extracted mineral content (muscovite flakes) were analyzed for major oxides and trace element contents at the Activation Laboratories, LTD., Canada using the ICP-MS analytical method. The method has a minimum detection limit of about 0.01 % for the major oxides and between 0.05–5 ppm in the trace and rare-earth elements. Acquired geochemical data were interpreted using simple computer software programme (Microsoft Excel 2007) based on established standard procedures by authors in pegmatite geochemistry.

## Results and discussion

Pegmatites occur in several locations in the area of study. They outcrop mostly as veins or as giant outcrops reaching a height of more than 5 m. This is probably because the host rocks (most likely schist) have been weathered away leaving behind the more resistant pegmatite vein. The most preferred orientation trend for these veins is the NNW – SSE, which is between 140° and 170°. Also these pegmatites occur in high angle structures as over 94 % have dip values greater or equal to 50° (Oden, 2010). These rocks, which are either hydrothermal injections or formed from facies metamorphism and anatexis of country rock (Ekwueme, 1990) are distributed across the entire study area and are hosted by two main rock units. And these are the metamorphic (schists and gneisses)

and the igneous (granodiorite) rocks. Detailed description of these host rocks have been described by Ekwueme, (1989); Theresa and Ekwueme, (1996); and Igonor et al., (2010) among others.

The pegmatite veins range in exposed length from about 1.5 m to 20 m and width of between 0.2 m and 8.4 m. The pegmatites are generally coarse grained with large crystal grains of representative minerals visible in hand specimen. Quartz grains range from about 1 cm × 2 cm to greater than 2 cm × 3 cm, while black tourmaline (schorl) of more than 4 cm in length is sometimes present. Variation in mineral composition of the pegmatite results in the various shades of colour observed in the pegmatites. Where orthoclase and/or albite is dominant, the colour is pinkish to white, while dense amount of schorl + biotite results in a dark-coloured rock type. The Akwa-Ibami area is characterized by a higher degree of weathering and deformation of host rock, massive ridges (up to 200 m × 20 m) and veins of pegmatites are undeformed and generally trending in the NE-

SW direction. Undeformed veins and dykes that are not too extensive and protected by their host (granodiorites) from intensive weathering characterize the Igbofia area. Aplitic dykes are associated with the pegmatites of Igbofia and Iwuru area which is a common feature of granitic pegmatites. Similarly, the Igbofia and Iwuru pegmatites run conformably with the general structural trend of the host rocks in the study area, that is, NE-SW. Some of these pegmatite veins trend in the NW-SE direction.

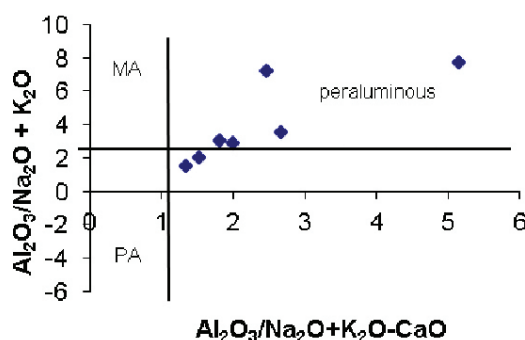


**Figure 2:** Plot of  $Al_2O_3/(Na_2O + K_2O)$  vs  $Al_2O_3/(Na_2O + K_2O - CaO)$  showing the peraluminous nature of the pegmatites from study area (after Maniar and Piccoli, 1989).

**Table 1:** Major oxides compositions of pegmatites of parts of Oban massif (south eastern Nigeria)

Oxides Wt %	T1	T2	T3	T4	T5	T6	T7	T8
	<b>Igbofia pegmatites</b>		<b>Akwalbami pegmatites</b>			<b>Iwuru pegmatites</b>		
SiO <sub>2</sub>	73.01	71.58	69.10	67.60	69.50	72.89	73.01	53.05
TiO <sub>2</sub>	0.04	0.18	0.04	0.07	0.19	0.06	0.07	1.66
Al <sub>2</sub> O <sub>3</sub>	16.01	15.00	14.00	15.50	14.50	12.01	12.00	16.89
Fe <sub>2</sub> O <sub>3</sub>	4.98	5.09	2.50	1.40	2.98	2.50	2.10	15.70
MnO	0.02	0.04	0.05	0.07	0.09	0.05	0.02	0.08
MgO	1.53	1.10	1.65	0.17	1.04	0.19	2.11	2.10
CaO	1.04	4.49	1.35	3.17	3.73	2.47	2.17	2.03
Na <sub>2</sub> O	0.10	0.14	0.18	0.07	0.09	0.29	0.11	0.02
K <sub>2</sub> O	3.01	0.65	10.04	11.12	5.57	6.28	5.89	6.32
P <sub>2</sub> O <sub>5</sub>	ND	ND	ND	ND	ND	ND	ND	ND
Total	100.27	99.81	99.86	99.61	99.99	98.70	99.04	99.94
<b>MAI</b>	<b>negative</b>		<b>positive</b>			<b>positive</b>		

N.B: T1, T2 – average of samples from Igbofia area; T3, T4, T5 – average of samples from Akwa Ibami area; T6, T7, T8 – average of samples from Iwuru area. T5 and T8 are muscovite extracts. Average values are of five samples in each case; MAI = Modified-Alkali-Lime-Index. ND – not detected.

Results of the major oxide geochemistry of the pegmatites from study area are as shown in Table 1. The results show that Igbofiapegmatites are the most siliceous and aluminous, while Iwurupegmatites are the poorest in  $\text{SiO}_2$  and Cabut richer in Fe. Generally, the pegmatites are high in aluminous content and are seen to be peraluminous (Figure 2). But Iwuru pegmatite is relatively slightly depleted in alumina content. Based on the high silica and alkali plus low CaO content, the pegmatites of Akwalbami and Iwuru area, are more granitic in composition, while the Igbofia area tends towards granodioritic composition because of their high silica, CaO, MgO, and low alkali content. The areas have a reasonably high Fe-number ranging between 0.66 and 0.77. The calculated Modified-Alkali-Lime-Index (MALI) shows positive values for both Akwalbami and Iwuru areas, while it is negative for the Igbofia group with a narrow range.

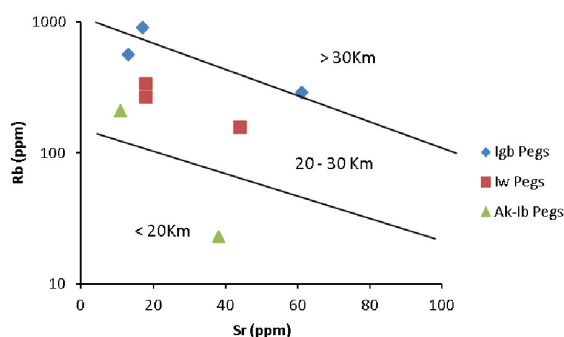


**Figure 4:** Plot of Rb vs Sr showing the likely depth of origin for the pegmatites of study area (after Brown et al., 1979).

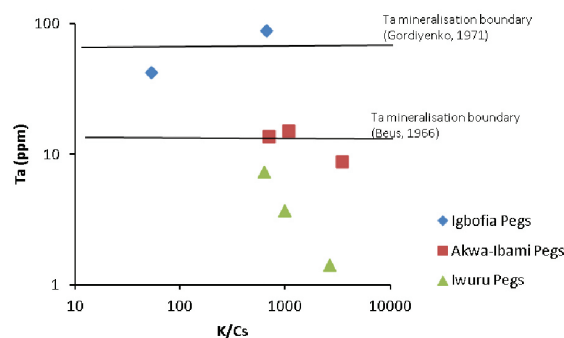


**Figure 5:** Plots of Ta vs K/Cs of pegmatites from study area (after Beus, 1966 and Gordiyenko, 1971).

Table 2 shows values of trace elements and elemental ratios for the pegmatites from study area. This shows selected trace elements such

as Ba, Sr, Zr, Rb, Ta, Nb and Cs having average concentrations of 71.15 ppm, 27.5 ppm, 16.61 ppm, 344.7 ppm, 18.14 ppm, 71.7 ppm and 24.5 ppm respectively. Trace element ratios of K/Ba and K/Cs have very high average values of 430.43 and 1291.30 while Ta:Cs ratio is far below 10 for all samples.

According to Frost et al., (2001), a reason these rocks are peraluminous could be as a result of the parent melt having another aluminous phase present, which could be aluminous biotite or muscovite, garnet or an  $\text{Al}_2\text{O}_5$  polymorph. Also Miller, (1985) believes that such rocks could have formed from strongly peraluminous melt which was derived from the melting of biotite bearing metaluminous felsic rocks.

According to Ekwueme and Matheis, (1995) it is inferred that the magma which produced these pegmatites must have been alkaline in nature hence the high alkali content of these pegmatites.

The high Fe-number of the pegmatites probably reflects a high modal proportion of a ferromagnesian mineral e.g. biotite (Frost et al., 2001). And the narrow range in the Fe-number values signifies similarity in source rock composition and or nearness in degree of melting undergone by rocks (Patino and Beard, 1996; Nabelek et al., 1991). Similarly, the narrow range in MALI supports the theory of similar parent source for the pegmatites of the study area (Frost et al., 2001).

The moderately high values of Cs indicate moderately high alkali metal fractionation (Cerny, 1982, 1989). Ta:Nb ratio ranges between 0.1 to 0.41. This suggests a preference for possible Nb enrichment. But Ta and Nb values are obviously too low for any profitable mineralization in tantalum and or niobium. Also since residual fluids, which form Ta rich pegmatites, are enriched in Ga (Cerny, 1982), the low level of Ga in the pegmatites of study area indicates a near impossibility of Ta mineralization. The higher than normal content of Rb (150 ppm – Taylor, 1965) is indicative that the melts which formed these rocks, have undergone high degree of partial melting of source material. It can be said that the pegmatites of study area, originate from average depth intrusions (20-30 km) since pegmatites originating from deeper intrusions have been shown to have similar low values of

**Table 2:** Trace element and elemental ratio composition of pegmatites of parts of Oban massif, SE Nigeria

Elements (ppm)	T1	T2	T3	T4	T5	T6	T7	T8
Ba	84	23	54	51	168	84	51	118
Rb	212	23	563	914	288	265	337	156
Sr	11	38	13	17	61	18	18	44
Y	1	1	1	4	3	1	1	5
Zr	26	39	3	18	21	8	9	9
Nb	131	259	33	53	38	14	13	32
Th	6	1	1	2	2	5	2	2
Pb	5	12	18	29	14	13	18	16
Ga	37	34	27	42	23	19	23	16
Zn	533	2133	2236	1246	5247	2851	3385	3280
Cu	11	14	18	20	25	20	15	47
Ni	1	5	6	4	8	7	14	15
V	2	4	3	3	17	7	6	18
Cr	7	28	36	20	44	39	36	104
Hf	3	4	0.3	2	2	1	1	0.4
Cs	15	27	13	62	22	9	29	18
Sc	0.3	2	0.4	1	2	0.3	1	2
Ta	53	429	14	15	1	4	7	
Co	1	1	1	1	2	1	3	4
Li	11	56	5	7	73	43	15	118
Be	124	580	5	49	59	11	6	331
K/Ba	500	104	856	847	174	289	575	98
Na/K	7	22	0.8	1	0.27	0.1	1	0.4
Rb/Sr	19	0.6	43	54	5	15	19	4
K/Rb	47	105	82	47	83	92	90	74
K/Cs	667	89	3527	700	1077	2641	997	634
Th/U	2	0.4	0.4	0.3	0.1	1	0.3	1

N.B: T1, T2 – average of samples from Igbofia area; T3, T4, T5 – average of samples from Akwa Ibami area; T6, T7, T8 – average of samples from Iwuru area. T5 and T8 are muscovite extracts. Average values are of five samples in each case.

Zr and aplite area less commonly found in association with them (Cerny, 1992). This fact is further buttressed by the graph of Rb vs Sr (Figure 4). Also the low Zr content is indicative of an almost no crustal derivation. Since these pegmatites have, Ta:Cs ratio far below 10, they conveniently group in the lack to low mineralized pegmatites of the world. (Moller and Morteani, 1989; Cerny, 1992.)

Low values of K/Ba and K/Cs are believed to be indicative of mineralized pegmatites (Garba, 2001). Thus the extremely high values in pegmatites of study area suggest that these pegmatites are barren and unmineralised. Further

economic mineralization of these pegmatites from Oban massif was evaluated using variation plots of Ta vs K/Cs (Figure 5), Ta vs Ga (Figure 6), K/Rb vs Rb (Figure 7), and K/Rb vs Cs (Figure 8). As any rock falling below the defining line of mineralization of Beus, (1966) and Gordiyenko, (1971) is considered barren, while those plotting above the lines are considered mineralized, the pegmatites from Iwuru are barren as they plot far below both mineralization boundaries. But the pegmatites of Igbofia and Akwa-Ibami have a very low mineralization potential as they are seen to plot above the defining line of Beus, (1966), but below that

of Gordiyenko, (1971). On the contrary, in the work of Kingsley and Ekwueme (2009), these same pegmatites seem to be high in mineralization. A scrutiny of the work showed a mistake in the calculation of the K/Rb and K/Cs data, which is pertinent in inferring the mineralization of pegmatite. Pegmatites from the Igbofia-Akwaibami-Iwuru area when compared with pegmatite from other parts of the country (the seven (7) fields of Okunlola, 2004) are depleted in silica but more enriched in  $\text{Fe}_2\text{O}_3$ , though has a lesser Fe-number except in comparison to those of BirniWari-Kushakafield. This lesser Fe-number is due to a relatively higher MgO content of the pegmatites from study area. Average alumina content is only similar to those of the Nassarawa-Keffi field but more depleted than pegmatites from the other six fields. Comparing alkali content, those of the study area is greater than those of Nassarawa-Keffi, Lema-Share, and BirniWari-Kushakabut less than those of the other four fields. According to Bateman and Chappell, (1979), rocks with  $\text{SiO}_2$  less than 70 % and Fe-number less than 0.6 are usually magnesian. This agrees with the pegmatites of study area. Further, Frost and Frost (1997), posits that such magnesian rocks are related to magmas which follow relatively oxidizing differentiation trends.

## Conclusion

The Igbofia-Akwaibami-Iwuru pegmatites are members of the Precambrian pegmatites of Nigeria formed in the Pan-African Orogeny. They are hosted by Precambrian rocks of Oban Basement Complex comprised of mainly schist and granodiorites. They are peraluminous, alkali rich, and tend towards granitic composition. These pegmatites from all reasonable indications and variation diagrams discriminations, are barren and unmineralised and thus have little or no economic potential as it pertains to rare-metals especially Ta-Nb minerals. This is in disagreement with Kingsley and Ekwueme, (2009). This disagreement stems from the wrong calculation of K/Rb and K/Cs ratios in their work, which invariably led to a wrong interpretation of mineralization potential as these ratios are important in pegmatite mineralization evaluation.

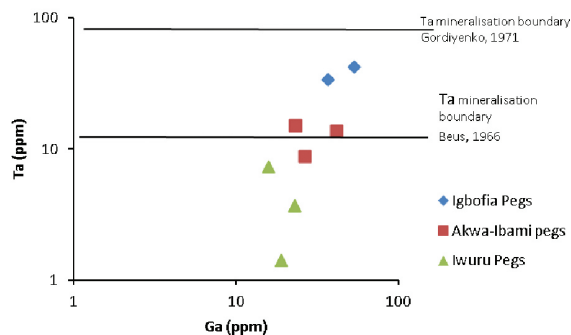


Figure 6: Plot of Ta vs Ga for pegmatites of study area.

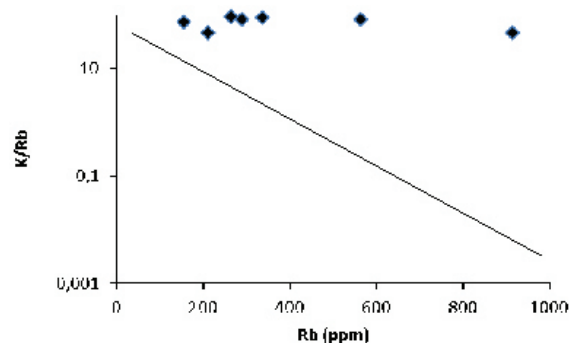


Figure 7: Plot of K/Rb vs Rb for pegmatites of study area (after Straurov et. al., 1966).

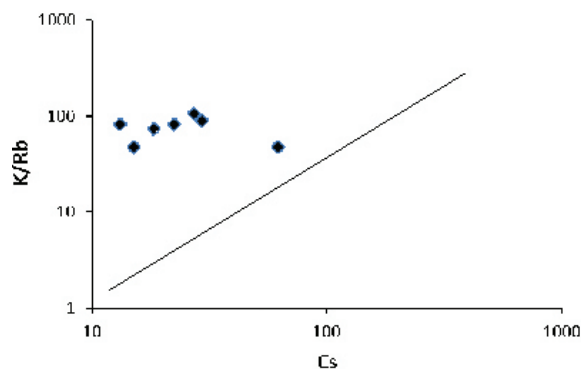


Figure 8: Plot of K/Rb vs Cs for pegmatites of study area (after Moller and Morteani, 1987).

## References

- Bateman, R. C. and Chappell, B. W., (1979). Crystallization, fractionation, and solidification of the Tuolumne intrusive series, Yosemite National Park, California. Geological society of America bulletin, Vol. 90, pp. 465-482.
- Beus, A. A., (1966). Distribution of tantalum and niobium in muscovite from granite pegmatites. Geokhimiya. 10: 1216-1220.

- Brown, E. H., Babcock, R. S., and Clark, M. D., (1979). Geology of Precambrian rocks of Grand Canyon: in Petrology and Structure of Vishu complex. Prec. Res. Vol. 8, pp. 219–241.
- Cerny, P., (1982). Anatomy and classification of granitic pegmatites: in CERNY PETR (ed.), short course in granitic pegmatites. Mineralog. Assoc. Canada short course handbook, Vol. 8, pp. 1–39.
- Cerny, P., Trueman, D.L., Ziehlke, D. V., Goad, B. E., and Paul, B. J. (1981). The Cat Lake-Winnipeg River and Wekusko Lake pegmatite fields, Manitoba; Manitoba Dept of Energy and Mines, economic geology Report ER 80–1, 216p.
- Ekwueme, B. N. and Matheis, G. (1995). Geochemistry and economic value of pegmatites in the Precambrian basement of southeast Nigeria in : R. K. Srivastava and R. Chandra (Eds.), magmatism in relation to diverse tectonic settings. Oxford and IBH Publ. Co. PVT Ltd. New delhi, p. 375–392.
- Ekwueme, B. N. and Schlag, C. (1989). Compositions of monazites in pegmatites and related rocks of Oban massif, southeast Nigeria: implications for economic mineral exploration. IGCP No. 255 Newsletter/bulletin, 2, 15–20.
- Ekwueme, B. N., (1989). Tectonothermal evolution of the Oban massif, Nigeria. 28th Intern. Geol. Congr. Washington D. C., Abstr. Vol. 4, pp. 439–440.
- Ekwueme, B.N., (1990d). On the occurrence of crystalline (basement complex) rocks in SW Ugep, Nigeria. Jour. Min. geol. Vol. 26(1), pp. 69–74.
- Frost, B. R., Barnes, C. G., Collins, W. J., Arculus, R. J., Ellis, D. J. and Frost, C. D. (2001). A geochemical classification for granitic rocks. *Journ. Of petrology*, Vol. 42, pp. 2033–2048.
- Frost, C. O. and Frost, B. R., (1997). High K, iron-enriched Rapakivi-type granites. The tholeiite connection. *Geology*, Vol. 25, pp. 647–650.
- Garba, I., (2001). Late Pan-African tectonic structures and origin of gold and tin-tantalum mineralization in Nigeria. 37th Ann. Intern. Conf. Nigerian Mining and Geosc. Soc. Jos, Nigeria, abstract. P9.
- Gordiyenko, V. V., (1971). Concentration of Li, Rb, and Cs in the potash feldspar and muscovite as criteria for assessing the rare-metal mineralization in granitic pegmatites. *Intern. Geology Rev.* 13:131–142.
- Igonor, E. E., Oden, M. I., and Ukwang, E. E. (2010). Geochemical evaluation of basement rocks within Igbofia-uyanga-Iwuru area, SE Nigeria. 46th Annu. Conf. Nig. Min. Geosci. Soc., Calabar, Nigeria, abstract, pp. 9
- Jacobson, R. and Webb, J.S., (1946). The pegmatites of central Nigeria. *Geol. Surv. Nig. Bull.*, 17
- Kingsley, A. E. and Ekwueme, B. N., (2009). Mineralization of pegmatites in parts of the Oban massif, south-eastern Nigeria: a preliminary analysis. *Chin. Jour. Geochem.* Vol. 28, pp. 146–153.
- Maniar, P. D. and Piccoli, P. M., (1989). Tectonic discrimination of granitoids. *Geol. Soc. Ame. Bull.* Vol. 101, pp. 635–643.
- Matheis, G and Caen-Vanchette, M. (1983). Rb-Sr isotopic study of rare-metal bearing and barren pegmatites in the Pan-African reactivation zone of Nigeria. *Journ. Of African Earth Science*, Vol. 1, pp. 35–40.
- Miller, C. F. (1985). Are strongly peraluminous magmas derived from politic sedimentary sources? *Journ. Geology*, Vol. 93, pp. 673–689.
- Moller, P., and Morteani, G., (1987). Geochemical guide for tantalum pegmatites. *Economic Geology*, Vol. 12, pp. 1885–1897.
- Oden, M. I. (2010). The pegmatite veins of western Oban massif: tectonic and lithological controls on physical properties. 46thannu. Conf. Nig. Min. Geosci. Soc., Calabar, Nigeria, Abstract, pp. 7
- Okunlola, O. A., (2004). Metallogeny of Tantalum-Niobium mineralization of Precambrian pegmatites of Nigeria. Book of abstract, Nigeria Mining and Geosciences Soc.: Int. Conf. Maiduguri. pp. 24
- Patinodouce, A. E. and Beard, J. S. (1996). Effects of P, F (O<sub>2</sub>) and Mg/Fe ratio on dehydration melting of model metagreywackes. *Journ. Of Petrology*, Vol. 37, pp. 999–1024.
- Raeburn, C., (1927). Tinstone in the Calabar District. *Geol. Surv. Nigeria Bull.* 11: 72–88.
- Straurov, O. O., Stolyarov, I. S. and Iocheva, E. I., (1966). Geochemistry and origin of Verkh – Isetgranitoid massif in central Ural. *Geochem. Intern.* Vol. 6, pp. 1138–1146.
- Taylor, R.S., (1965). The application of trace element data to problems of Petrology. In: L. Ahvens, F., Press, S. K. Runcorn and C. Urey(eds.), *Physics and Chemistry of the Earth*, Pergamon Press, Oxford, vol. 6, pp. 133–214.
- Varlamoff, N., (1972). Central and West African rare-metal granitic pegmatites, related aplites, quartz veins and mineral deposits. *Mineral Deposita (Berl.)* 7: 202–216.

# Sedimentological characteristics, provenance and hydrocarbon potential of Post Santonian sediments in Anambra Basin, Southeastern Nigeria

## Sedimentološke značilnosti, izvor in potencial ogljikovodikov postsantonijevih sedimentov v kadunji Anambra v jugovzhodni Nigeriji

Matthew E. Nton<sup>1,\*</sup>, Shereef A. Bankole<sup>2</sup>

<sup>1</sup>Department of Geology, University of Ibadan, Ibadan, Nigeria

<sup>2</sup>Department of Chemical and Geological Sciences, Al-Hikmah University, Ilorin, Nigeria

\*Corresponding author. E-mail: matthew.nton@mail.ui.edu.ng

### Abstract

Field studies of outcrop samples from part of Anambra basin, southeastern Nigeria, were investigated to unravel the lithofacies distribution, provenance, palaeotectonic history as well as aspects of hydrocarbon potential of the basin. The sandstone facies of the Nkporo, Owelli, Mamu and Ajali Formations are cross bedded, medium to coarse grained, poorly sorted to moderately well sorted, negatively skewed and leptokurtic to platykurtic. Textural plots and multivariate parameters indicate fluvial to shallow marine environment. Paleocurrents signify southwest direction for the Nkporo and Ajali Formations while the Owelli Formation points to a northwest direction. The sandstones classify as quartz arenite with heavy mineral assemblages that revealed the presence of zircon, rutile, tourmaline, staurolite, sillimanite, kyanite, garnet and apatite; having ZTR index of 63 %. These typify products of weathering of basement rocks under humid climatic setting with long transportation and/or recycling history. Organic matter quantity of the shales ranges from mass fractions 0.89 % to 3.98 % TOC and Rock-eval parameters indicate immature, poor to fair hydrocarbon potential. Cross plots of rock eval parameters revealed gas prone terrestrially derived Types III and IV kerogen. It can be deduced that the sandstones were sourced from the Adamawa–Abakaliki folded belt and part of Oban Massif while the shales have prospect to generate gas at appropriate maturation, especially from the Nkporo Shale.

**Key words:** sedimentology, provenance, palaeoenvironment, hydrocarbon potential, Anambra Basin

### Izvleček

Vzorci izdankov iz dela kadunje Anambra v jugovzhodni Nigeriji so preiskali z namenom ugotoviti porazdelitev litofaciesov, izvor, paleotektonsko zgodovino in značilnosti naftnega potenciala v kadunji. Za faciese peščenjakov formacij Nkporo, Owelli, Mamu in Ajali so značilne navzkrižna plastovitost, srednja do debela zrnastost, slaba do srednja sortiranost, negativna asimetričnost in lepto- do platikurtičnost. Teksturni diagrami in multivariatni parametri nakazujejo rečno do plitvomorsko okolje. Paleotokovi imajo jugozahodno usmerjenost v formacijah Nkporo in Ajali ter severozahodno v formaciji Owelli. Peščenjaki spadajo h kremenovem arenitu s težkomineralnimi združbami, ki vsebujejo cirkon, rutil, turmalin, stavrolit, sillimanit, kyanit, granat in apatit z ZTR-indeksom 63 %. Predstavljajo produkte preperevanja kamnin podlage v vlažnem podnebju z dolgim transportom in/ali recikliranjem. Masni delež organske snovi v glinavcih se giblje med 0,89 % in 3,98 %. Vrednosti TOC in rock-eval nakazujejo nezrel, nizek do srednji potencial ogljikovodikov. Navzkrižni diagrami rock-eval-parametrov določajo plinsko usmerjeni kerogen terestričnega izvora tipov III in IV. Sklepajo, da so bili peščenjaki napajani iz nagubanega pasu Adamawa–Abakaliki in delno masiva Oban. Glinavci, zlasti glinavec Nkporo, utegnejo ob primerni dozorelosti proizvajati plin.

**Ključne besede:** sedimentologija, izvor, paleookolje, potencial ogljikovodikov, kadunja Anambra

## Introduction

The origin of Anambra Basin is related to the evolution of the Benue Trough, which is also associated with the separation of the African plate from South American plate in the Mesozoic (Tijani et al., 2010). As reported by Akande & Erdtmann, (1998) it is logical to include the Anambra Basin in the Benue Trough, being a related structure that developed after the compressional stage. The basin covers an area of approximately 40 000 km<sup>2</sup> (Nwajide & Reijers, 1996) with approximate sediment thickness of 5 000 m (Uma & Onuoha, 1997). The Anambra basin is characterized by enormous lithogenic heterogeneity in both lateral and vertical extensions derived from a range of paleoenvironmental settings, ranging from Campanian to Recent (Akaegbobi, 2005).

The initial interest in search for oil and gas within the Lower Benue Trough (including the Anambra Basin) of Nigeria, aroused by the presence of favourable stratigraphic setting of interbedded shales and sandstones with occasional limestones (Agagu et al., 1985). The exploration for coal and petroleum in the Anambra Basin culminated into commercial production of coal in 1916 while oil exploration was abandoned as the efforts ended in a number of non-commercial discoveries. The search for commercial hydrocarbons in the Anambra Basin in Nigeria has been a concern, especially to oil companies and research groups, more so as oil is found in the nearby Niger Delta. In addition, sedimentological characteristics of different litho-units have not been fully discussed on a regional scale.

This study therefore examines sedimentological characteristics, provenance, palaeoclimatic and palaeodepositional conditions as well as aspects of hydrocarbon potential of the sediments of Anambra basin from outcrop studies. Such studies would be useful to researchers and explorationists.

## Location of study area and stratigraphy of Anambra basin

The study area lies within latitudes 5°55' N to 6°30' N and longitudes 7°20' E to 7°30' E and belongs to the Anambra Basin (Figure 1). The locations of sampling are shown as 1 to 7 in Figure 1.

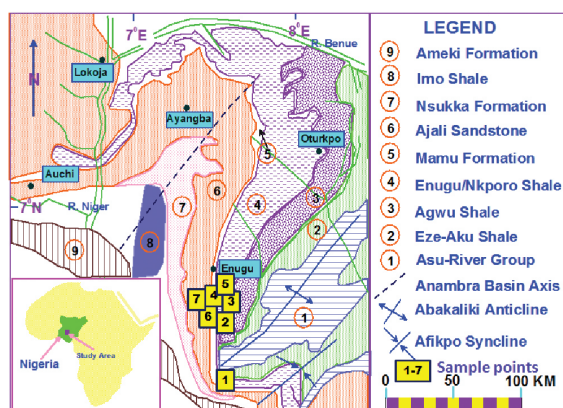


**Figure 1:** Regional stratigraphy of southeastern Nigeria with the sample points (after Tijani et al., 2010).

The oldest sediment in the southern Benue Trough is the Asu River Group (Nwajide, 1990). It consists of about 3 000 m of micaceous sandstones, mudstones, sandy shales, siltstone and limestone lenses. The succession was uplifted and became the topographic provenance (Abakaliki Anticlinorium), which supplied the bulk of the Anambra Basin fill (Hoque, 1977). According to Reyment (1965) and Burke et al. (1972), the sediments are of Albian to Turonian age and were deposited under shallow marine or near shore conditions. The Asu River Group is overlain by the Eze-Aku Formation, which is of Turonian age (Reyment, 1965; Nwajide, 1990). It comprises hard grey-black shales and siltstones with frequent facies changes to sandstones or sandy shales (Petters, 1978; Kogbe, 1989). The Awgu Formation conformably overlies the Eze-Aku Formation. It consists of grey to black well bedded, fissile shales, with thin interbeds of shelly limestone and fine to medium grained/moderately sorted sandstone. Based on the foraminiferal content, Agagu et al. (1985) assigned a Turonian-Santonian age and a shelf depositional environment to the Awgu Formation.

In the Santonian, there was a major tectonic event in which the Albian-Coniacian sediments were deformed, folded, faulted and uplifted (Benkhelil, 1989). This marked the period of sediments deposition within the Anambra Basin (Nwajide, 1990; Tijani et al., 2010). The oldest sediments within the basin is the Nkporo Group. It was deposited into the basin in Late Campanian and comprised Nkporo Shale, Owelli Sandstone and Enugu Shale (Reyment, 1965; Obi et al., 2001). The Nkporo Group is overlain by paralic succession made up of siltstone, shale, coal seam and sandstone units of Mamu Formation deposited in the Early Maastrichtian (Kogbe, 1989). On the basis of organic geochemical and biomarkers parameters, Nton & Awarun (2011), described the shale and coal units of the Mamu Formation as moderate to rich oil/gas prone, immature source rocks of terrestrial precursor.

The Mamu Formation is successively overlain by cross-bedded, tidal channel/fluvial deposits that constitute the Maastrichtian Ajali Sandstone (Ladipo, 1986). The Ajali Sandstone, formerly known as the false-bedded sandstone (Simpson, 1954) consists of friable, medium to coarse grained, poorly sorted, cross bedded sandstones with thin beds of whitish claystones as well as numerous bands of variegated carbonaceous shale (Reyment, 1965 and Agagu et al., 1985). Ajali Sandstone is succeeded by the Nsukka Formation (upper coal measure) which is of Late Maastrichtian age (Obi et al. 2003). It consists of carbonaceous mud rocks, sandstones, shales and coal seams (Nwajide, 1990; Obi et al, 2003). The Imo Shale (Paleocene) overlies the Nsukka Formation and comprises clayey shale with occasional ironstone and thin sandstone in which carbonaceous plant remains may occur (Kogbe, 1989). The Imo Shale is later succeeded by the Ameki Group (Reyment, 1965; Nwajide, 1990).

## Field sampling and analytical methods

Field exercise was carried out along road cuts within parts of the Anambra Basin (Figure 1). Altogether, seven (7) outcrop locations were encountered. At each location, the outcrop was

described, logged, and strike and dips of directional properties were taken. The lithologic profile at each location was sketched and the GPS reading taken as reference. Attempts were made at getting fresh samples which were made up of sandstones, shales and coals. Each sample was described and taken in a well labeled sample bag. Brief descriptions of the different outcrop locations are given below:

### *Location 1 (Leru Village)*

This is a road cut exposure at Leru village representing Nkporo Formation. It is about 54 m thick (Figure 2) and has a lateral extent of about 1.5 km. Based on the different lithologies observed, the formation can be differentiated into shale facies, sandstone facies and sandy shale facies. The basal part of the outcrop starts with a dark shale resting unconformably on a doleritic boulder (Figure 2). It has a vertical thickness of about 7 m and contains bivalves, gypsum and micrite. The dipping direction is  $296^\circ$  Az, trending in  $038^\circ$  N/ $218^\circ$  S direction and with a dip of  $6^\circ$ . This is overlain by a thin bed of ferruginised fine brown sandstone of about 5 cm with groove casts. This is later succeeded by a black shale of about 0.8 m containing micrite and gypsum nodules, joints and rootlets. The trending of the bed is  $40^\circ$  N/ $220^\circ$  S, dipping along  $300^\circ$  N with dip amount of  $7^\circ$ . It progresses into a thin ferruginised brown shale of about 5 cm, containing bivalves and groove structures which is succeeded by grey shale of about 1 m, having traces of bivalves and gypsum nodules. The section passes into an indurated mudstone of about 4 cm, trending in  $22^\circ$  N/ $202^\circ$  S direction; it has a dip amount of about  $6^\circ$ . It is overlain by a grey shale of 2 m thick, interbedded with mudstone and ferruginised at the upper part. The trend of the bed is  $22^\circ$  N/ $202^\circ$  S; it has a dipping direction of about  $226^\circ$  W and dip amount of about  $5^\circ$ . Next in succession is a grey shale with an estimated thickness of about 10 m. The shale is fissile and contains bivalves. Overlying the lower shale facies is a sandstone facies with graded, parallel laminated, poorly sorted, medium to coarse, friable sandstone bed of about 20 m thick (Figure 2). It dips  $270^\circ$  W, trends towards  $12^\circ$  N/ $192^\circ$  S and with dip amount of  $10^\circ$ . It continues into a parallel laminated, poorly sorted, friable medium to fine

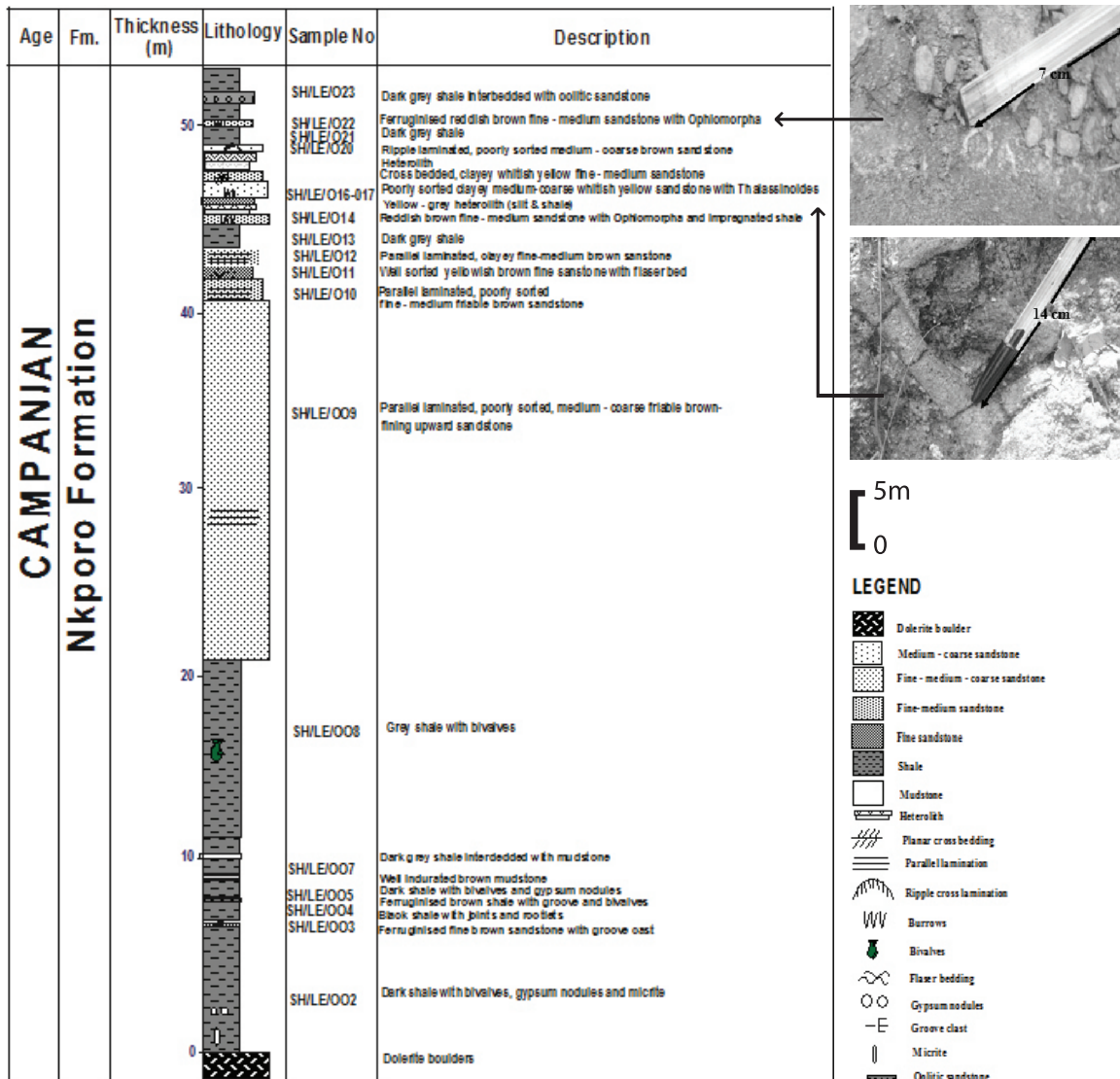


Figure 2: Lithologic section of Nkporo Formation exposed at Enugu-Port Harcourt express way in Leru Village. Co-ordinate: 5°55' N and 7°28' E.

grained brownish sandstone. It is 1.3 m thick, dips 282° W, trends along 30° N/210° S and with dip amount of 8°. Overlying this, is a well sorted friable, yellowish brown fine sandstone characterised with flaser bed and succeeded by a well sorted, friable, clayey, fine to medium grained brown sandstone.

The uppermost unit consists of sandy shale facies, made up of sequences of shale, sandstone and heterolith. A grey shale with a thickness of about 1.5 m marks the basal portion of this facies. It passes into ferruginised, reddish brown, fine to medium grained sandstone typified by presence of Ophiomorpha (Figure 2) and impregnated shale. The facies continues with a

heterolith of 0.7 m thick which is overlain by a friable, clayey, greyish yellow, fine grained sandstone, 0.3 m thick, and succeeded by a poorly sorted clayey, medium to coarse grained whitish yellow sandstone which is 1 m thick, containing Thalassinoides (Figure 2). The section grades into a bed of 0.4 m thickness that is cross bedded, whitish yellow medium grained sandstone. It is overlain by a heterolith of 1 m thickness and passes into a ripple laminated medium to coarse grained brown sandstone of 0.2 m thick with Ophiomorpha. This is overlain by dark grey shale which is 1 m thick, trending 40° N/220° S, dipping 308° W and having dip amount of about 7°. The dark grey shale is over-

lain by 0.2 m thick ferruginised reddish brown fine to medium grained sandstone with *Ophiomorpha* burrows. The section terminates with dark grey shale which is 3 m thick, interbedded with oolitic sandstone of 0.1 m thickness.

### **Location 2**

This is an exposure of Owelli Formation, encountered south of Enugu along Enugu-Port Harcourt road (Figures 1 and 3). It consists of shale, sand, coal and mudstone beds with a total thickness of about 21 m (Figure 3) and lateral extent of about 700 m. The sequence begins with a grey to brown weathered shale which is 2 m thick interbedded with thin mudstone. It is overlain by 1 m thick, grey-brown ferruginised shale which is succeeded by 2 m thick, poorly sorted, clayey, fine to medium grained brown sandstone with gypsum nodules. The sequence is overlain by 1.7 m dark grey shale, trending  $46^{\circ}$  N/ $226^{\circ}$  S, dipping  $314^{\circ}$  W and dip amount of about  $8^{\circ}$ . It is succeeded by 1.2 m thick dark grey shale trending  $44^{\circ}$  N/ $224^{\circ}$  S, dipping  $3120$  W and dip amount of about  $7^{\circ}$ . Overlying this, is a bed of about 1.1 m of laminated brown mudstone, overlain by 3 cm black coal bed showing considerable degree of partings. This is succeeded by a brown mudstone of about 1.5 m. The section continues with about 0.6 m thick parallel laminated fine to medium grained greyish white sandstone. The sequence is overlain by 0.7 m thick cross bedded yellowish white, poorly sorted, clayey, fine to medium sandstone. It continues into a poorly sorted, clayey, fine to medium grained whitish sandstone which is 0.4 m thick and characterized by herringbone structure (Figure 3). It trends  $60^{\circ}$  N/ $240^{\circ}$  S, dips  $150^{\circ}$  E and has a dip amount of about  $10^{\circ}$ . Successively overlying this, is a parallel laminated, ferruginised, reddish white, fine to medium sandstone about 1 m thickness and passing into a cross bedded, ferruginised, coarsening upward, fine to medium grained white sandstone of about 0.7 m with *Ophiomorpha* burrows. It is succeeded by poorly sorted, medium to coarse grained yellowish sandstone of about 2 m thick, characterised by *Ophiomorpha* burrows, which is overlain by a dark brown sandstone of about 1 m thick containing vertical burrows of the *Skolithos* ichnogenera (Fig-

ure 3). The section is capped by an indurated brown mudstone of about 4 m thick.

### **Location 3**

This location was encountered along the Enugu-Onitsha expressway at Agu Abor. It is a road cut exposure of Enugu Shale with a vertical thickness of about 16.5 m (Figure 4) and lateral extent of about 800 m. The section begins at base with dark grey weathered shale which is 3 m thick, with an extra-formational clast (Figure 4). It is overlain by dark grey shale of about 4.1 m thickness and continues into a parallel laminated siltstone which is about 0.1 m thick. The siltstone is succeeded by dark grey shale of about 2.5 m, bearing extra-formational clast. It passes into a heterolith and transits into dark grey shale of 1.2 m. The top of the section terminates with a dark grey shale of 4 m thickness, which is interbedded with ironstone of about 2.5 cm thickness.

### **Location 4**

This location, encountered at Onyeama Mine, along the Enugu-Onitsha Expressway, is the type section of Mamu Formation. With a total thickness of about 41 m, it consists of a sequence of siltstone, sandstone, coal, mudstone and shale (Figure 5). The sequence begins at the base with yellowish brown, fairly indurated siltstone, 1.5 m thick, and overlain by dark coal beds with high degree of partings which show increasing hardness in an upward direction. The coal beds have  $20^{\circ}$  N/ $200^{\circ}$  S strike, dip direction of  $120^{\circ}$  S and dip amount of  $4^{\circ}$ . The sequence is overlain by 25 m thick yellowish grey mudstone bearing bivalves. It is succeeded by 3 m thick well indurated grey siltstone and grade into well laminated, reddish brown fine sandstone of 2 m thick which is overlain by a yellow siltstone of 2 m thick. The sequence is successively overlain by reddish white, clayey, fine sandstone, then passes into a parallel laminated yellow fine sandstone which is 7.8 m thickness. This is overlain by parallel laminated grey siltstone about 1 m thick and the section is overlain by about 2 m thickness of overburden.

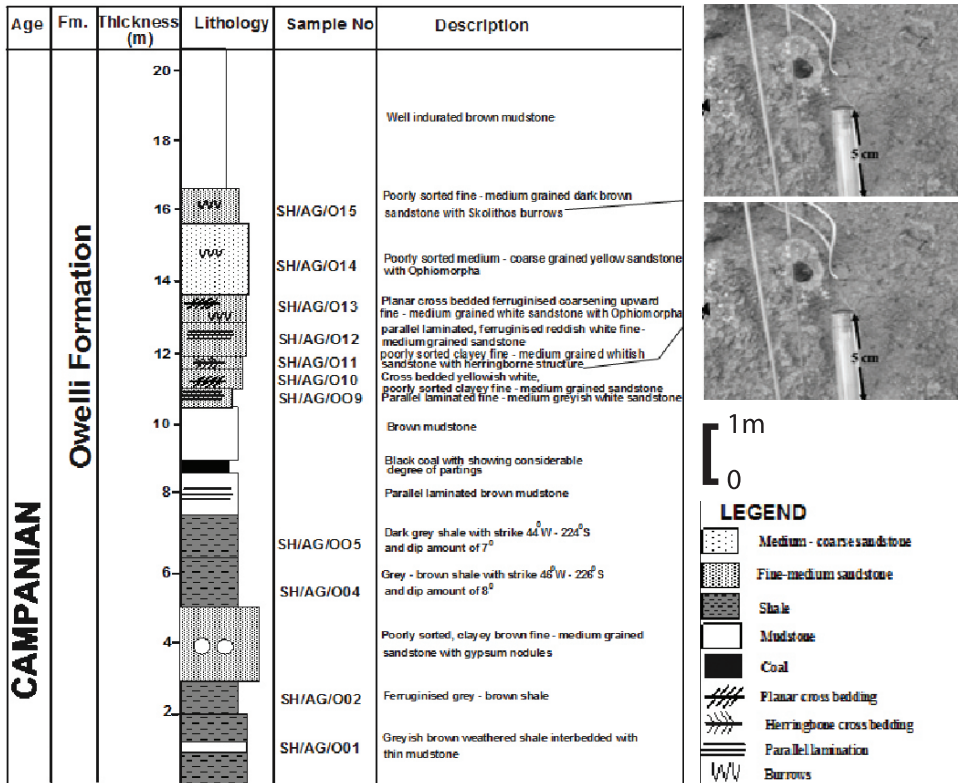


Figure 3: Lithologic section of Owelli Formation exposed at 30 km south of Enugu along Enugu-Port Harcourt expressway, Agbogugu junction. Co-ordinate:  $6^{\circ}16' N$  and  $7^{\circ}28' E$ .

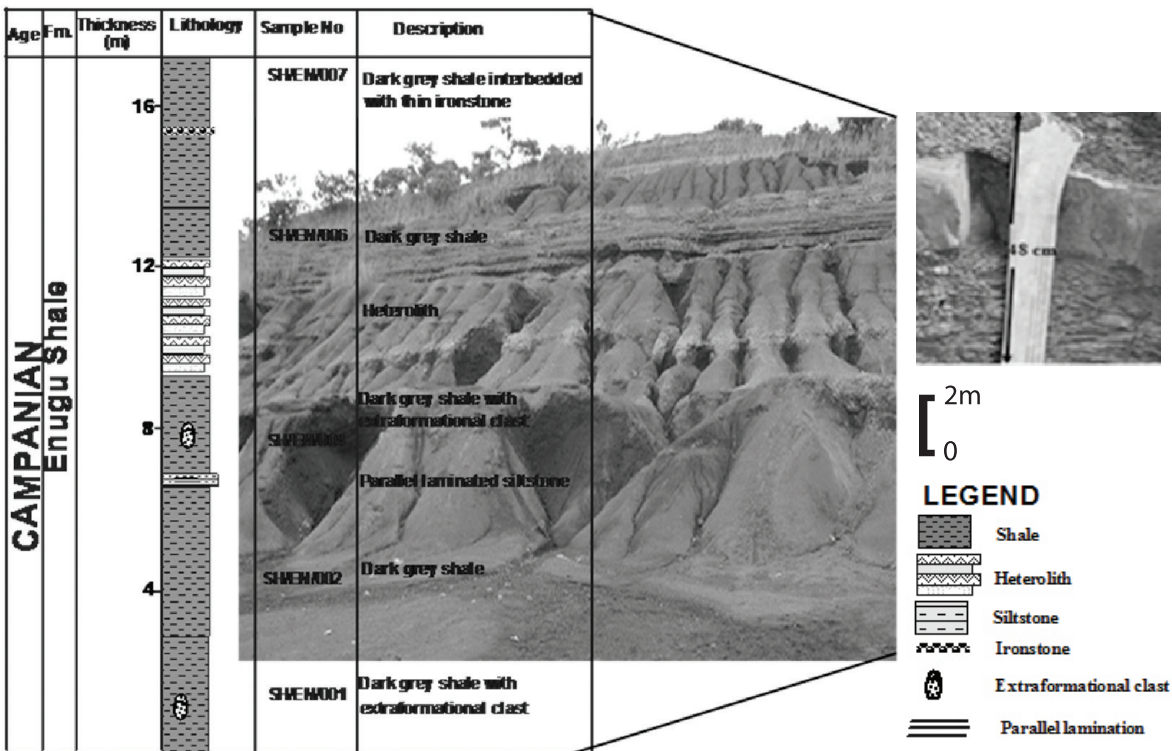
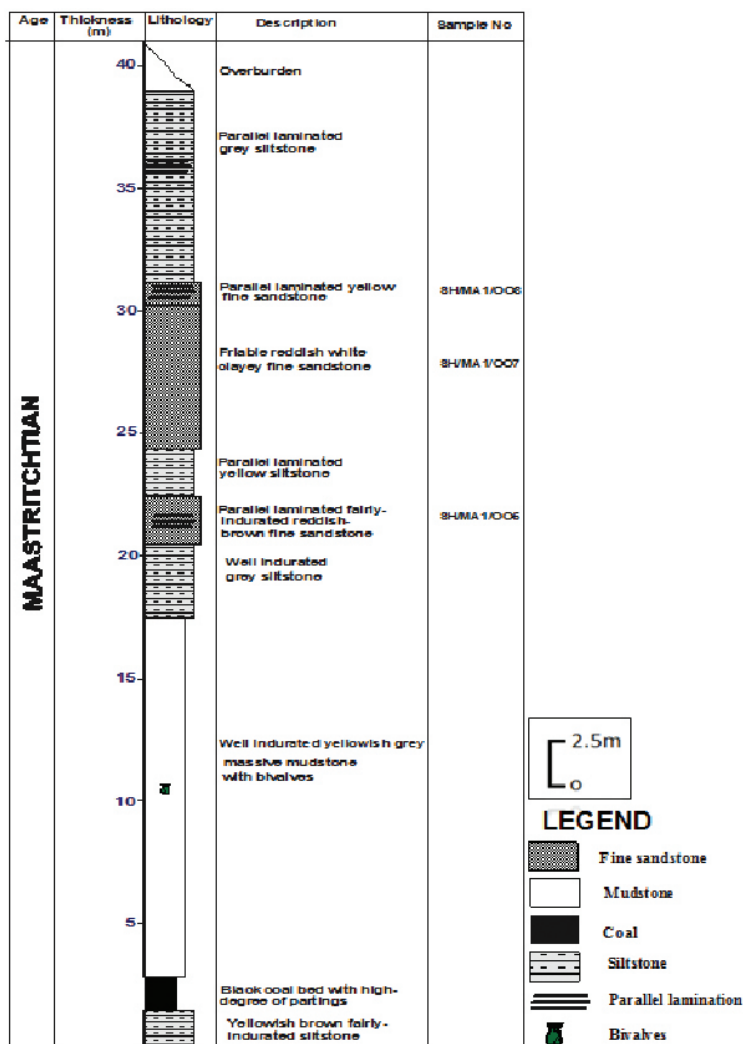


Figure 4: Lithologic section of Enugu Shale exposed at Agu-Abor near Onitsha road flyover at Enugu. Co-ordinate:  $6^{\circ}26' N$  and  $7^{\circ}29' E$ .



**Figure 5:** Lithologic section of Mamu Formation exposed at Onyema mine, 1.2 km away from NNPC Mega Petrol station at Agu-Abor. Co-ordinate: 6°25' N and 7°27' E.

### Location 5

This is a section of Mamu Formation exposed at Proda, half a kilometer away from the NNPC Mega Petrol Station at Agu-Abor, along Enugu-Onitsha expressway in Enugu. It has a vertical thickness of about 20 m (Figure 6) and a lateral extent of about over 500 m. It is made up of a sequence of siltstone, shale and sandstone. The section begins with parallel laminated grey siltstone of about 6.5 m thickness that is overlain by parallel laminated grayish to yellowish siltstone which is about 2.5 m thick. This is successively overlain by 1.5 m thick dark grey shale and then by 0.5 m thick parallel laminated fine grained sandstone. Overlying this sequence is a 5 m thick parallel laminated brownish yellow siltstone which is overlain by massive grayish

yellow siltstone about 2 m thickness and then capped by a heterolith of silt and sandstone of 2.5 m thickness.

### Location 6

This location shows a vertical thickness of 13 m of Ajali Sandstone (Figure 7) at Ngwo with a lateral extent of about 600 m. The basal bed is made up of poorly sorted, loose, clayey reddish fine grained sandstone which is succeeded by poorly sorted, loose, clayey, cross bedded, white fine grained sandstone. The overall sequence is capped by white colored, poorly sorted, loose, coarse grained sandstone, consisting of herringbone cross bedding and reactivation surface.

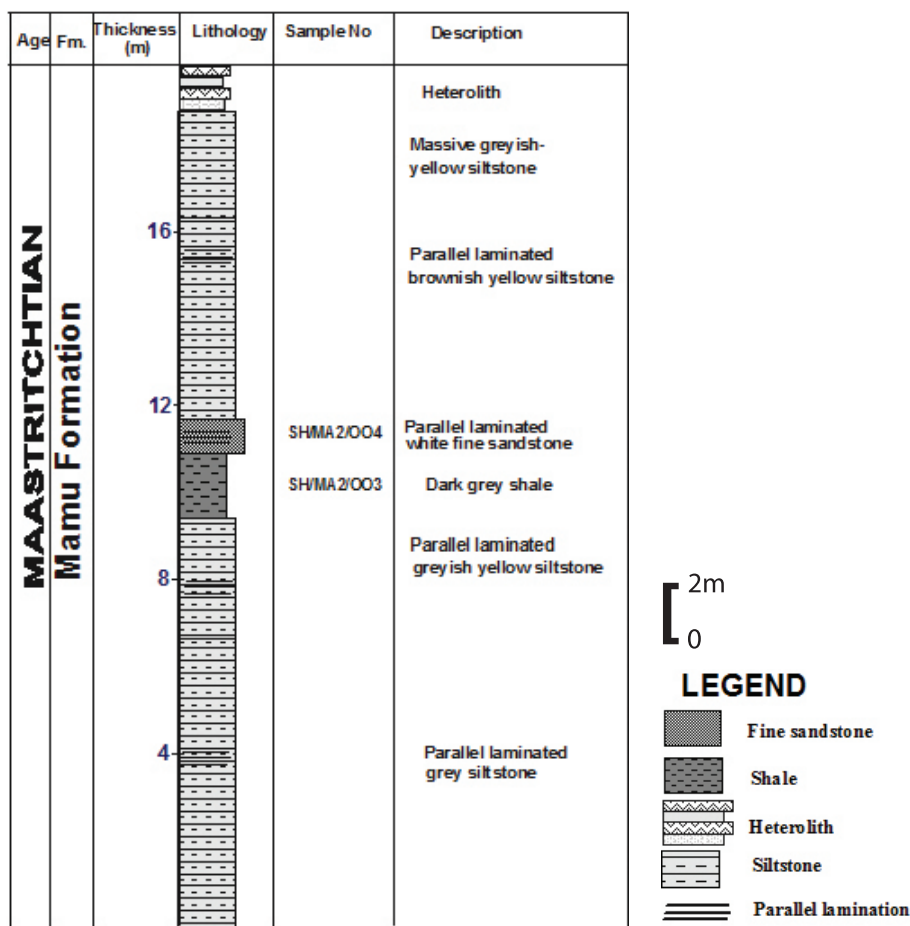


Figure 6: Lithologic section of Mamu Formation exposed at Proda, 465 m away from NNPC Mega Petrol station at Agu-Abor. Co-ordinate: 6°25' N and 7°28' E.

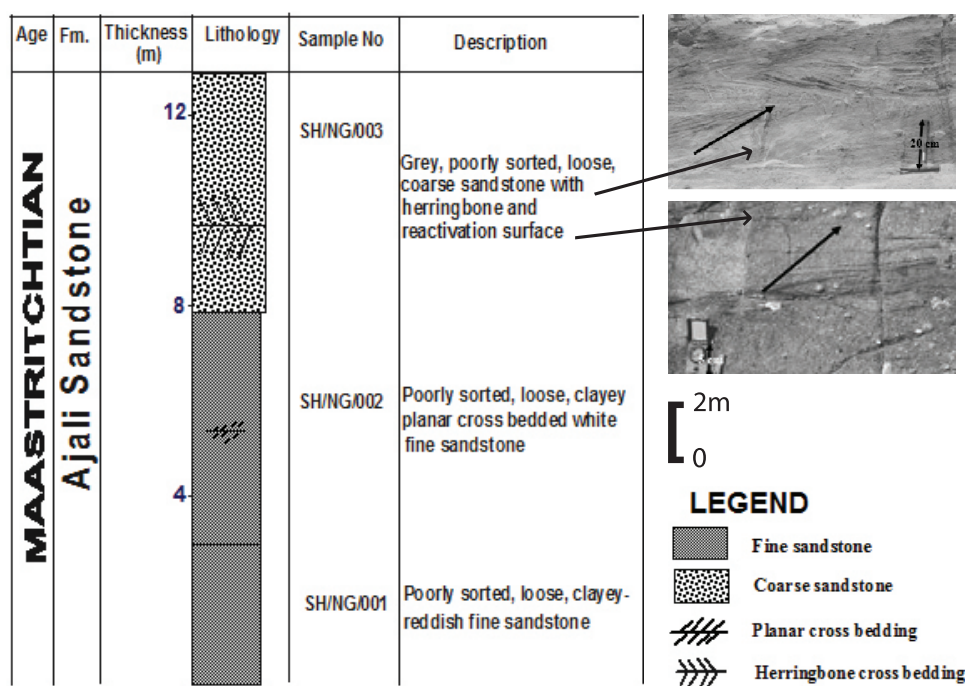


Figure 7: Lithologic section of Ajali Sandstone exposed at Ngwo, Enugu. Co-ordinate: 6°22' N and 7°27' E.

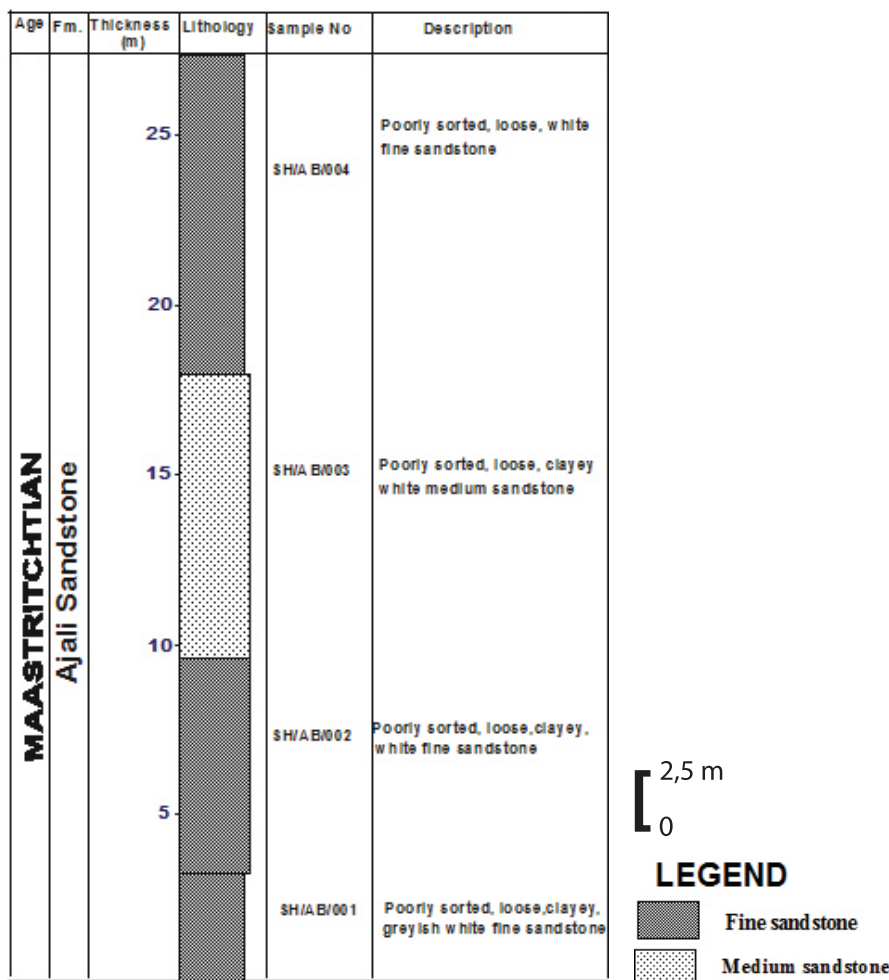


Figure 8: Lithologic section of Ajali Sandstone exposed at Abor, Enugu. Co-ordinate: 6°21' N and 7°24' E.

### Location 7

This location represents an exposure of Ajali Sandstone at Abor. The overall sequence is 27 m thick (Figure 8), and its lateral extent is about 400 m. The base is made up of poorly sorted, loose, clayey, grey – white, fine grained sandstone of about 3 m thick. It trends 163° with dip amount of 8°. It is succeeded by poorly sorted, clayey, loose, clayey white sandstone of about 6.8 m, trending 3°, and dip direction of 210° S and dip amount of 6°. This is successively overlain by 7.8 m thick, poorly sorted, loose, clayey, white medium grained sandstone. It trends 10° with dip direction of 150° S and dip amount of 6°. This is succeeded by poorly sorted, loose, white fine grained sandstone (2 m), trending 5° with dipping direction of 220° S and dip amount of 6°.

### Analytical methods

#### Grain size analysis

Twenty eight (28) representative sandstone samples were selected to be disaggregated for grain size studies. 100 g of each disaggregated sample was measured out and subjected to standard grain size analysis using a set of sieves at ½ phi interval and sieved on a Ro-tap shaker for fifteen minutes. Cumulative plots were drawn for each sample and statistical parameters were computed based on the concept of Folk (1974). The analysis was conducted at the Sedimentological Laboratory, University of Ibadan, Nigeria.

#### Paleocurrent analysis

Rosette diagrams were constructed and Mean Vector Azimuths (MVA) (Turker, 1996) were

calculated based on dips and azimuths of planar cross bedding earlier taken in the field. The formula for calculating the mean vector azimuth is stated below:

$$MVA = \tan^{-1} (\sum n \sin \sigma) / (\sum n \cos \sigma)$$

Where  $\sigma$  is the azimuth in degree

### Heavy mineral studies

5 g each of sandstone samples was subjected to heavy mineral analysis. Bromoform extracts of heavy minerals from 26 sandstones samples were rinsed with acetone and later mounted on slides. Point counting method of the non-opaque assemblages was done in the Petrology Laboratory, University of Ibadan, using a binocular petrological microscope. Photomicrographs of salient features were taken.

### Thin section petrography

Twenty (20) sandstones samples were impregnated in resin and thin sectioned by standard methods. The slides preparations were done at the Department of Geology and Mineral Sciences, University of Ilorin. Petrographic examination, entailing point counting of the minerals, was carried out using a petrological microscope Model Brunel, at the Petrology Laboratory, University of Ibadan, Nigeria. This study is based on the concepts of Dickinson (1970) and Ingersoll et al. (1984).

### TOC and Rock-Eval pyrolysis analyses

A total of ten (10) shale samples were pulverized and sieved through 0.2 mm sieve. 100 mg of each sieved sample was treated in concentrated HCl, to remove carbonates. The acid was drained off with a filtration apparatus fitted with a glass microfiber film. The filtrate was placed in a LECO crucible and dried at 110 °C for a minimum of 1 h. Later, each sample was analyzed with a LECO 600 Carbon Analyser for TOC determination.

Arising from TOC adequacy, 80 mg of each pulverized shale sample was heated in an inert atmosphere to determine the S1, S2 and S3 groups of compounds which were measured as peaks. Samples were heated at 300 °C for 3–5 min, to produce S1 peak by vaporizing the free hydrocarbons. The temperature of the oven was then increased by 25 °C/min to 600 °C, and the S2

and S3 peaks were measured from the pyrolytic degradation of the kerogen in the sample.

The analysis was determined by Rock-Eval II pyroanalyser which has a TOC module. These analyses were carried out at State Key Geochemistry Laboratory, China. The work flow pattern for the study is shown in Figure 9. Details of the analytical procedures can be found in Bankole (2011).

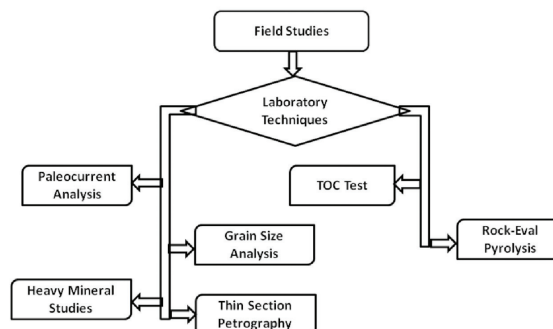


Figure 9: Flow Chart of Laboratory Analyses.

## Results and discussion

### Grain size characteristics

The results of the statistical parameters are presented in Table 1. The sandstone units of the Nkporo Formation are medium to coarse grained, poorly sorted to moderately well sorted, very negatively skewed to positively skewed and very leptokurtic to very platykurtic (Table 1). The Owelli Sandstones are medium to coarse grained, poorly sorted to moderately well sorted, negatively skewed to positively skewed and very leptokurtic to platykurtic (Table 1). The sandstone facies of the Mamu Formation is fine grained, moderately sorted to well sorted, negatively skewed and very leptokurtic. The Ajali Sandstone is medium to coarse grained, poorly sorted to moderately well sorted, negatively skewed to nearly symmetrical and leptokurtic to mesokurtic. Typical grain size probability plots for some samples (Figure 10) contain the upper two segments of a normal three segmented classes of suspension, saltation and bed load, and indicate fluvial setting (Visher, 1969).

Bivariate plots of the grain size parameters such as mean size vs. sorting (Friedman, 1961;

Moiola & Weiser, 1968), sorting vs. median (Stewart, 1958; Moiola & Weiser, 1968) are shown in Figure 11 and Figure 12, respectively. These show that the sediments are mainly product of river processes. Arising from linear discriminant function after Sahu (1964) which is presented in Table 2, it can be seen that the sediments were deposited in shallow marine to fluvial (deltaic) environment.

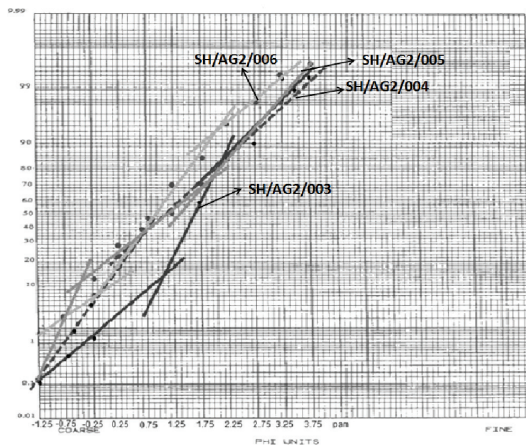


**Figure 10:** Typical probability plots for some studied sandstone samples.

**Table 1:** Summary of grain size parameters

Size Parameter	Range ( $\phi$ )	Average Value ( $\phi$ )	Interpretation	Standard deviation
<b>AJALI SANDSTONE (7 samples)</b>				
Median	1.00–1.60	1.24	Medium to coarse grained	0.19
Mean	0.92–1.58	1.16	Medium to coarse grained	0.21
Sorting	0.55–1.06	0.86	Poorly sorted to moderately sorted	0.15
Skewness	–0.29–0.03	–0.12	Negatively skewed to nearly symmetrical	0.12
Kurtosis	0.96–1.43	1.14	Leptokurtic to mesokurtic	0.15
<b>MAMU FORMATION (4 samples)</b>				
Median	2.40–2.95	2.66	Fine grained	0.28
Mean	2.28–2.93	2.60	Fine grained	0.30
Sorting	0.46–0.84	0.64	Moderately sorted to well sorted	0.17
Skewness	–0.29–(–0.20)	–0.25	Negatively skewed	0.04
Kurtosis	1.51–2.09	1.79	Very leptokurtic	0.28
<b>OWELLI SANDSTONE (7 samples)</b>				
Median	0.5–1.35	0.94	Medium grained to coarse grained	0.32
Mean	0.08–1.38	0.86	Medium grained to coarse grained	0.43
Sorting	0.69–1.08	0.89	Poorly sorted to moderately sorted	0.15
Skewness	–0.31–0.19	–0.08	Negatively skewed to positively skewed	0.16
Kurtosis	0.77–1.70	1.12	Leptokurtic to platykurtic	0.28
<b>NKPORO FORMATION (10 samples)</b>				
Median	0.25–1.45	1.00	Medium to coarse grained	0.38
Mean	0.50–1.42	1.01	Medium to coarse grained	0.34
Sorting	0.50–1.03	0.82	Poorly sorted to moderately well sorted	0.20
Skewness	–0.44–0.18	–0.02	Very negatively skewed to Positively skewed	0.21
Kurtosis	0.00–1.74	1.05	Leptokurtic to Very kurtic	0.46

**Table 2:** Deduced depositional environments based on linear discriminant function (after Sahu 1964)

Sample No	Formation	Location	Calculated values	Interpretation	
SH/NG/001	Ajali Sandstone	Ngwo	-2.52	Shallow marine	
SH/NG/002			-6.58	Shallow marine	
SH/NG/003			-6.06	Shallow marine	
SH/AB/001		Abor		-6.65	Shallow marine
SH/AB/002				-7.76	Fluvial
SH/AB/003				-8.73	Fluvial
SH/AB/004				-10.44	Fluvial
SH/MA1/005		Mamu Fm.	Onyeama	-2.09	Shallow marine
SH/MA1/007	-2.70			Shallow marine	
SH/MA1/008	Proda		-4.93	Shallow marine	
SH/MA2/004			-6.83	Shallow marine	
SH/AG/009	Owelli Sandstone	Agbogugu	-7.89	Fluvial	
SH/AG/010			-6.49	Shallow marine	
SH/AG/011			-3.52	Shallow marine	
SH/AG/012			-7.44	Fluvial	
SH/AG/013			-10.57	Fluvial	
SH/AG/014			-5.00	Shallow marine	
SH/AG/015			-8.07	Fluvial	
SH/LE/003			Nkporo Formation	Leru	-6.92
SH/LE/009	-7.44	Fluvial			
SH/LE/010	-4.50	Shallow marine			
SH/LE/011	-4.38	Shallow marine			
SH/LE/012	-8.23	Fluvial			
SH/LE/014	-10.09	Fluvial			
SH/LE/016	-3.93	Shallow marine			
SH/LE/017	-7.05	Shallow marine			
SH/LE/020	-7.46	Fluvial			
SH/LE/022	-0.89	Shallow marine			

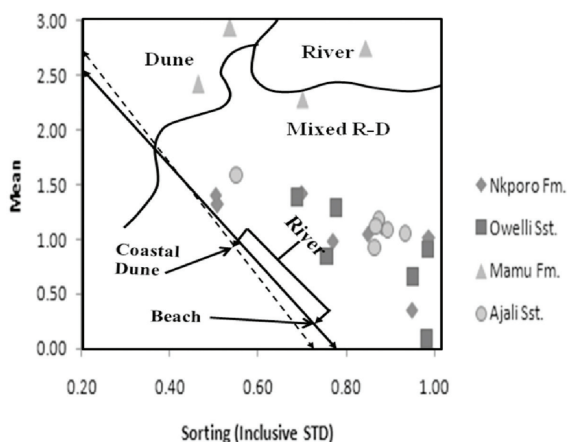


**Figure 11:** Bivariate plot of grain size mean against sorting (inclusive standard deviation) after Friedman (1961), Moiola & Weiser (1968).

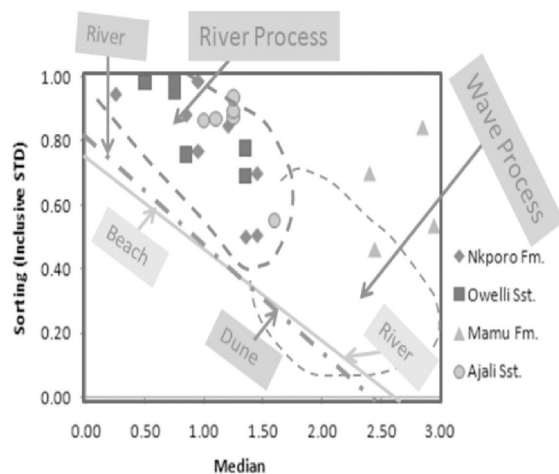


**Figure 12:** Bivariate plot of grain size sorting (inclusive standard deviation) against median after Stewart (1958), Moiola & Weiser (1968).

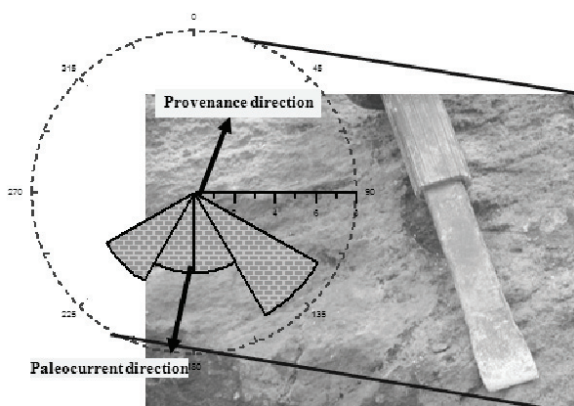


**Figure 13:** Rosette diagram for Nkporo Formation exposed at Leru village (note the paleocurrent and provenance directions).

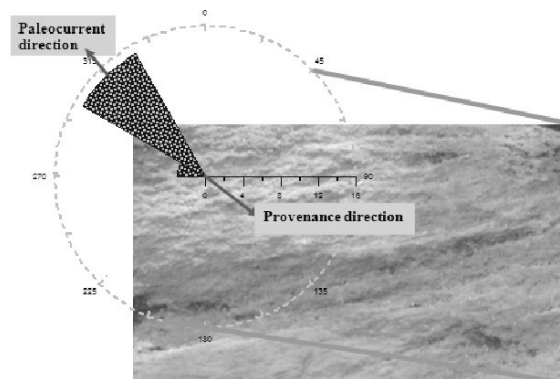


**Figure 14:** Rosette diagram for Owelli Sandstone exposed at Agbogugu junction (note the paleocurrent and provenance directions).

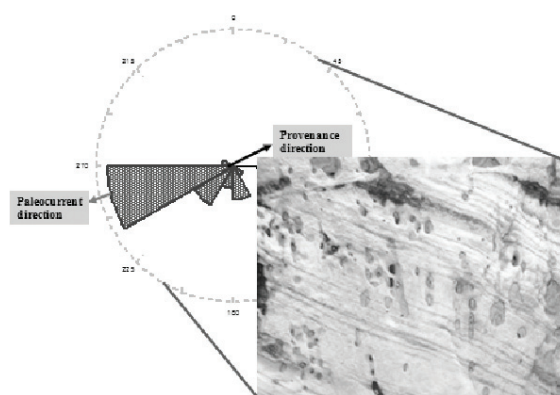


**Figure 15:** Rosette diagram for Ajali Sandstone exposed at Ngwo (note the paleocurrent direction and the provenance direction).

### Provenance

Paleocurrent analysis gives the following mean vector azimuths of 225°, 315° and 234° for Nkporo, Owelli, and Ajali Sandstone, respectively. The mean vector azimuths and the rose diagrams suggest that the source of the sediments is confined to the northeast with little contribution from southeastern part of the basin (Figures 13–15).

The presence of zircon, rutile, tourmaline, garnet, apatite, kyanite, sillimanite, and staurolite in the heavy mineral suites (Table 3) also revealed that the sediments were derived from basement complex of both igneous and metamorphic origin (Feo-Codecido, 1956). The zircon, tourmaline, rutile (ZTR) index (Hubbert, 1962) ranges between 58 % and 75 % and indicates fairly mineralogically matured sediments. The sandstone petrography (Table 4) revealed

quartz arenite with quartz being the main constituent (> 95 %), low feldspar and low lithic fragment contents (Figure 16). This suggests that the sediments have been subjected to intense weathering, prolonged transportation and/or have been reworked or recycled (Pet-tijohn et al., 1973; Akarish & El-Gohary, 2008).

### ***Paleoclimatic and Paleotectonic Deductions***

Suttner et al. (1981) utilized Quartz, Feldspar and Rock Fragment (QFR) ternary plot to separate climatically induced compositional differences in Holocene sands. Based on their concept, the sandstones of Anambra Basin

(Figure 17) were sourced from a metamorphic humid climatic setting, probably during the Campanian to Maastrichtian times. According to Dickinson & Suczek (1979), the detrital framework mode of sandstone composition is a function of the plate tectonic setting of the provenance. The QFR diagram based on this concept shows that the sandstones plotted within the rifted and uplifted continental block setting (Figure 18). This corresponds with the findings of Olade (1975), who posited that the Nigerian basement was domed and rifted in the pre-Early Cretaceous times to form the ensialic Benue aulacogen.

**Table 3:** Heavy mineral assemblages (%) of the sandstone facies of the studied sediments

Formation	Location	Sample No	Z	T	R	K	St	Si	G	Ap	ZTR
Ajali Sandstone	Ngwo	SH/NG/001	8	6	7	-	3	-	5	-	72
		SH/NG/002	10	9	13	-	5	2	7	1	68
		SH/NG/003	13	9	10	4	4	3	6	2	63
	Abor	SH/AB/001	25	18	20	10	11	8	7	2	62
		SH/AB/002	12	14	10	5	6	4	5	1	63
		SH/AB/003	14	13	10	5	8	2	1	-	60
		SH/AB/004	20	18	19	5	10	5	6	-	69
Mamu Formation	Onyeama	SH/MA1/005	12	8	9	4	7	3	7	1	57
	Proda	SH/MA2/004	10	7	8	3	4	2	6	1	61
Owelli Sandstone	Agbogugu	SH/AG2/001	11	9	13	-	6	-	5	-	75
		SH/AG2/002	9	8	6	-	4	-	6	1	68
		SH/AG2/004	12	14	10	6	7	4	7	-	60
		SH/AG2/005	8	7	6	-	3	4	7	-	60
		SH/AG2/006	7	8	9	-	4	-	5	-	73
		SH/AG2/007	10	7	8	3	5	3	6	2	57
		Nkporo Formation	Leru	SH/LE/003	11	8	14	2	8	-	9
SH/LE/009	11			8	12	-	7	-	3	4	69
SH/LE/010	14			10	11	3	5	3	4	3	66
SH/LE/011	9			8	10	-	4	4	5	2	64
SH/LE/012	13			12	10	3	6	5	5	4	60
SH/LE/013	11			8	14	2	8	-	9	2	61
SH/LE/014	16			13	26	10	14	7	8	5	56
SH/LE/016	10			9	13	5	7	6	8	3	52
SH/LE/017	18			10	12	4	3	4	6	-	70
SH/LE/020	15			9	10	3	5	3	7	2	63
SH/LE/022	20	18	19	8	12	10	10	1	58		

\*Z = Zircon, R = Rutile, T = Tourmaline, K = Kyanite, St = Staurolite, Si = Sillimanite, G = Garnet, Ap = Apatite

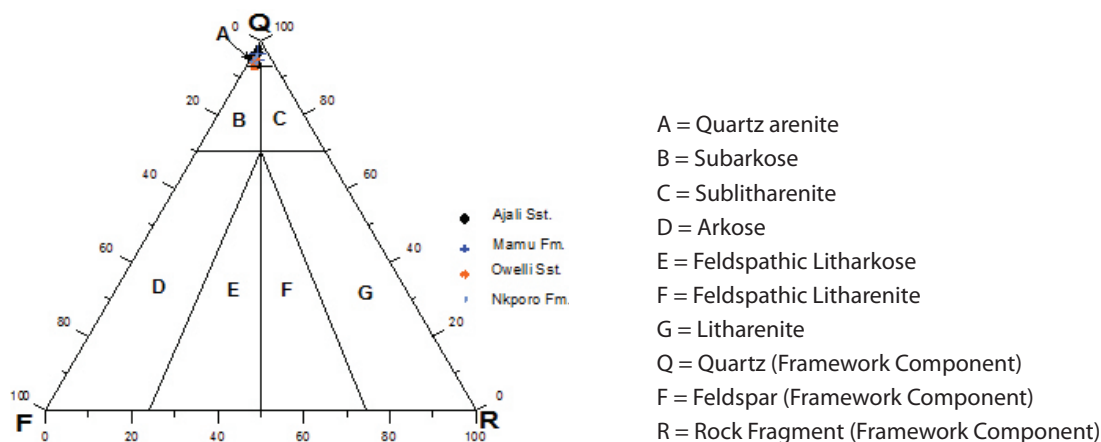


Figure 16: Ternary classification of sandstones based on framework components (after Folk, 1974).

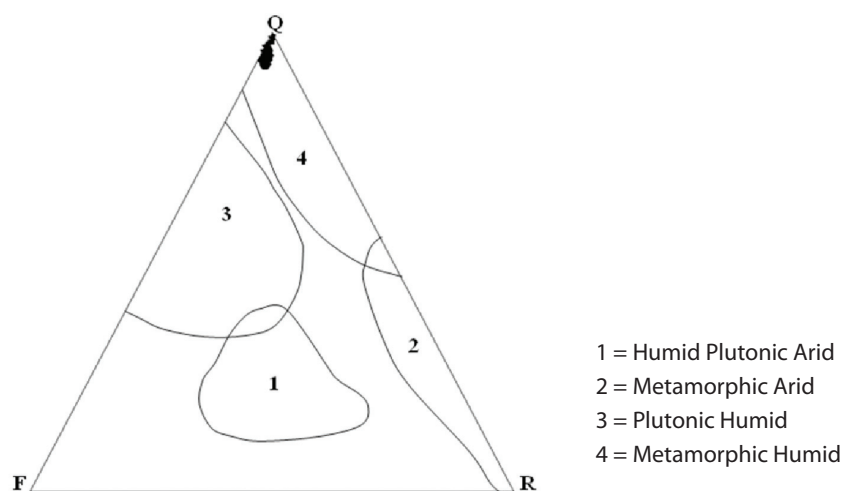


Figure 17: Ternary plot of QRF showing the paleoclimatic setting of the different formations (after Suttner et al., 1981).

### Hydrocarbon Potential Organic matter quantity

The results of organic geochemical parameters are shown in Table 5. The shaly facies of Nkporo Formation have TOC values ranging between mass fractions 0.89 % and 3.59 % (av. 2.4 %, Table 5); the shale sequence of Owelli Formation have between 0.96 % and 1.17 % TOC while that of Enugu Shale has TOC range between 2.09 % and 3.98 % The value for Mamu Formation is 2.63 % TOC. These values imply that the organic matter content is adequate for hydrocarbon generation (Tissot & Welte, 1984) and can further be categorized as good to very good source rocks (Peters, 1986).

The values of the source potential (S1 + S2) of the samples range generally from 0.28 mg to 4.18 mg HC in 1 g rock, while the values of S2 ranges from 0.28 mg to 4.13 mg HC in g rock (Table 5). These values are indicative of insignificant oil rich source rocks but of gas generative potential (Peters, 1986). The source potential values (S1 + S2) of samples SH/LE/008 and SH/LE/021 are respectively 4.18 mg HC in 1 g TOC and 4.08 mg HC in g TOC for the Nkporo Formation and a value of 3.0 mg HC in 1 g TOC (SH/EN/007) for the Enugu Shale. The corresponding values for hydrocarbon yield (S2) for the same samples are (4.13, 4.04 and 2.97) mg

**Table 4:** Thin section petrographic data for different sandstone facies

Formation	Location	Sample No	Qm (%)	Qp (%)	Qt = Qm + Qp (%)	F (%)	Lt (%)
Ajali Sandstone	Ngwo	SH/NG/001	80.0	15.0	95.0	4.5	0.5
		SH/NG/002	87.0	9.0	96.0	3.8	0.2
		SH/NG/003	83.0	15.0	98.0	1.5	0.5
	Abor	SH/AB/001	90.0	7.0	97.0	2.0	1.0
		SH/AB/002	82.0	14.0	96.0	3.4	0.6
		SH/AB/003	79.0	15.0	94.0	4.3	1.7
		SH/AB/004	83.5	10.0	93.5	4.0	2.5
Mamu Formation	Onyeama	SH/MA1/005	79.3	15.7	95.0	3.6	1.4
	Proda	SH/MA2/004	84.0	12.8	96.8	2.2	1.0
Owelli Sandstone	Agbogugu	SH/AG/009	77.0	17.0	94.0	4.7	1.3
		SH/AG/010	76.4	19.0	95.4	3.2	1.4
		SH/AG/004	81.0	12.0	93.0	4.7	2.3
		SH/AG/013	79.0	14.0	93.0	5.0	2.0
		SH/AG/014	83.0	12.0	95.0	3.6	1.4
Nkporo Formation	Leru	SH/LE/009	74.0	19.0	93.0	4.5	2.5
		SH/LE/012	78.0	16.0	94.0	5.0	1.0
		SH/LE/014	85.0	10.0	95.0	3.8	1.2
		SH/LE/016	81.0	15.0	96.0	2.7	1.3
		SH/LE/017	75.6	18.0	93.6	4.3	2.1
		SH/LE/022	82.0	12.0	94.0	3.8	2.2

\*Qm = Monocrystalline quartz; Qp = Polycrystalline quartz; F = Feldspar; Lt = Lithic fragment; Qt = total quartz.

HC in g TOC. Such values according to Tissot & Welte, (1984) and Akande et al., (2005) indicate moderately rich source rocks with fair oil potential.

#### Type of Organic matter

The quality of organic matter content of a source rock determines the type of hydrocarbon generated (Tissot & Welte, 1984). Cross plots of hydrogen index versus  $T_{max}$  (Figure 19) and hydrogen index versus oxygen index (Figure 20) reveal Type III and Type IV kerogens. It is well known (e.g. van Krevellen, 1981) and many authors after him that type III kerogen is terrestrially derived, and dominated by vitrinite and lesser amount of inertinite (Nton et al., 2009) and produces less paraffinic oil. Though type III kerogen may contain terrestrially derived liptinite, but in an insignificant amount consisting of sporinite and resinite (e.g. Akande et al., 2005).

Peters (1986) suggested that at thermal maturity equivalent to a vitrinite reflectance of 0.6 % ( $T_{max} = 435^{\circ}\text{C}$ ), rocks with HI > 300 mg HC in 1 g TOC produce oil; those with HI between 150 mg HC/ in 1 g TOC and 300 mg HC in 1 g TOC produce oil and gas; those with HI between 50 mg HC/ in 1 g TOC and 150 mg HC/ in 1 g TOC produce gas and those with HI < 50 mg HC in 1 g TOC are inert. Arising from this study, only four samples: SH/MA/003 (Mamu Formation), SH/EN/007 (Enugu Shale), SH/LE/008 and SH/LE/021 (Nkporo Shale) contain HI between 50 mg HC in 1 g TOC and 150 mg HC in 1 g TOC. In actual fact, the  $T_{max}$  for the samples from Mamu Formation and Enugu shales are <435 °C which may not support this generalization. Therefore only two samples from Nkporo Shale (20 %) can be termed gas prone while the majority (80 %) are inert with HI < 50 mg HC in 1 g TOC.

**Table 5:** Summary of the Rock-Eval pyrolysis parameters

Sample No	Location	Formation	TOC (wt%)	TOC (wt%)			Tmax (°C)	Ro (%)	HI	OI	S2/S3	S1/TOC*100	S1+S2	PI
				S1	S2	S3								
SH/MA/003	Onyeama	Mamu Formation	2.63	0.05	1.86	0.38	429	0.57	71	14	0.03	2	1.91	0.03
SH/EN/001	Enugu-Ont. Exp.Rd.	EnuguSh.	2.09	0.02	0.72	1.16	429	0.57	34	56	0.03	1	0.74	0.03
SH/EN/004			2.21	0.02	1.01	0.15	428	0.56	46	7	0.02	1	1.03	0.02
SH/EN/007			3.98	0.03	2.97	1.48	429	0.57	75	37	0.01	1	3.0	0.01
SH/AG/004	Agbogugu	Owelli Sandstone	1.17	0.01	0.37	1.56	439	0.76	32	133	0.03	1	0.38	0.03
SH/AG/005			0.96	0	0.28	0.74	444	0.85	29	77	0	0	0.28	0
SH/LE/002	Leru	Nkporo Formation	2.28	0.02	0.88	1.15	426	0.52	39	50	0.02	1	0.90	0.02
SH/LE/008			3.59	0.05	4.13	1.84	438	0.74	115	51	0.01	1	4.18	0.01
SH/LE/013			0.89	0.01	0.28	0.5	421	0.43	31	56	0.04	1	0.29	0.03
SH/LE/021			2.86	0.04	4.04	0	436	0.7	141	0	0.01	1	4.08	0.01

\*Notes:

TOC - total organic carbon, wt. %

S1 - volatile hydrocarbon (HC) content, mg HC/g rock

S2 - remaining HC generative potential, mg HC/g rock

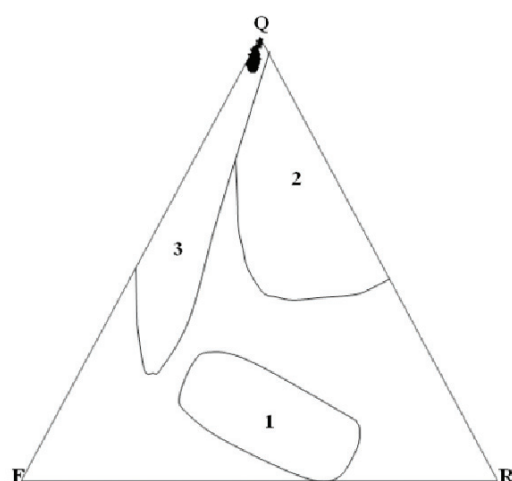
S3 - carbon dioxide content, mg CO<sub>2</sub>/g rock

PI - Production index = S1/(S2 + S2)

HI - Hydrogen Index = S2 × 100/TOC (mg HC in g rock)

OI - Oxygen index = S3 × 100/TOC, mg CO<sub>2</sub>/g TOC

Cal. R0/% = 0.018 03 × T<sub>max</sub> - 7.16



- 1 = Magmatic Arc Provenance
- 2 = Recycled Orogen Provenance
- 3 = Continental Block Provenance

**Figure 18:** Ternary plot of QRF showing paleotectonic settings (after Dickinson & Suczek, 1979) for the different formations discussed in this paper.

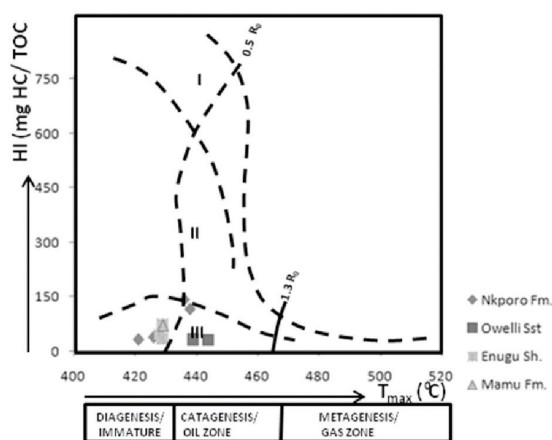


**Figure 19:** Classification of Kerogens on the HI-Tmax (adapted from Akande et al., 2005).

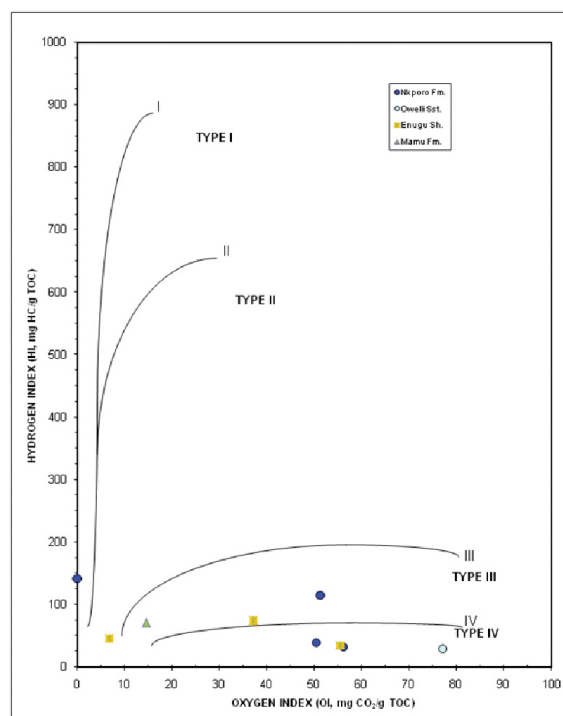


**Figure 20:** Plot of HI versus OI indicating the kerogen types (Note that all treated samples are of the Types III/IV i.e. vitrinite/inertinite-rich type of kerogen).

### Maturity of the organic matter

Thermal maturity describes the extent of heat-driven reactions which convert sedimentary organic matter into petroleum (Peters & Moldowan, 1993). In general, the extent of maturity depends on the relation of organic matter to the oil generation window. The  $T_{max}$  is a thermal stress parameter, dependent primarily on time/temperature conditions and can only

be approximately related to the stage of petroleum generation for the rock type.

The  $T_{max}$  values presented in Table 5 show that the sediments of Nkporo Formation have values between 421 °C and 444 °C, indicating immature to marginally mature organic matter. Arising from the low values of the hydrocarbon yield i.e. S2 (Table 5) maturity status based on the  $T_{max}$  appear unreliable in determining the maturity level. Based on the production index (PI) values range of between 0.00 and 0.03, it is quite certain that all the samples are thermally immature at the present level of consideration.

## Summary and conclusions

Outcrop samples from road cut exposures within the Anambra basin were sampled from the respective formations namely; Nkporo Formation, Owelli Sandstone, Enugu Formation, Mamu Formation and Ajali Sandstone for sedimentological characteristics, provenance, palaeoclimatic and tectonic deductions as well as appraise aspects of the hydrocarbon potential. Textural characteristics show that the sandstones are mainly moderately sorted, coarse to nearly symmetrical and leptokurtic. Cross plots of statistical parameters show that the sandstones are mainly fluvial deposits. The sandstones are mature with quartz content ranging from 93.0–96.8 %; feldspars from 2.2 % to 5.0 % while rock fragments are from 0.2–2.5 % and classify the treated sandstones as quartz arenites. Heavy mineral assemblages include zircon, tourmaline, garnet, apatite and rutile with ZTR maturity index ranging from 60 to 72 % (Ajali Sandstone); 57–61 % (Mamu Formation), 57–73 % (Owelli Sandstone) and 52–70 % (Nkporo Formation). These indicate a source in basement rocks, mainly the metamorphic and igneous rocks sourced from the Adamawa-Abakaliki folded belt and Oban massif which were rifted, uplifted and within a humid climatic setting.

Organic matter content is adequate, immature with Types III and IV kerogen that indicate terrestrial derivation. It is envisaged that there is the possibility of securing mature sediments with moderate oil potential at depth, particularly within the Nkporo Shale and Enugu Shale.

## Acknowledgements

The authors are grateful to the staff and management of State Key Laboratory of Organic Geochemistry, Chinese Academy of Science, Guangzhou, China, for assistance in laboratory analysis. The corresponding author also appreciates the cordial working relationship with colleagues and students at the Department of Geology, University of Ibadan, Nigeria.

## References

- Agagu, O. K. Fayose, E. A. & Petters, S. W. (1985): Stratigraphy and sedimentation in the Senonian Anambra Basin of eastern Nigeria. *Journal of Mining and Geology*; Vol. 22, No. 1, 26–36.
- Bankole, S. A. (2011): Sedimentological and Geochemical studies of part of the Post–Santonian sediments within the Anambra Basin, Southeastern Nigeria. Unpublished M.Sc Dissertation, Department of Geology, University of Ibadan, Nigeria; 133p.
- Akaegbobi, I. M. (2005): The Crabs eye-view of the organic sedimentological evolution of the Anambra basin, Nigeria: Hydrocarbon source potential and economic implications, Faculty of Science, University of Ibadan Lecture, University of Ibadan Press, 42p.
- Akande, S. O. & Erdtmann, B. D. (1998): Burial metamorphism (thermal maturation) in Cretaceous sediments of the Southern Benue Trough and Anambra Basin, Nigeria. *American Association of Petroleum Geologist Bull.*; Vol. 82, No. 6, 1191–1206.
- Akande, S. O., Ojo, O. J., Erdtmann, B. D. & Hetenyi, M. (2005): Paleoenvironments, organic petrology and Rock-Eval studies on source rock facies of the Lower Maastrichtian Patti Formation, Southern Bida Basin, Nigeria. *Journal of African Earth Sciences*, Vol. 41, 394–406.
- Akarish, A. I. M. & El-Gohary, A. M. (2008): Petrography and geochemistry of Lower Paleozoic sandstones, East Sinai, Egypt: Implications for provenance and tectonic setting. *Journal of African Earth Science*, Vol. 52, 43–54.
- Benkheilil, J. (1989): The origin and evolution of the Cretaceous Benue Trough, Nigeria. *Journal of African Earth Science*, Vol. 8, 251–282.
- Burke, K. C., Dessavaugie, T. F. J. & Whiteman, A. J. (1972): Geological history of Benue valley and adjacent areas. In: Dessavaugie, T. F. J. & Whiteman A. J. Ed. *African Geology*, University of Ibadan Press, Nigeria, 187–205.
- Dickinson, W. R. (1970): Interpreting detrital modes of greywacke and arkose. *Journal of Sed. Petrol.*, Vol. 40, 695–707.
- Dickinson, W. R. & Suczek, C. A. (1979): Plate tectonics and sandstone compositions. *American Association of Petroleum Geologists Bull.*, Vol. 163, 2164–2182.
- Feo-Codécico, G. (1956): Heavy mineral techniques and their application to Venezuelan Stratigraphy. *American Association of Petroleum Geologist Bull.*, Vol. 40, 948–1000.
- Folk, R. L. (1974): *Petrology of sedimentary rock*. Hemphil Book Store Austin, Texas, 78703, 182 pp.
- Friedman, G. M. (1961): Distinction between dune, beach and river sands from their textural characteristics. *Journal of Sed. Petrol.*, Vol. 70, 737–753.
- Hoque, M. (1977): Petrographic differentiation of tectonically controlled Cretaceous sedimentary cycle, southeastern Nigeria. *Sedimentary Geology*. Vol. 17, 235–245.
- Hubbert, J. F. (1962): A Zircon-Tourmaline -Rutile maturity index and interdependence of the composition of heavy mineral assemblages with the gross composition and texture of sandstones. *Journ. Sed. Petrol.*, Vol. 32, pp. 440–450.
- Ingersoll, R. V., Bullard, T. F., Folk, R. L., Grimm, J. P., Pickle, J. D. & Sares, S. W. (1984): The effects of grain size on data modes: a test of the Gazzi-Dickinson point counting method. *Journal of Sed. Petrol.*, Vol. 46, 620–632.
- Kogbe, C. A. (1989): *The Cretaceous and Paleocene sediments of southern Nigeria*. In: CA. Kogbe. Ed. 2nd ed. Lagos: Elizabeth Publishers; 273–286.
- Ladipo, K. O. (1986): Tidal shelf depositional model for Ajali Sandstone, Anambra Basin, southeastern Nigeria. *Journal of African Earth Sciences*; Vol. 5, No. 2, 177–185.
- Moiola, R. J. & Weiser (1968): Textural parameters: an evaluation. *Journal of Sed. Petrol.*, Vol. 260, 45–53.
- Nton, M. E. & Awarun, A. O. (2011): Organic geochemical characterization and hydrocarbon potential of subsurface sediments from Anambra basin, SE Nigeria. *Mineral Wealth*; Vol. 162, pp. 23–42.
- Nton, M. E., Ikhane, P. R. & Tijani, M. N. (2009): Aspect of Rock-Eval studies of the Maastrichtian-Eocene sediments from subsurface, in the eastern Dahomey Basin southwestern Nigeria. *European Journal of Scientific Research*; Vol. 25, No. 3, 417–427.
- Nwajide, C. S. (1990): Cretaceous sedimentation and paleogeography of Central Benue Trough. In:

- Ofoegbu, C. O. Ed. *The Benue Trough, Structure and Evolution*. International Monograph Series, Braunschweig; 19–38.
- Nwajide C. S & Reijers, T. J. A. (1996): Sequence architecture in outcrops: examples from the Anambra Basin, Nigeria. *Nigerian Association of Petroleum Explorationist Bull.*; Vol. 11, 23–33.
- Obi, G. C., Okogbue, C. O. & Nwajide, C. S. (2001): Evolution of the Enugu Cuesta: A tectonically driven erosional process. *Journal of Pure and Applied Sciences*; Vol. 7, No. 2, 321–330.
- Obi, G. C. & Okogbue C. O. 2003. Sedimentary response to tectonism in the Campanian-Maastrichtian succession, Anambra Basin, southeastern Nigeria. *Journal of African Earth Sciences* 4: 314–323.
- Olade, M. A. (1975): Evolution of Nigeria Benue Trough (Aulacogen): A tectonic model. *Geological Magazine*, Vol. 122, 575–583.
- Petters, S. W. (1978): Stratigraphic evolution of the Benue Trough and its implications for the Upper Cretaceous Paleogeography of West Africa. *Journal of Geology*; Vol. 86, 311–322.
- Peters, K. E. (1986): Guidelines for evaluating petroleum source rocks using programmed pyrolysis. *American Association of Petroleum Geologists Bull.*; Vol. 70, No. 3, 318–329.
- Peters, K. E. & Moldowan, J. M. (1993): *The biomarker guide: Interpreting molecular fossils in petroleum and ancient sediments*, Prentice Hall: Englewood Cliff, NJ.
- Pettijohn, F. J., Potter, P. E. & Siever, R. (1973): *Sand and sandstones*. 1st ed. Springer Verlag, New York, pp. 250.
- Reyment, R. A. (1965): In: *Aspects of Geology of Nigeria*. Ibadan University Press, pp. 145.
- Sahu, B. K. (1964): Depositional mechanisms from the size analysis of clastic sediments. *Journal of Sed. Petrol.*, Vol. 34, 73–83.
- Simpson, A. S. (1954): The Nigerian coal field. The geology of parts of Owerri and Benue Provinces. Geological Survey of *Nigeria Bull.*; Vol. 24, pp. 85.
- Stewart, H. B, Jr. (1958): Sedimentary reflections of depositional environments in San Miguel Lagoon, Baja, California, Mexice. *American Association of Petroleum Geologists Bulletin*; Vol. 42, 2567–2618.
- Suttner, L. J., Basu, A. & Mack, G. H. (1981): Climate and origin of quartz arenite. *Journal Sed. Petrol.*; Vol. 51, No. 4, 1235–1246.
- Tijani, M. N., Nton, M. E. & Kitagawa, R. (2010): Textural and geochemical characteristics of the Ajali Sandstone, Anambra basin, SE Nigeria: Implication for Its provenance. *C. R. Geoscience.*; Vol. 342, 136–150.
- Tissot, B. P. & Welte, D. H. (1984): *Petroleum formation and occurrence*. 2nd ed. Springer-Verlag, Berlin, pp. 699.
- Tucker, M. E. (1996): *Sedimentary rocks in field*. 2nd ed. John Wiley & Sons Ltd, Baffin Lane, Chichester West Sussex PO19 1UD, England, pp. 152.
- Uma, K. O. & Onuoha, K. M. (1997): Hydrodynamic flow and formation pressures in the Anambra Basin, southern Nigeria. *Hydrological Sciences Journal*, Vol. 42, No. 2, 141–152.
- Visher, G. S. (1969): Grain size distribution and depositional processes. *Journ. Sed. Petrol.*; Vol. 39, 1074–1106.

# Life cycle assessment of an intermodal steel building unit

## Ocena trajnostnega cikla intermodulne jeklene gradbene enote

Darko Milanković<sup>1</sup>, Branislav Milanović<sup>1</sup>, Boris Agarski<sup>1</sup>, Milana Ilić<sup>1</sup>, Branislava Crnobrnja<sup>1</sup>, Aleš Nagode<sup>2</sup>, Borut Kosec<sup>2</sup>, Igor Budak<sup>1,\*</sup>

<sup>1</sup>University of Novi Sad, Faculty of Technical Sciences, Trg D. Obradovića 6, 21000 Novi Sad, Serbia

<sup>2</sup>University of Ljubljana, Faculty of Natural Sciences and Engineering, Aškerčeva 12, SI-1000 Ljubljana

\*Corresponding author. E-mail: igor.budak@gmail.com

### Abstract

To minimize and in the near future eventually eliminate the negative environmental impacts, such as emissions, waste, energy and excessive raw material consumption, the life cycle assessment of buildings is essential. This paper provides an insight in environmental life cycle assessment (LCA) of a typical intermodal steel building unit (ISBU).

**Key words:** Life Cycle Assessment (LCA), intermodal steel building unit, environmental impact

### Izveček

Za zmanjšanje in v bližnji prihodnosti tudi odpravo negativnih vplivov na okolje, kot so onesnaženje, odpad, prekomerno izkoriščanje energije in surovin, je ocena trajnostnega cikla zgradb neobhodna. V prispevku je prikazan primer ocene trajnostnega cikla (LCA) tipske intermodulne jeklene gradbene enote (ISBU).

**Ključne besede:** ocena trajnostnega cikla (LCA), intermodulne jeklene gradbene enote, vpliv na okolje

## Introduction

The built environment is a major contributor to both social and economic development and represents a large portion of real capital in many countries; but it's also a primary source of environmental impacts. Furthermore, existing building stock requires continuous investments for repair and renovations. The notion that building structures that would last for centuries is the best environmental solution to our problems does not match with our existing building use trends and knowledge of the built environment.

Buildings will be replaced with newer designs that are more suited towards the needs of future occupants. Energy is an essential input to every production, transport, and communication process and is thus a driver for the economy as well as social development of any nation. The building construction industry consumes 40 % of the materials, entering the global economy and generates approximately 45 % of the global output of greenhouse gases and the agents of acid rain. <sup>[1-3]</sup> The growing concern of environmental problems, such as global warming, which have been linked to the extended use of energy, has increased both the importance of all kinds of so-called "energy saving measures", and the necessity for an increased efficiency in all forms of energy utilization. <sup>[4]</sup> As a consequence of the latest reports on climate change and the need for a reduction in CO<sub>2</sub> emissions, huge efforts must be made in the future to conserve high quality, or primary energy, resources. <sup>[5]</sup> While consuming large amounts of energy, building industry has also caused a large burden on the environment due to the environmental emissions by the production of building materials and the running of building system. <sup>[6]</sup> Extraction or purification of materials from their natural ores is an activity that consumes energy, generates waste, and also contributes to environmental damage with negative impacts such as resource depletion, biological diversity losses, and other. On the other hand they provide the necessary infrastructure for many productive activities such as industries, services, commerce, and utilities, and thus satisfy a very basic human need. However, due to

this very basic nature of buildings, stakeholders in development sometimes do not consider the environmental impacts of building, especially in developing economies. <sup>[7]</sup>

## Methodology

As a significant tool of environmental management, life-cycle assessment has become an internationally recognized criterion. It is the basis for establishing an environmental policy and is generally used to guide the clean production, development of green production, and the environmental harmonization design. A life cycle assessment (LCA) is a technique to assess environmental impacts associated with all the stages of a product's life from cradle to grave (i.e., from raw material extraction through materials processing, manufacture, distribution, use, repair and maintenance, and disposal or recycling). LCA can help avoid a narrow outlook on environmental concerns by <sup>[8]</sup>:

- compiling an inventory of relevant energy and material inputs and environmental releases,
- evaluating the potential impacts associated with identified inputs and releases, and
- interpreting the results to help make a more informed decision.

The LCA process is a systematic, phased approach and consists of four components <sup>[9,10]</sup>:

- goal definition and scoping,
- inventory analysis,
- impact assessment, and
- interpretation.

The goal of this study is to estimate the environmental impacts of a typical intermodal steel building unit (Figure 1 and Table 1).

The system studied includes the part of a life cycle of the building, including manufacturing of building materials, construction, operation, and maintenance. For the demolition and disposal stage, due to lack of relevance data, land-filling is assumed. Transport for each life cycle stage was also included. Only the structure and envelope of the selected building are assessed. Special emphasis is put on energy consumption. The functional unit for this estimation was defined as one intermodal steel building unit



**Figure 1:** Intermodal steel building unit (ISBU).

**Table 1:** Input data gathered for assessment of ISBU

Building parameters	Specifications
Dimensions	12.2 m × 2.4 m × 2.6 m
Service life	approx. 25 years
Floor area	approx. 30 m <sup>2</sup>
Office volume	67.7 m <sup>3</sup>
Structure	Construction steel
Envelope	Construction steel
Foundation	Reinforced concrete
Coverings	Gypsum, Plaster, Insulation
Floor finish	Linoleum
Windows	PVC

for a period of 25 years which is used for office purpose (Figure 2).

The second step of the LCA is inventory analysis. It contains the data collection and calculation procedures, and is of key importance since this data will be the basis for the study. Inventory is also tied to the scoping exercise since data collection and other issues may lead to refinement or redefinition of the system boundaries. Data needed were gathered from EcoInvent Database v2.2 and other scientific and technical publications and sources.<sup>[11, 12]</sup>

The LCA process has three major phases:

- building materials production phase,
- use phase, and
- the end of life phase.

Each of them includes production, transportation, and distribution.



**Figure 2:** Case study: Intermodal steel building units used for office purposes.

### **Life cycle assessment**

The assessment follows the LCI analysis first categorizes the impacts (resources consumption and emissions) into a range of impact categories. The characterization step is then performed, which converts the quantities of various types of impacts under each category into equivalent quantities of a reference impact (e.g. methane into an equivalent amount of CO<sub>2</sub> under the global warming category), yielding one single impact indicator for each impact category. Each impact indicator retains the unit of measurement of the quantity.

In this case, the BEES method is employed. BEES is the acronym for Building for Environmental and Economic Sustainability, a software tool developed by the National Institute of Standards and Technology (NIST). BEES combines a partial life cycle assessment and life cycle cost for building and construction materials into one tool. Results are presented in terms of life

cycle assessment impacts, costs, or a combination of both. BEES strives to assist the architect, engineer, or purchaser to choose a product that balances environmental and economical performance, thus finding cost effective solutions for protecting the environment. BEES uses the SETAC method of classification and characterization.

Characterization results are presented in Figure 3. The impact of ISBU is represented via 12 impact categories according to BEES methodology. Figure 4 presents the results of energy consumption compared during the production and installation stage and operation and use stage.

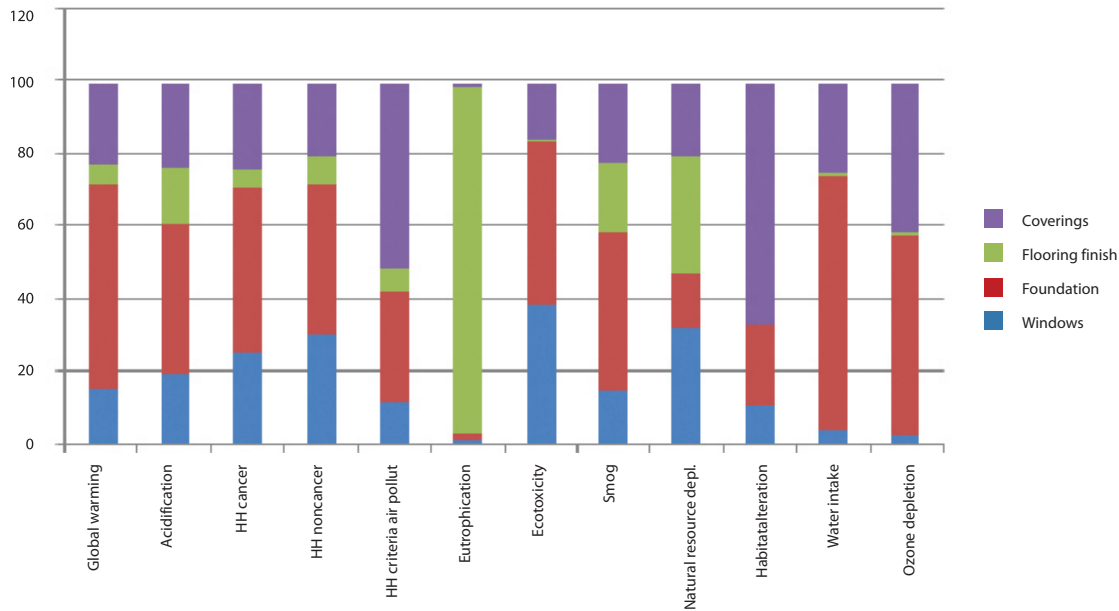


Figure 3: Characterization results of an ISBU production stage.

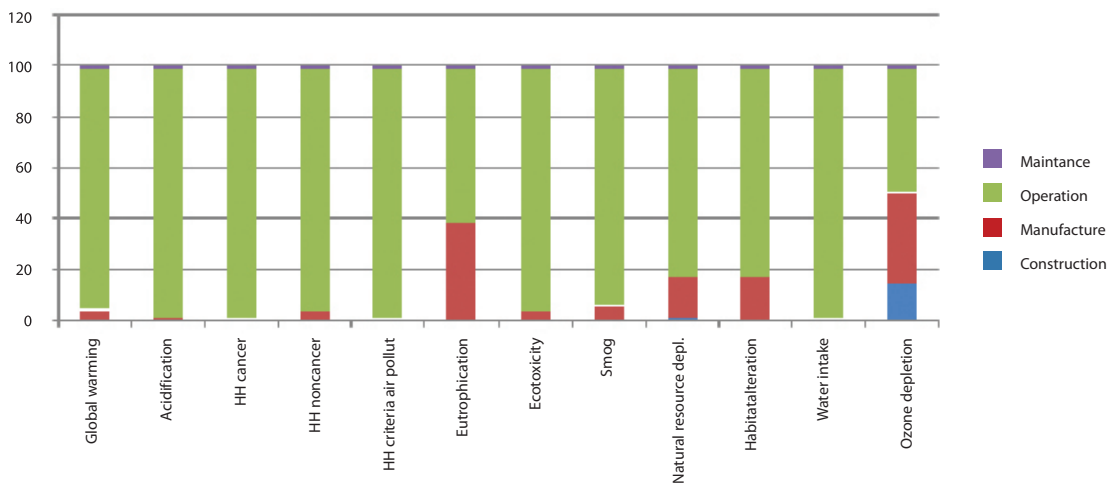


Figure 4: Characterization results of an ISBU regarding energy consumption.

## Discussion

Based on the results obtained, ISBU that is analyzed indicates certain problem areas observed in the product life cycle and that within three main impact categories:

- water intake,
- ozone depletion and
- global warming.

The largest impact within the above mentioned categories results from processes of cement production that is used for the foundation on which the object is installed and also steel from which structure and envelope is built. Processes observed in the use phase of the ISBU life cycle with its influence on the environment stands out from the rest, mainly because of the total electricity consumption in the assumed lifetime of 25 years. These problems can be successfully overcome if the existing structure is adapted to the rigorous requirements of a Leadership in Energy and Environmental Design (LEED) certification. A LEED certified office is designed and constructed in accordance with the rigorous guidelines of the LEED for offices green building certification program. LEED for offices is a consensus developed, third party verified, voluntary rating system which promotes the design and construction of high performance green offices. Main advantages of ISBU modules are:

- strong building construction,
- earthquake proof,
- fire proof,
- strong, corrosion resistant construction steel,
- extreme security,
- recyclable - green construction and modifications,
- saves trees,
- unibody construction,
- ideal for multiple floors and levels,
- fast construction,
- insulation: bonds easily with space-age,
- ceramic insulations,
- easily adapted to prefab automation, and
- easily adapted to custom homes/offices.

Intermodal steel building units (ISBU) have become very popular and trendy for use as homes, storages, prefabs, and business construction purposes. Only recently has the world begun to

realize their value in housing, office construction, storage and emergency shelters. The possibilities are virtually endless.

## Conclusions

The goal of the presented study is the determination of the impact of intermodal steel building units (ISBU) life time on the environment. For materials and methods in discussed in this work, a combination of input-output and process analysis was used in assessing the potential environmental impact associated with the system under study according to the standard ISO 14040 methodology.

The study covered the whole life cycle of the ISBU including design, materials production, construction, occupation, maintenance, demolition, and disposal.

Globally, the main reason for so high interest in intermodal steel building units is off-course the relatively low cost of construction.

## Acknowledgement

A part of result presented in this paper is obtained in the framework of the project "Continuous quality improvement of products and processes throughout the entire life cycle", TR 114-451-1924/2011-02, supported by the Provincial Secretariat for Science and Technological Development of AP Vojvodina, Republic of Serbia.

## References

- [1] Kutz, M. (2007): *Environmentally Conscious Mechanical Design*, John Wiley & Sons, New Jersey.
- [2] Rebitzer, G., Ekvall, T., Frischknecht, R., Hunkeler D., Norris, G., Rydberg, T., Schmidt, W. P., Suh, S., Weidema, B. P., Pennington, D. W. (2004): *Life cycle assessment: Part 1: Framework, goal and scope definition, inventory analysis, and applications*, *Environment International*, Vol. 30, No. 5, 701–720.
- [3] Pennington, D. W., Potting, J., Finnveden, G., Lindeijer, E., Jolliet, O., Rydberg, T., Rebitzer, G. (2004): *Life cycle assessment Part 2: Current impact assessment*

- practice, *Environment International*, Vol. 30, No. 5, 721–739.
- [4] Osman, A., Ries, R. (2007): Life cycle assessment of electrical and thermal energy systems for commercial building, *International Journal of Life Cycle Assessment*, Vol. 12, No. 5, 308–316.
- [5] Borjesson, P., Gustavsson, L. (2000): Greenhouse gas balances in building construction: wood versus concrete from life-cycle and forest land-use perspectives, *Energy Policy*, Vol. 28, No. 9, 575–588.
- [6] Seliger, G. (2007): Sustainability in Manufacturing recovery of resources in product and material cycles, Springer Verlag, Berlin/Heidelberg.
- [7] Anderson, J., Shiers, D. E., Sinclair, M. (2002): The greenguide to specification: an environmental profiling system for building materials and components, Blackwell Science, Malden.
- [8] ISO 14040: Environmental Management–Life Cycle Assessment–Principles and Framework. International Organization for Standardization (ISO), Paris, 2006.
- [9] Suh, S., Huppes, G. (2005): Methods for Life Cycle Inventory of a product. *Journal of Cleaner Production*, Vol. 13, No. 7, 687–697.
- [10] Burchart – Korol, D. (2011): Significance of environmental life cycle assessment (LCA) method in the iron industry. *Metalurgija*, Vol. 50, No. 3, 205–208.
- [11] Kosec, B., Senčič, S., Sokovič, M., Karpe, B. (2008): Foundry waste management; *International journal for quality research*, Vol. 2, No. 2, 129–133.
- [12] Abele, E., Anderl, R., Birkhoffer, H. (2005): Environmentally – Friendly Product Development, Methods and Tools, Springer Verlag, London.

# Mineralogical and chemical characterization of major basement rocks in Ekiti State, SW-Nigeria

## Mineraloške in kemične značilnosti glavnih kamnin podlage v državi Ekiti v JZ Nigeriji

Abel O. Talabi<sup>1,\*</sup>

<sup>1</sup>Ekiti State University, Faculty of Science, Department of Geology, Ado-Ekiti, Nigeria

\*Corresponding author. E-mail: soar\_abel@yahoo.com

### Abstract

Mineralogy and chemical composition of rocks constitute a reliable means of rocks' classification. Migmatite which occur in association with quartz schist/quartzite, Pan African Granites and charnockitic bodies around Ekiti State, southwestern Nigeria, were studied with a view to elucidate their mineralogical, compositional characteristics and their evolution.

Mineralogical determinations from optical studies revealed a high proportion of granular quartz and accessory muscovite in the quartz schist/quartzite. The migmatite on the other hand comprises mainly of quartz and feldspar (volume fractions  $\leq 70\%$ ) with minor muscovite, biotite and opaque minerals. Both Pan-African granite and charnockitic rocks have similar mineralogical composition with quartz and feldspar as dominant minerals. However, the charnockites have more mafic minerals compared to the granites.

Chemical analysis of the rocks involving major elements revealed the siliceous nature of all the rock units (migmatites, quartz-schist/quartzite, granites and the charnockites) in the study area. Three oxides ( $\text{SiO}_2$ ,  $\text{Al}_2\text{O}_3$  and  $\text{Fe}_2\text{O}_3$ ) constitute about 70–75 % of the chemical composition in migmatites, granites and the charnockites while in quartz-schist/quartzite, it was over 80 %. The chemical compositions as well as different variation plots suggest sedimentary origin for the granite, migmatite and quartz-schist/quartzite rocks while the charnockite has a preference for igneous source. The  $(\text{Na}_2\text{O}+\text{K}_2\text{O}) - \text{CaO}$  versus  $\text{SiO}_2$  plot indicated that majority of the rock units (migmatite, granite and charnockite) are in alkali-calcic and calcic-alkali categories while quartz-schist/quartzite is of calcic affinity.

**Key words:** mineralogy, Ekiti State, optical studies, major elements, Igneous source

### Izvleček

Mineraloška in kemična sestava kamnin je zanesljiva osnova za njihovo klasifikacijo. Razvit je migmatit v združbi s kremenovim metamorfnim skrilavcem/kvarцитom. V študiji so preiskovali panafriške granite in charnokitska telesa z namenom pojasniti značilnosti njihove mineraloške in kemične sestave ter njihov razvoj. Z mineraloško optično preiskavo so ugotovili v kremenovem metamorfnem skrilavcu/kvarcitu velik volumenski delež zrnatega kremenca in akcesorni muskovit. Po drugi strani vsebuje migmatit predvsem ( $\leq 70\%$ ) kremen in glinenec s podrejenim muskovitom, biotitom in neprozornimi minerali. Panafriški graniti in charnokitske kamnine imajo podobno mineraloško sestavo s prevladujočima kremenom in glincem, vendar vsebujejo charnokiti v primerjavi z graniti več mafičnih mineralov.

Kemične analize glavnih elementov so razkrile silicijsko naravo vseh kamninskih enot (migmatitov, kremenovega metamorfnega skrilavca/kvarcita, granitov in charnokitov) na raziskovanem območju. Trije oksidi ( $\text{SiO}_2$ ,  $\text{Al}_2\text{O}_3$  and  $\text{Fe}_2\text{O}_3$ ) obsegajo kar 70–75 % kemične sestave migmatitov, granitov in charnokitov, medtem ko je ta delež pri kremenovem kristalastem skrilavcu/kvarcitu več kot 80 %. Kemična sestava in različni variacijski diagrami nakazujejo sedimentno poreklo granitnih, migmatitnih in kremenovo metamorfno skrilavih/kvarcitnih kamnin in prednostno magmatski vir charnokita. Diagram  $(\text{Na}_2\text{O}+\text{K}_2\text{O}) - \text{CaO}$  s  $\text{SiO}_2$  prikazuje, da pripada večina kamnin (migmatit, granit in charnokit) alkalijsko-kalcijevim in kalcijsko-alkalijskim kategorijam, le kremenov kristalasti skrilavec/kvarcit kalcijski.

**Ključne besede:** mineralogija, država Ekiti, optične preiskave, glavne prvine, magmatsko poreklo

## Introduction

Ekiti State in Southwestern Nigeria is underlain primarily by the basement complex rocks of Pre-Cambrian age comprising gneisses and migmatites, quartz-schist/quartzite, Pan-African granites and charnockite with migmatites covering over 50 % of the whole area (Talabi & Tijani, 2011).

Most rocks are made up of major and trace elements. These rocks components are subjected to intensive weathering processes especially in the tropical area (like Ekiti State) with subsequent release of regolith products into the groundwater of the area. The weathering processes are characterized by intensive desilicification and ionic lost from the rock forming minerals. Crystalline rocks are formed by interlocking silicate minerals such as quartz, feldspars, micas, hornblende, pyroxenes, olivine and a host of minor accessories. Chemical weathering involves the dissolution of these minerals resulting in the formation of both soluble as well as solid phase products. History of the various transformations are documented in form of mineralogical and chemical dynamism of the rock.

A diligent search revealed scanty literature on the subject matter regarding the study area. Many of the research works in the study area were on geophysical assessment of the groundwater potential and hydrochemistry. Owoade et al. (1989) worked on hydrogeology and water chemistry in the weathered crystalline rocks of southwestern Nigeria and concluded that kaolinite was found to be the stable clay weathering product and that groundwater resides in the weathered regolith in the area. Bolarinwa & Elueze (2005) also reviewed the geochemical trends in the weathered profiles above granitic gneiss and schist of Abeokuta area, southwestern Nigeria. The research indicated that the  $Fe_2O_3$  rich laterite is low in  $Na_2O$ ,  $K_2O$ ,  $CaO$  and  $MgO$  due to the removal of alkaline and earth elements, through leaching of the topsoil and laterite. Emofurieta & Salami (1993) while looking on the geochemical dispersion patterns associated with laterization process at Ile-Ife reported that the soils derived from the melanocratic bands are  $SiO_2$  rich, compared to soils derived from the leucocratic bands. Based

on their average  $SiO_2/Al_2O_3 + Fe_2O_3$  ratios, the soils derived from the melanocratic bands are lateritic whilst the leucocratic derivatives are non laterite. This study therefore was to characterise the major basement rocks in Ekiti state using mineralogy and chemistry of the rocks.

## Study area

Ekiti State is located between latitudes  $7^{\circ} 15' - 8^{\circ} 5' N$  and longitudes  $4^{\circ} 44' - 5^{\circ} 45' E$  covering an approximate area of about 6 353  $km^2$  (Figure 1). The area lies entirely in the tropical climate with two distinct seasons; rainy and dry seasons. These two seasons have elastic boundaries in view of the recent global climatic variability. However, in general, on yearly basis, the rainy season commences in April and terminates in October while the dry season spans through November to March. The temperature is high throughout the year (mean annual temperature is  $27^{\circ} C$ ). The relative humidity is high (60–80 %) most months of the year while the mean annual rainfall is 1 500 mm. The study area is located in a hummocky terrain having a well pronounced undulating topography with prominent hills characterized by steep slope with elevation between 200 m and 500 m above mean sea level. Prominent hilly features include inselbergs, whalebacks and other categories of residual hills which are commonly associated with massive granite bodies. The inselbergs are striking feature of the Pan African granites occurring as picturesque prominent hills, rising sharply above their surrounding plains.

### *Geology of the study area*

The study area is an Archaean-Early Proterozoic terrain underlain by the basement complex of southwestern Nigeria (Clark, 1985, Alagbe & Raji, 1990, Oyinloye & Ademilua, 2005). Furthermore, Oversby (1975) and Olarewaju (1981), indicated that the study area is composed of migmatite-gneiss-quartzite complex, with supracrustal rocks relics. In this study, geological appraisal through systematic mapping reveal the following distinguishable lithologies namely: Migmatite-gneiss, Quartzite/Quartz-Schist, the Pan-African granite, Charnockite, Aplite and Pegmatite (Figure 2). The

rocks are not evenly distributed but migmatites predominate, covering a greater proportion of the study area (Figure 2).

## Material and method

The principal aim of the study was to establish the basic mineralogy and fabric properties of major rock types in the study area. Twenty (20) fresh representative samples comprising of 5 samples each of migmatite, quartz-schist/quartzite, granite and charnockite were subjected to thin section study. The nature of outcrop, colour, texture, mineralogy and structures were noted on the field. As for the geochemical investigations, collected samples were dried at temperature of 60 °C, crushed using a jaw crusher and pulverized with the ball milling machine and sieved to 80 mesh. Elemental compositions of the rocks were determined using Atomic Absorption Spectrophotometer (Unicam 969 model).

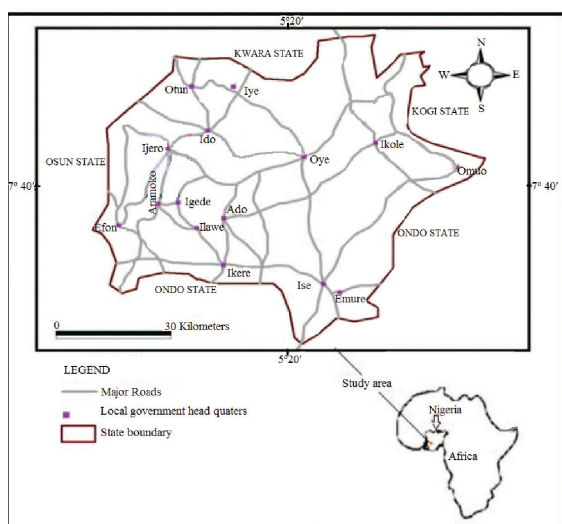


**Figure 1:** Location map of Nigeria showing the study area (Talabi & Tijani, 2011).

Ten (10) grams of each sample was weighed and put in a clean digestion bottle. Using a calibrated plastic syringe, 15 ml of 40 % hydrochloric acid was added with the help of an automatic pipette. Subsequently, ten (10 ml) of hydrofluoric acid was added. To avoid the escape of silicon fluoride ( $\text{SiF}_4$ ) gas during mixing of the two acids the digestion bottle was

tightly closed. The digestion bottle was later put on a water bath and warmed up to 70 °C for about two hours and allowed to cool down to 25–30 °C. A 100 ml saturated boric acid was added to the solution and the bottle was closed tightened. The bottle was put on a water bath up to 70 °C until the milky solution became clear. Distilled water was added to it after cooling to make a solution of 250 ml; part of distilled sample was put in a sample container which was then analyzed with a dilution factor of 25. Major elemental oxides such as  $\text{SiO}_2$ ,  $\text{Al}_2\text{O}_3$ ,  $\text{K}_2\text{O}$ ,  $\text{Na}_2\text{O}$ ,  $\text{CaO}$ ,  $\text{MgO}$ ,  $\text{Fe}_2\text{O}_3$  and  $\text{TiO}_2$  were obtained using Atomic Absorption Spectrophotometer (Unicam 969 model) with a precision of +0.5. The geochemical results were subjected to variation plots to infer the petrogenesis of the rocks.

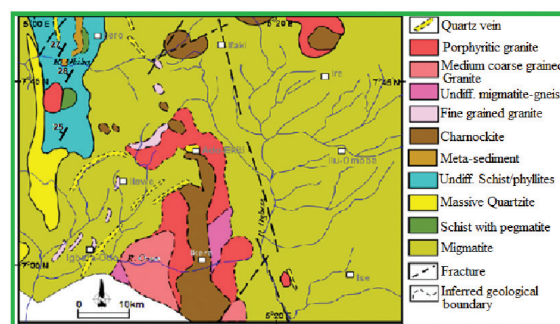


**Figure 2:** Geologic Map of Study area (Talabi & Tijani, 2011).

## Results and discussion

### Field petrographic features

Generally, geological appraisal through systematic mapping revealed outcrops of gneisses and migmatites representing highly denuded hills while quartz-schist/quartzite, Pan-African granites (porphyritic and fine-medium grained) and charnockite commonly form ridges, hills and whalebacks in the study area. The rocks are not evenly distributed but migmatites predominate, covering a greater proportion of the study area. The Pan-African granites comprise of felsic and mafic minerals. The felsic minerals contain quartz, orthoclase, plagioclase feldspar and muscovite. Quartz is colourless, white and occasionally grey in colour while orthoclase display white, pink or buff grey colour. Plagioclase feldspar is often white, pink, grey or

dark grey coloured while muscovite is the flaky mineral of the mica group displaying colourless colour. The mafic group comprise of the black coloured biotite and the dark green to black hornblende. The biotite is differentiated from hornblende in terms of hardness. The former has a hardness range of 2–2.5 and can easily be scratched with a pen-knife while the later range of hardness is 5–6 on the Mohs scale of hardness.

### ***Gneisses and migmatites***

Gneisses and Migmatites cover over 65 % of the study area (Figure 2) into which the other successions of rocks have been emplaced. Typical outcrops of migmatites and gneisses in the study area are presented in Figures 3(a–d). Field observation revealed close structural relationship between quartzite and the intrusive granitic and charnockitic rocks. Migmatite rock exposures occur as highly denuded hills of essentially fine texture while the pegmatites are very coarse-grained with phenocrysts of feldspar over 2500 mm in length, usually of granitic composition and forming at a late stage of crystallization. In the study area, the migmatite-gneiss rocks composed of a mafic portion, made up of biotite, hornblende and opaque minerals while the felsic portion is quartzofeldspatic. Compositional variation in the rock outcrops are indicated by closely spaced alternating bands of leucocratic minerals (quartz and feldspars) and melanocratic minerals indicated by the preponderance of biotite minerals (Figure 3a). The banded gneisses with alternating parallel light and dark coloured bands are common in the study area especially at Ado, Iworoko, Ikere, Ise and Emure. Figure 3c shows drag folds of leucocratic veins and ptymatic structures while figure 3d represents a typical granite gneiss at Ado-Ekiti with alternating light and dark coloured bands.

### ***Quartz-schist/quartzite***

Quartz-schist/quartzite is a hard, non foliated metamorphic rock derived from sandstone during tectonic compression, a process where heat and pressure beneath the ground increases to form new rocks. Found on hills and mountains, quartzite endures little wear or decomposition based on its elevated locations.

The quartz-schist/quartzite in the study area exhibits white to gray colour due to varied iron oxide content in the rock. A few good massive quartzite outcrops rising up to 100 m above the surrounding terrain occur around Ado-Ekiti, while the ones at Ikogosi are highly schistose with muscovite flakes littering its environment. However, around the south western part of Ilawe-Ekiti, the quartzite rock exists as rubbles. Quartzite is very resistant to chemical weathering and often forms ridges and resistant hill-tops. The nearly pure silica content of the rock provides little to soil formation and therefore the quartzite ridges are often bare or covered only with a very thin layer of soil and little vegetation.

### ***The Pan-African granites***

The Pan-African granites (ca. 600 Ma) occur as intrusions within the migmatite-gneiss-quartzite complex (Oyinloye, 2002, Oyinloye, 2011, Folorunso & Okonkwo, 2011, Omosanya et al., 2012 and Okonkwo & Folorunso, 2013). The granitic rocks outcropped as domes and small hills in the area. The granites are distinguishably unique because of their visible minerals, lack of foliation, fine-medium grained texture (Figure, 3e) and compact interlocking crystals that developed during the crystallisation of magma. However, granitic rocks of porphyritic texture (Figure 3f) occur around Ado-Ekiti, Ikere-Ekiti and close to Ikole-Ekiti. Some of the outcrops occur as well-rounded boulders devoid of any preferred orientation of component minerals. The contact relationship of the Pan-African granites with the surrounding country rock are abrupt in few cases while most are gradational over very short distances. Generally, the porphyritic granite is light coloured with signs of having been fairly weathered.

### ***Charnockites***

The charnockitic rocks outcropped as pavement and oval or semi-circular hills of between five and ten meters (10 m) high with a lot of boulders at some outcrops. They are generally massive, dark-greenish in colour with medium to coarse grained texture. The fresh outcrops with little or no sign of weathering have a lot of quartz, aplite and pegmatite intrusions occurring in it. The general trend of the intrusions

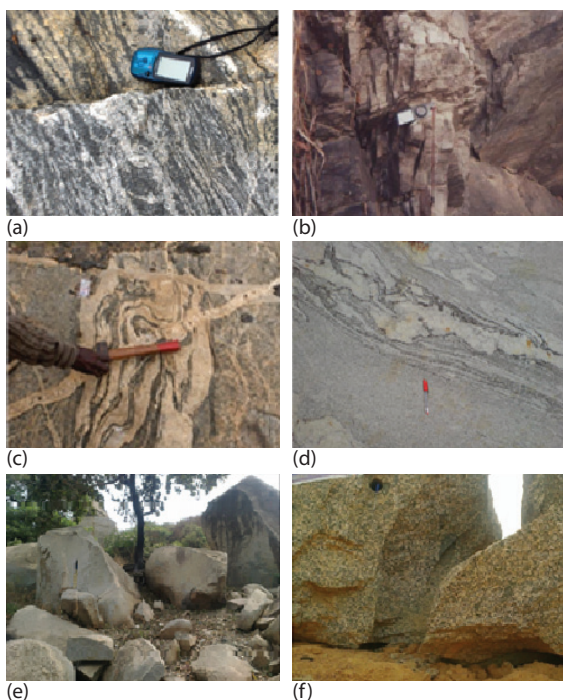


**Figure 3:** Typical rock outcrops from the study area [(a) Migmatite, (b) Migmatite outcrop with pegmatite intrusion, (c) and (d) Granite gneiss, (e) Fine-medium grained granite, (f) Porphyritic granite.

is N-S. The dominant trend of the joints that occur on the rock is N-S. The rock outcropped around Ado, Ikere, Otun, Ifaki, Itapa and Ikole areas. Two mode of charnockite occurrence have been revealed through field observation. The charnockites that occur along the margins of Older Granites bodies especially the porphyritic granites as exemplified by the charnockitic outcrops in Ado, Ikere and Igbara-Odo areas. The other mode of occurrence comprise of charnockites that aligned in a NW-SE direction as shown by the charnockitic rocks at Oye, Itapa and Ijelu areas. The contact relationship of the charnockites to the surrounding rocks is variable. In some places on the one hand, gradational contact was observed between the charnockites and the surrounding Older Granites while on the other hand the contact is abrupt from migmatitic and granitic gneisses to the charnockitic rocks.

At Ifaki, the charnockites showed cross-cutting intrusive contacts with surrounding country rocks while at Ikere, the charnockites appear on slightly weathered surfaces said to have been broken up into xenolithic blocks by a foliated porphyritic granite. Furthermore, on the

fresh surfaces, it is difficult to distinguish the contact between the granite and charnockite because the feldspars of the granite have the same greenish colour as the feldspars in the charnockite. However, the colouration fades away with increased weathering of the charnockite. Megascopic examination with the aid of hand lens revealed the presence of quartz, alkali feldspar, plagioclase and biotite as major minerals in the charnockitic rocks in the study area.

In summary, field observations highlight gneiss and migmatite, granite, quartz-schist/quartzite and Charnockite as major rock units in the study area with variable mineralogical composition. Granite contains more minerals that are susceptible to weathering i.e. high percentage of mafic minerals (biotite and hornblende) which got easily weathered because the iron (Fe) in their crystals structures can easily be oxidized. However, the quartz in such rocks will show mild resistance to weathering. The weathering of rocks and minerals are significant to mineral and chemical evolution of rocks.

#### ***Microscopic evaluation of rocks in the study area***

Thin section petrography of the migmatite/gneiss shows abundance of feldspar (microcline), quartz, muscovite, biotite and opaque minerals. Microcline occurs as large euhedral crystals exhibiting cross hatched twinning, biotite content is low, occur in disoriented masses and mineral alignment is poorly developed. Other minor components include ferromagnesian minerals like hornblende (Figures 4 & 5). Quartz and feldspar alone constitute up to volume fractions 70 % of the rock in thin section (Table 1). Feldspar is second to quartz in abundance while minerals such as garnet and magnetite constitute the opaque minerals.

The quartzites/quartz-schist shows predominance of quartz, accessory muscovite and opaque minerals (Figures 6 & 7). Quartz occurs as granoblastic and euhedral crystals with well-defined outlines. It exhibits weak birefringence, low relief with wavy extinction. Few grains however appear cloudy. Muscovite that forms supporting minerals occupy intergranular spaces of interlocking quartz crystals and often is the platy brightly coloured minerals.

Quartz and muscovite constitute up to volume fractions 88 % of the rock in thin section (Table 2).

**Table 1:** Modal composition of Migmatite (in volume fractions)

Minerals	Sample 1	Sample 2	Sample 3	Average
Quartz	43	45	44	44
Feldspar	25	26	27	26
Hornblende	8	10	9	9
Pyroxene	-	-	-	-
Biotite	9	10	8	9
Muscovite	6	5	4	5
Opaque	9	4	8	7
Total	100	100	100	100

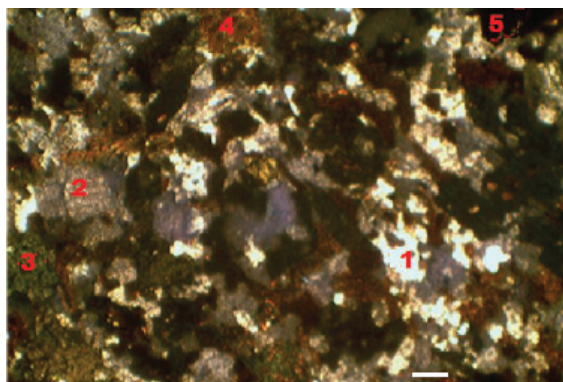


**Figure 4:** Photomicrograph of migmatite gneiss in transmitted light showing quartz (1), plagioclase (2), hornblende (3), biotite (4) and opaque mineral (5). Bar scale is 2 mm crossed polars.

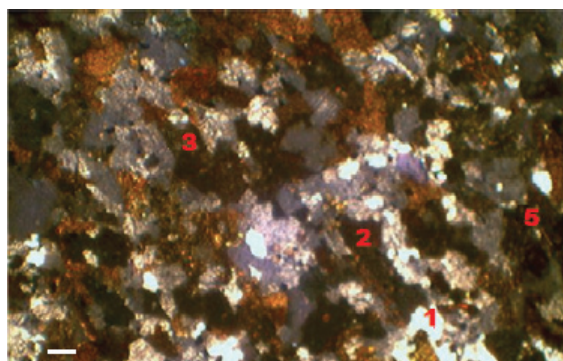


**Figure 5:** Photomicrograph of migmatite gneiss in transmitted light showing quartz (1), biotite (2), hornblende (3), microcline (4) and opaque mineral (5). Bar scale is 2 mm crossed polars.

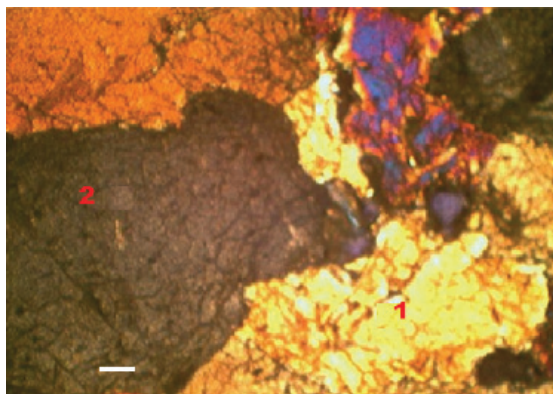


**Figure 6:** Photomicrograph of quartzite in transmitted light showing quartz (1) and muscovite (2). Bar scale is 2 mm crossed polars.

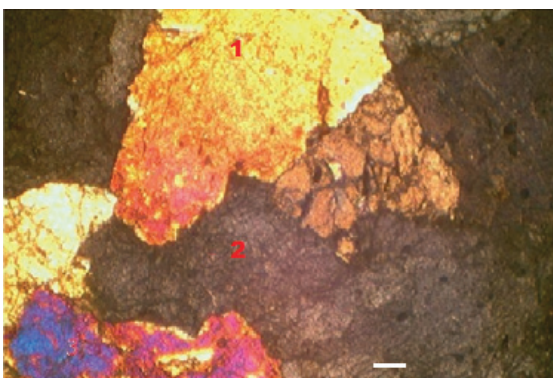


**Figure 7:** Photomicrograph of quartz-schist showing quartz (1), muscovite (2) and muscovite. Bar scale is 2 mm crossed polars.

**Table 2:** Modal composition of Quartzite (in volume fractions)

Minerals	Sample 1	Sample 2	Sample 3	Average
Quartz	59	57	58	58
Feldspar	-	-	-	-
Hornblende	-	-	-	-
Pyroxene	-	-	-	-
Biotite	8	7	9	8
Muscovite	29	31	30	30
Opaque	4	5	3	4
Total	100	100	100	100

Quartz, feldspars, hornblende, biotite and some opaque minerals (probably iron oxide) were the major minerals identified in thin section of the Pan-African granite. The feldspars are large, well-formed crystals of albite with carlsbad twinning. The hornblende content in the

granite is low. Quartz occurs as irregular masses of colourless and unaltered grains. Biotite is mainly the green and brown coloured minerals with medium relief. Figures 8 & 9 display the photomicrographs of porphyritic granite while Figures 10 & 11 represent that of fine-medium grained granite. In all the photomicrographs, quartz form the dominant mineral. All the quartz grains display low first order interference colour. Biotite displays the anomalous red colour interference. However, the polysynthetic twinning of plagioclase was not conspicuous.

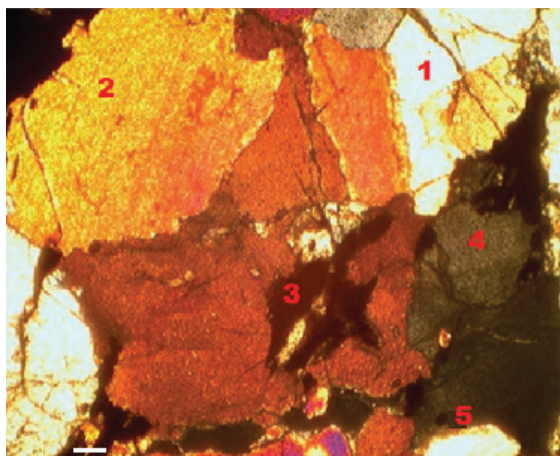


**Figure 8:** Photomicrograph of porphyritic granite in transmitted light showing quartz (1), muscovite (2), biotite (3), hornblende (4) and opaque mineral (5). Bar scale is 2 mm crossed polars.

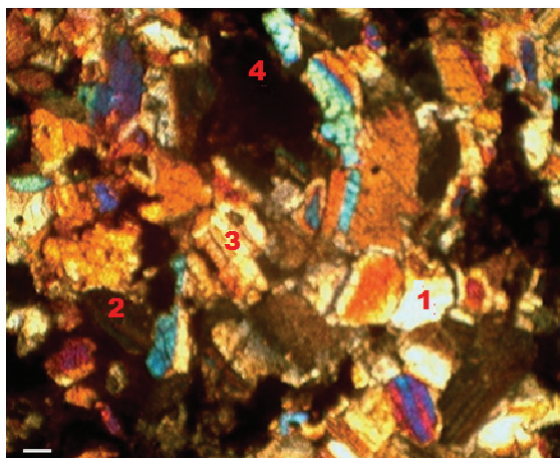


**Figure 9:** Photomicrograph of porphyritic granite in transmitted light showing quartz (1), hornblende (2), plagioclase (3) and biotite (4). Bar scale is 2 mm crossed polars.

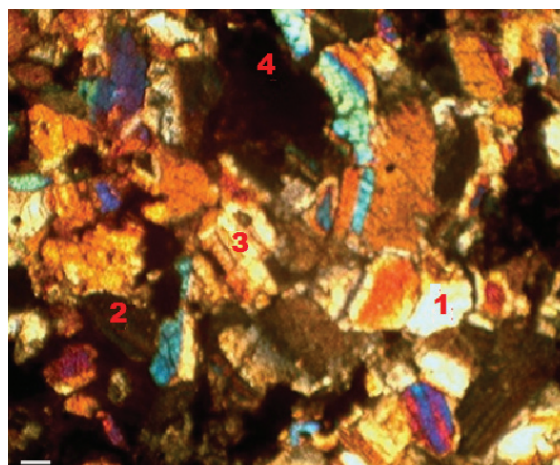


**Figure 10:** Photomicrograph of fine-medium granite in transmitted light showing quartz (1), biotite (2) and hornblende (3). Bar scale is 2 mm crossed polars.

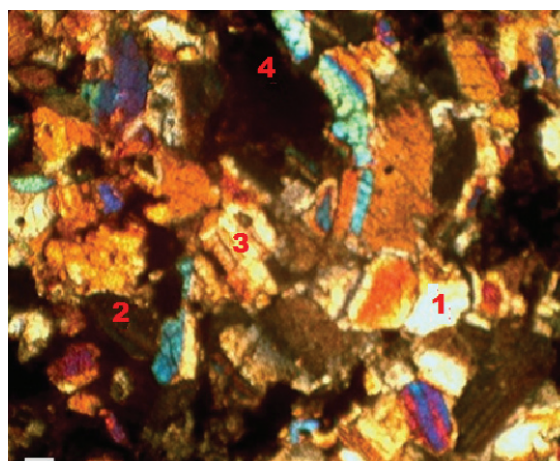


**Figure 11:** Photomicrograph of fine-medium granite showing biotite (1), quartz (2) and hornblende (3). Bar scale is 2 mm crossed polars.

The modal analysis of the thin sections of the porphyritic granite (Table 3) gave an average of (45, 15, 10, 8, 15, and 7) % quartz, feldspar, hornblende, biotite, muscovite and opaque mineral, respectively. Also, that of the fine-medium grained granite (Table 4) gave (48, 32, 5, 7 and 4) % quartz, feldspar, hornblende, pyroxene, biotite and opaque minerals, respectively.

**Table 3:** Modal composition of porphyritic granite (in volume fractions)

Minerals	Sample 1	Sample 2	Sample 3	Average
Quartz	45	44	46	45
Feldspar	13	18	14	15
Hornblende	8	9	13	10
Pyroxene	-	-	-	-
Biotite	8	9	7	8
Muscovite	16	14	15	15
Opaque	7	8	6	7
Total	100	100	100	100

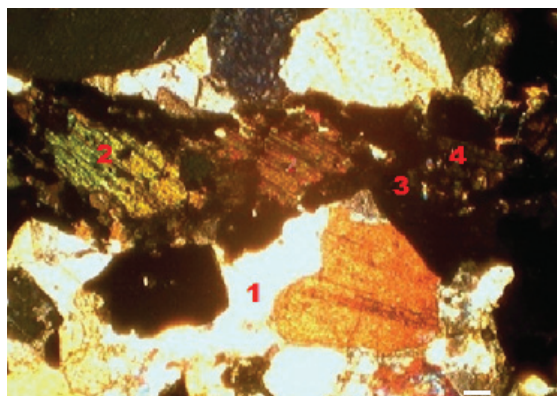
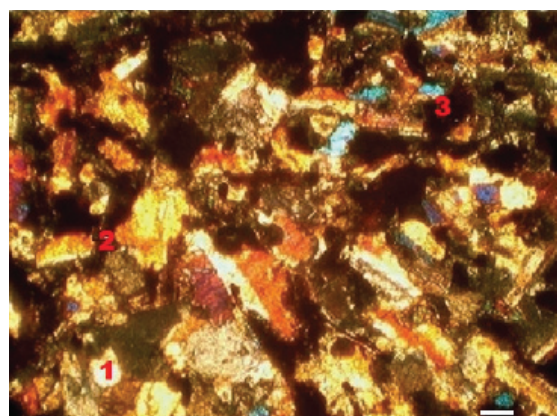
**Table 4:** Modal composition of fine-medium grained granite (in volume fractions)

Minerals	Sample 1	Sample 2	Sample 3	Average
Quartz	47	48	49	48
Feldspar	32	31	33	32
Hornblende	6	5	4	5
Pyroxene	7	9	5	7
Biotite	5	4	3	4
Muscovite	-	-	-	-
Opaque	3	3	6	4
Total	100	100	100	100

In thin section generally, the minerals constituting the charnockitic rock include quartz, plagioclase, hornblende, biotite, pyroxene, muscovite and opaque minerals (Figures 12 & 13). The modal analysis of the thin sections of the rock (Table 5) gave an average of (45, 35, 8, 5, 2, 3 and 2) % quartz, plagioclase, hornblende, pyroxene, biotite, muscovite and opaque minerals, respectively.

### Geochemistry

Geochemical analysis of five fresh samples of each rock unit was carried out and few variation diagrams were plotted to establish petrologic and petrogenetic processes of the basement rocks in the study area. The major elemental composition of the rocks in the study area is presented in Table 6.

**Figure 12:** Photomicrograph of charnockite in transmitted light showing quartz (1), plagioclase (2), biotite (3) and hornblende (4) Bar scale is 2 mm crossed polars.**Figure 13:** Photomicrograph of charnockite in transmitted light showing quartz (1), hornblende (2), and biotite (3). Bar scale is 2 mm crossed polars.**Table 5:** Modal composition of charnockite (in volume fractions)

Minerals	Location 1	Location 2	Location 3	Average
Quartz	47	44	45	45
Feldspar	33	37	35	35
Hornblende	7	9	8	8
Pyroxene	6	4	6	5
Biotite	2	3	1	2
Muscovite	2	1	3	3
Opaque	3	2	2	2
Total	100	100	100	100

In the migmatite rock unit,  $\text{SiO}_2$  concentration in mass fractions ranged from 66.50–69.80 %,  $\text{Al}_2\text{O}_3$  ranged from 14.65–15.46 %,  $\text{Fe}_2\text{O}_3$  ranged from 2.13–3.46 % (Table 6). This trend though with variations, was observed in other rock units as  $\text{SiO}_2$  in granite ranged from 71.89–75.02 % while  $\text{SiO}_2$  in charnockite ranged from 65.21–67.77 %. The  $\text{Al}_2\text{O}_3$  concentrations in granite and charnockite ranged from 14.98–15.68 % and 10.22–13.03 % respectively. The  $\text{Fe}_2\text{O}_3$  content in granites ranged from 2.19–2.44 % while it ranged from 2.81–4.16 % in the charnockitic rocks. These three oxides ( $\text{SiO}_2$ ,  $\text{Al}_2\text{O}_3$  and  $\text{Fe}_2\text{O}_3$ ) constitute about 70–75 % of the chemical composition of the rock units in the study area. The geochemical data were plotted on discriminatory diagrams to establish the geochemical evolution of the rock. The major element composition revealed different evolutionary trend for the various rock units as evidenced in Figure 14, showing a negative correlation with  $\text{Si}_2\text{O}$ . All the major element composition apparently decreased with increasing  $\text{Si}_2\text{O}$  content and showed medium to high-K affinity i.e fell mainly into the calc-alkaline and high-K calc-alkaline series as revealed in the plot of  $\text{K}_2\text{O}$  versus  $\text{SiO}_2$  (Figure 14) after Peccerillo & Taylor (1976). Furthermore, a plot of  $\text{Na}_2\text{O} + \text{K}_2\text{O}-\text{CaO}$  versus  $\text{SiO}_2$  diagram after Frost et al. (2001) (Figure 15) categorised most rock units into the alkali-calcic and calcic-alkali series. However, the quartz-schist/quartzite fell in the calcic group signifying abundance of quartz and muscovite in the rock unit. The overall decreasing trend of the various variation diagrams suggested high fractionation of mafic minerals like biotite.

The origin of the basement rocks of southwestern, Nigeria is controversial. Rahaman & Occan (1978) suggested that the charnockitic rocks were original igneous rocks which retained their anhydrous affinity during the Pan-African orogeny. Elueze, (1982) worked on the petrochemistry of Precambrian gneisses and migmatites in the western part of Nigeria, concluded that the varied petrochemical features of the rocks were considered to be related to the progenetic affinity of the rocks, implying that the units were derived from heterogeneous progenitors. Okunlola et al., (2009) suggested arenaceous sedimentary ancestry for

the quartz schist and an igneous ancestry most probably mafic extrusive volcanics for the amphibole schist in Ibadan area, southwestern Nigeria. In addition, provenance indicators, such as Ba, in the quartz schists suggested derivation of this sedimentary protolith from the weathering of largely granitic rocks. However, Ademeso & Adeyeye, (2011), suggested a preference for igneous fields by the granite gneiss of Arigidi area, S/W, Nigeria. Oyinloye, (2011) in his research work on “Geology and Geotectonic Setting of the Basement Complex Rocks in South Western Nigeria: Implications on Provenance and Evolution” discovered that a mineral monazite was present in the basement rocks (amphibolite and granite gneisses) at Ilesha area, southwestern, Nigeria. The implication of presence of monazite in the amphibolite which is supposed to be purely igneous is that the initial magma from which the precursor rocks were formed had input from a crustal or sedimentary source. Data from the present study when subjected to the plot of  $\text{K}_2\text{O}$  versus  $\text{Na}_2\text{O}$  (Pettijohn, 1975) indicates that migmatite, granite and quartz-schist/quartzite samples plotted in the field of arkoses while charnockite samples plotted in the greywackes (Figure.16). In addition,  $\text{Na}_2\text{O}/\text{Al}_2\text{O}_3$  versus  $\text{K}_2\text{O}/\text{Al}_2\text{O}_3$  plot (Garrells & Mackenzie, 1971) shows that granite plotted in the sedimentary field, quartz-schist/quartzite plotted in both fields while migmatite and charnockite plotted in the igneous field. However, further classification using the plot of alumina saturation versus alkalinity (after Maniar & Piccoli, 1989) i.e.  $[\text{Al}_2\text{O}_3 / (\text{Na}_2\text{O} + \text{K}_2\text{O}) \text{ vs. } \text{Al}_2\text{O}_3 / (\text{Na}_2\text{O} + \text{K}_2\text{O} + \text{CaO})]$  classified three of the rock units (migmatite, granite and charnockite) as peraluminous plotting mostly in the S – type field of Maniar & Piccoli (1989) granite classification diagram (Figure 18). Deductions from the various discriminatory diagrams suggest sedimentary origin for the granite, migmatite and quartz-schist/quartzite rocks while the charnockite has a preference for igneous source.

In summary, the major chemical composition of the analysed rock samples revealed  $\text{SiO}_2$ ,  $\text{Al}_2\text{O}_3$ ,  $\text{Fe}_2\text{O}_3$ ,  $\text{MgO}$ ,  $\text{CaO}$ ,  $\text{K}_2\text{O}$ ,  $\text{TiO}_2$ ,  $\text{P}_2\text{O}_5$ ,  $\text{MnO}$  as major oxides. Granite has more  $\text{SiO}_2$  content than the migmatite and charnockite. However, charnockite is richer in  $\text{Fe}_2\text{O}_3$  content. In addition,

variation diagram of  $(\text{Na}_2\text{O} + \text{K}_2\text{O}) - (\text{CaO})$  vs  $\text{SiO}_2$  diagram after (Frost, et al., 2001) indicates that most of the rocks in the study area are in

the alkali-calcic and calcic-alkali series and in the S – type peraluminous field suggesting sedimentary protolith.

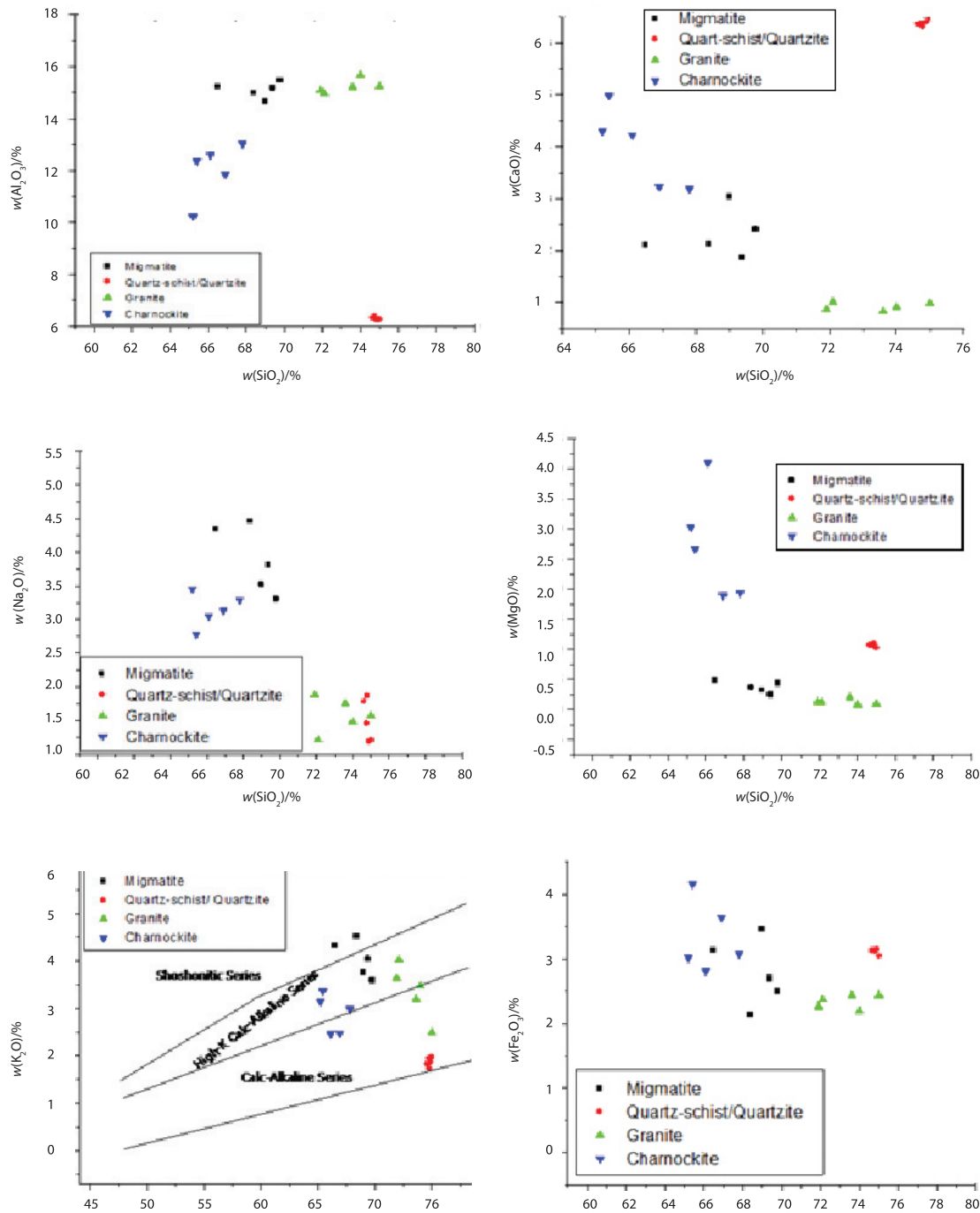


**Figure 14:** Harker diagrams showing variations of major element oxides with silica for the rocks in the study area. The  $\text{K}_2\text{O}$  vs  $\text{SiO}_2$  diagram after Peccerillo and Taylor (1976) indicates a high- $\text{K}$  affinity of the rock units.

**Table 6:** Chemical composition (in mass fractions) of rocks in the study area

Sample Code	Locality	SiO <sub>2</sub>	Al <sub>2</sub> O <sub>3</sub>	Fe <sub>2</sub> O <sub>3</sub>	MnO	CaO	MgO	Na <sub>2</sub> O	K <sub>2</sub> O	TiO <sub>2</sub>	P <sub>2</sub> O <sub>5</sub>	LOI	Total
<b>Rock Type</b>													
<b>Migmatite</b>													
Mf1	Oye	69.80	15.46	2.50	0.20	2.40	0.43	3.30	3.58	0.08	0.04	2.01	99.80
Mf2	Iworoko	69.40	15.18	2.70	0.34	1.86	0.24	3.80	4.04	0.09	0.06	2.21	99.92
Mf3	Are	68.40	14.98	2.13	0.38	2.12	0.36	4.46	4.51	0.10	0.05	2.35	99.84
Mf4	Igbemo	66.50	15.22	3.13	0.26	2.10	0.48	4.34	4.32	0.07	0.04	3.32	99.78
Mf5	Ogbesse	69.00	14.65	3.46	0.40	3.03	0.31	3.52	3.76	0.06	0.05	2.02	100.30
	Min.	66.50	14.65	2.13	0.20	1.86	0.24	3.30	3.58	0.06	0.04	2.01	
	Max.	69.80	15.46	3.46	0.40	3.03	0.48	4.46	4.51	0.10	0.06	3.32	
	Mean	68.60	15.10	2.78	0.32	2.30	0.36	3.88	4.04	0.08	0.05	2.38	
	Std. Dev.	1.29	0.30	0.52	0.08	0.45	0.10	0.51	0.38	0.02	0.01	0.54	
<b>Quartz - schist/quartzite</b>													
Q6	Ado	75.02	6.25	3.04	2.17	6.48	1.02	1.20	1.97	0.04	0.01	2.62	99.82
Q7	Ado	74.92	6.22	3.14	2.16	6.40	1.10	1.18	1.86	0.03	0.02	2.72	99.75
Q8	Ilawe	74.78	6.34	3.13	2.18	6.38	1.08	1.45	1.94	0.04	0.02	2.68	100.02
Q9	Ijero	74.80	6.28	3.12	2.17	6.31	1.06	1.86	1.72	0.03	0.03	2.63	100.01
Q10	Ogbesse	74.65	6.30	3.13	2.15	6.36	1.07	1.78	1.82	0.04	0.02	2.66	99.98
	Min.	74.65	6.22	3.04	2.15	6.31	1.02	1.18	1.72	0.03	0.01	2.62	
	Max.	75.02	6.34	3.14	2.18	6.48	1.10	1.86	1.97	0.04	0.03	2.72	
	Mean	74.83	6.28	3.11	2.17	6.39	1.07	1.49	1.86	0.04	0.02	2.66	
	Std. Dev.	0.14	0.05	0.04	0.01	0.06	0.03	0.32	0.10	0.01	0.01	0.04	
<b>Granite</b>													
Gf11	Ado	75.00	15.24	2.44	0.09	0.98	0.09	1.57	2.49	0.03	0.23	2.15	100.3
Gf12	Ado	72.10	14.98	2.37	0.12	1.01	0.12	1.21	4.02	0.05	0.15	2.05	98.13
Gf13	Itapa	74.00	15.68	2.19	0.10	0.91	0.08	1.48	3.47	0.02	0.03	2.04	100.00
Gf14	Ikere	71.90	15.10	2.26	0.08	0.86	0.13	1.88	3.64	0.04	0.11	2.16	98.15
Gf15	Oshin	73.60	15.22	2.43	0.11	0.82	0.20	1.75	3.19	0.06	0.01	2.28	99.63
	Min.	71.90	14.98	2.19	0.08	0.82	0.08	1.21	2.49	0.02	0.01	2.04	
	Max.	75.00	15.68	2.44	0.12	1.01	0.20	1.88	4.02	0.06	0.23	2.28	
	Mean	73.30	15.24	2.34	0.10	0.92	0.12	1.58	3.36	0.04	0.11	2.14	
	Std. Dev.	1.33	0.27	0.11	0.02	0.08	0.05	0.26	0.57	0.02	0.09	0.10	
<b>Charnockite</b>													
Cf21	Ado	66.1	12.58	2.81	0.1	4.22	4.11	3.05	2.46	1.13	0.61	2.8	99.95
Cf22	Ikere	65.2	10.22	3.02	0.21	4.3	3.03	3.45	3.14	1.01	0.56	3.55	97.70
Cf23	Afao	65.4	12.36	4.16	0.17	4.98	2.67	2.78	3.36	1.1	0.67	2.55	100.20
Cf24	Ire	66.9	11.85	3.64	0.15	3.22	1.89	3.13	2.47	0.98	0.71	2.82	97.75
Cf25	Igbole	67.8	13.03	3.08	0.14	3.18	1.94	3.29	2.98	1.04	0.53	3.18	100.20
	Min.	65.2	10.22	2.81	0.1	3.18	1.89	2.78	2.46	0.98	0.53	2.55	
	Max.	67.8	13.03	4.16	0.21	4.98	4.11	3.45	3.36	1.13	0.71	3.55	
	Mean	66.3	12.01	3.34	0.15	3.98	2.73	3.14	2.88	1.05	0.62	2.98	
	Std. Dev.	1.07	1.09	0.55	0.04	0.77	0.91	0.25	0.4	0.06	0.07	0.39	

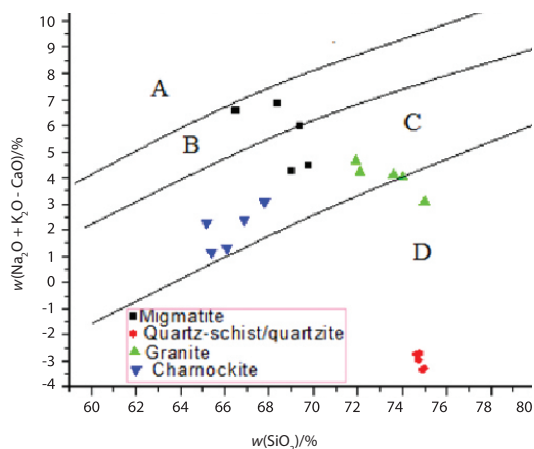


**Figure 15:**  $Na_2O + K_2O - CaO$  versus  $SiO_2$  diagram after Frost et al. (2001) showing the classification of the major rocks into A (alkalic), B (alkali-calcic), C (calcic-alkali) and D (calcic) groups.

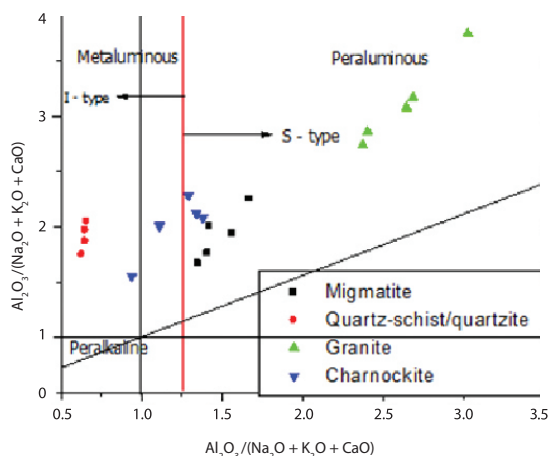


**Figure 18:** Plot of alumina saturation vs alkalinity after Maniar & Picooli (1989) highlight the major rock units in the study area.

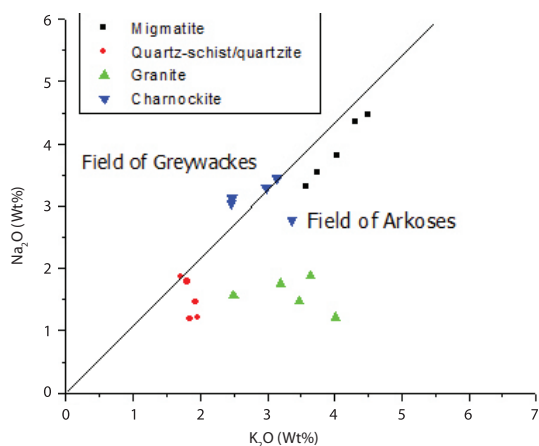


**Figure 16:**  $Na_2O$  versus  $K_2O$  Discrimination Diagram (Pettijohn, 1975).

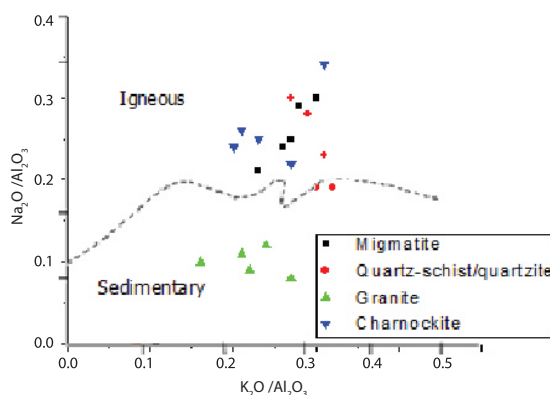


**Figure 17:**  $Na_2O/Al_2O_3$  versus  $K_2O/Al_2O_3$  plot for some basement rocks in Ekiti State (Garrells & Mackenzie, 1971).

### Conclusion

This study revealed that gneiss/migmatite, quartz-schist/quartzite, the Pan-African granites and charnockites as major rock units in the study area. Mineralogically, quartz and feldspar are dominant in most of the rock units. Chemical assessment of the rocks indicated  $SiO_2$ ,  $Al_2O_3$ ,  $Fe_2O_3$ ,  $MgO$ ,  $CaO$ ,  $K_2O$ ,  $TiO_2$ ,  $P_2O_5$ ,  $MnO$  as major oxides while variation diagrams of  $K_2O$  versus  $SiO_2$  suggested that the rocks in the study area are calcic-alkali and alkali-calcic dominated. The various discriminatory diagrams suggest sedimentary origin for the granite, migmatite and quartz-schist/quartzite rocks while the charnockite has a preference for igneous source.

### References

Ademeso, O. & Adeyeye, O. (2011): The Petrography and Major Element Geochemistry of the Granite Gneiss of Arigidi area, S/W, Nigeria. *Nature and Science*, 2011; 9(5), pp. 7–12.

Alagbe, S. A. & Raji, B. A. (1990): Groundwater Resources of the basement complex in a semi arid region: a case study of the Kan Gimi River Basin, Kaduna State. In: *proceedings of First Biennial National Hydrology Symposium*; pp. 559–571. National Water Resources Publication, Maiduguri, Nigeria.

Bolarinwa, A. T. & Elueze, A. A. (2005): Geochemical trends in weathered profiles above granite gneiss

- and schists of Abeokuta area, southwestern Nigeria. *Journal of Mining and Geology*. Vol. 41 (1), pp. 19–31.
- Clark, I. D. (1985): Groundwater abstraction from the basement complex areas of Africa. *J. Eng. Geol.*, Vol. 18, pp. 25–34.
- Elueze, A. A. (1982): Petrochemistry of Precambrian Gneisses and Migmatites in the Western part of Nigeria. *Revista de Geociências*, Volume 12 (1–3), pp. 301–306.
- Emofurieta, W. O. & SALAMI, A. O. (1993): A comparative study on two Kaolin deposits in south-western, Nigerian. *Journal Mining and geology*. Vol. 24, Nos. 1 and 2, pp. 15–27.
- Folorunso, I. O. & Okonkwo, C. T. (2011): Petrographic investigation of Oke-Awun rocks, southwestern Nigeria. *International Journal of Science and Advanced Technology* (ISSN 2221-8386) Vol. 1, No. 10, pp. 162–165.
- Frost, B. R., Barnes, C. G. & Collins, W. J. (2001): A geochemical classification for granitic rocks. *Journal of Petrology*, 42 (11), 2033–2048.
- Garrels, R. M. & Mckenzie, F. F. (1971): *Evolution of Sedimentary Rocks*. WM Norton and Co., New York, p. 394.
- Maniar, P. D. & Piccoli, P. M. (1989): Tectonic discrimination of granitoids. *Geological Society of American Bulletin*, 101, 635–643.
- Okonkwo, C. T. & Folorunso, I. O. (2013): Petrochemistry and Geotectonic Setting of Granitic Rocks in Aderan Area, S.W. Nigeria. *Journal of Geography and Geology*; Vol. 5, No. 1, pp. 30–44. ISSN 1916-9779 E-ISSN 1916-9787.
- Okunlola, O. A, Adeigbe, O. C. & Oluwatoke, O. O. (2009): Compositional and Petrogenetic features of schistose rocks of Ibadan area, southwestern Nigeria. *Earth sci. res. j.*, Vol. 13., No. 2, pp. 119–133.
- Olarewaju, V. O. (1981): Geochemistry of the charnockitic and granitic rocks of the basement complex around Ado-Ekiti, southwestern Nigeria. Ph. D. Thesis, University of London, U. K.
- Omosanya, K., Adebawale Sanni, R., Laniyan, T., Mosuro, G., Omosanya, H. & Falana, L. (2012): Petrography and Petrogenesis of Pre-Mesozoic rocks, Ago-Iwoye NE, SW Nigeria. In: (Ed.) Gordon S. Lister, *General Contributions, Journal of the Virtual Explorer*, Electronic Edition, ISSN 1441-8142, Vol. 40, No. 1.
- Oversby, V. N. (1975): Lead isotope study of Aplites the precambian basement rocks near Ibadan, southwestern Nigeria. *Earth and Planetary Science Letters*. 27, p. 177–180.
- Owoade, A., Hutton, L. G., Moffat, W. S. & Bako, M. D. (1989): Hydrogeology and water chemistry in the weathered crystalline rocks of southwestern Nigeria. *Groundwater Management- Quantity and Quality* (Proceedings of the Benidorm Symposium). IAHS Publ. no. 188.
- Oyinloye, A. O. (2002): Geochemical Studies of granite gneisses: the implication on source determination. *Jour. Chem. Soc. Nigeria*, 26 (1), 131–134.
- Oyinloye, A. O. & Ademilua, O. L. (2005): The nature of aquifer in the crystalline basement rocks of Ado-Ekiti, Igede-Ekiti and Ogbara odo areas, southwestern Nigeria pak. *J. Sci. Ind. Res.* Vol. 48(3): pp. 154–161.
- Oyinloye, A. O. (2011): *Geology and Geotectonic Setting of the Basement Complex Rocks in South Western Nigeria: Implications on Provenance and Evolution*. Earth and Environmental Sciences, Dr. Imran Ahmad Dar (Ed.), ISBN: 978-953-307-468-9, In Tech, Available from <http://www.intechopen.com/books/earth-and-environmental-sciences/geology-and-geotectonic-setting-of-the-basement-complex-rocks-in-south-western-nigeria-implications>.
- Peccerillo, A., & Taylor, S. R. (1976): Geochemistry of Eocene calc-alkaline volcanic rocks from the Kastamonu area, northern Turkey. *Contributions to Mineralogy and Petrology*, Vol. 58, 63–81. <http://dx.doi.org/10.1007/BF00384>45>.
- Pettijohn, T. J. (1975): *Sedimentary Rocks*. Harper and brothers, New York, 718 pp.
- Rahaman, M. A. & Ocan, O. (1978): On the Relationship in the Precambrian Migmatite Gneiss of Nigeria. *Jour of Mining Geo*, Vol. 15 (1), pp. 23–32.
- Talabi, A. O. & Tijani, M. N. (2011): Integrated remote sensing and GIS approach to groundwater potential assessment in the basement terrain of Ekiti area southwestern Nigeria. *RMZ – Materials and Geoenvironment*, Vol. 58, No. 3, pp. 303–328.



Event note

## Students from the Department of Materials and Metallurgy became World Champions of the 7th Virtual Steelmaking Challenge

Študenta Oddelka za materiale in metalurgijo sta postala svetovna prvaka v virtualni izdelavi jekla

### Matjaž Knap

University of Ljubljana, Faculty of Natural Sciences and Engineering, Aškerčeva cesta 12, SI-1000 Ljubljana, Slovenia  
Corresponding author. E-mail: matjaz.knap@omm.ntf.uni-lj.si

On February 19, 2013, Andraž Bradeško and Anže Tekavčič, students from the Department of Materials and Metallurgy of the Faculty of Natural Sciences and Engineering, University of Ljubljana, won the Grand Final of the 7th Virtual Steelmaking Challenge and became world champions 2013. They won in the Student category; moreover their result beat the result of the winners in the Industry category.



**Figure 1:** Anže Tekavčič, Andraž Bradeško and their mentor, assistant professor Matjaž Knap, PhD, with the cup for winning the 7th Virtual Steelmaking Challenge.

**Slika 1:** Anže Tekavčič, Andraž Bradeško in mentor doc. dr. Matjaž Knap s pokalom za zmago na 7th Virtual Steelmaking Challenge

Dne 19. februarja 2013 sta Andraž Bradeško in Anže Tekavčič, študenta Oddelka za materiale in metalurgijo Naravoslovnotehniške fakultete Univerze v Ljubljani, zmagala v velikem finalu tekmovanja v virtualni izdelavi jekla 7th Virtual Steelmaking Challenge in postala svetovna prvaka v virtualni izdelavi jekla za leto 2012/2013. Zmagala sta v kategoriji študentov, hkrati pa je bil njun rezultat boljši od tistega, ki so ga dosegli zmagovalci v kategoriji mladih inženirjev.



**Figure 2:** Participants from the Department of Metals and Metallurgy at the regional online competition.

**Slika 2:** Tekmovalci z Oddelka za materiale in metalurgijo na regionalnem tekmovanju prek interneta

The two students are in their third year of the study of Materials Engineering at the Department of Materials and Metallurgy, and were preparing for this challenge under the mentorship of assistant professor Matjaž Knap, PhD, who accompanied them during the Grand Final in Brussels. The great importance of this event for the steel industry is shown by the fact that the awards were presented by the president of the World Steel Association (the sponsor of the competition) and the CEO of Severstal Mr. Alexei Mordashov. World Steel Association from Brussels is an organization that includes the most important steel producers in the world. The production of its members (16 out of 20 world biggest steel producers) comprises 85 % of the world steel production.

The competition was divided into two categories, the Student category and the Industry category. The two students qualified for this year's final as the regional champions in the Student category for the European region which includes the former Soviet Union. Regional champions from North America, Central and South America, East Asia and Oceania, Middle East, India and Africa also participated in the Grand Final.

This year, the first round of the competition was held on two days: on Tuesday, November 13, and on Wednesday, November 21, 2012. Each time, the participants had 24 hours to virtually make steel that meets all the standards regarding the quality as well as purity. The first phase of the competition took place online, with the goal of finding the cheapest way to make steel. The first round of the competition comprised of 1 148 teams from 37 countries that performed over 42 000 simulations. The regional competition was attended by 17 teams from the Department of Metals and Metallurgy of the Faculty of Natural Sciences and Engineering, University of Ljubljana. On both days of the competition, they gathered in the conference room at the Institute of Metals and Technology and together tried to optimize the process and individually achieve the best possible result. They did a great job – 9 teams ranked in the first 10 participants from Europe. By doing so, they performed better than previous generations who always ended just below the top.

Oba sta študenta 3. letnika Inženirstva materialov na Oddelku za materiale in metalurgijo in sta se na tekmovanje pripravljala pod mentorstvom doc. dr. Matjaža Knapa, ki ju je spremljal tudi na velikem finalu v Bruslju.

O veliki odmevnosti dogodka in pomenu za jeklarsko industrijo priča podatek, da je priznanja podelil Alexey Mordashov, predsednik World Steel Association (pokrovitelj tekmovanja) in CEO Severstala. World Steel Association iz Bruslja je organizacija, ki združuje najpomembnejše svetovne proizvajalce jekla. Proizvodnja njenih članov (16–20 največjih svetovnih proizvajalcev) obsega 85 odstotkov svetovne proizvodnje jekla.

Tekmovanje je potekalo v dveh kategorijah: v študentski kategoriji in kategoriji mladih inženirjev. V letošnji finale tekmovanja sta se študenta uvrstila kot zmagovalca v kategoriji študentov za področje Evrope in bivše Sovjetske zveze. Poleg njiju so v velikem finalu sodelovali regionalni zmagovalci iz Severne Amerike, Srednje in Južne Amerike, Vzhodne Azije in Oceanije ter z Bližnjega vzhoda, Indije in Afrike.

Prvi krog tekmovanja je letos potekal v dveh terminih, in sicer v torek, 13. novembra, in v sredo, 21. novembra 2012. Tekmovalci so vsakič imeli na voljo 24 ur, da so virtualno izdelali jeklo, ki je ustrezalo vsem zahtevanim standardom, tako glede kvalitete kot tudi čistosti. Prva faza tekmovanja je potekala prek interneta in zmagal je tisti, ki je naredil jeklo najceneje.

V prvem krogu tekmovanja je sodelovalo 1148 ekip iz 37 držav, ki so opravili več kot 42 000 simulacij. Regijskega tekmovanja se je udeležilo tudi 17 ekip iz Oddelka za materiale in metalurgijo Naravoslovnotehniške fakultete Univerze v Ljubljani, ki so se oba dneva tekmovanja zbrali v sejni sobi na Inštitutu za kovinske materiale in s skupnimi močmi poskušali optimirati proces ter posamično doseči čim boljši rezultat. Odrezali so se odlično, saj se je kar devet ekip uvrstilo v prvo deseterico udeležencev iz Evrope. S tem so nadgradili uspehe prejšnjih generacij, ki so se uvrščale tik pod vrh.

Na tekmovanje se študenti Oddelka za materiale in metalurgijo pripravljajo in se ga udeležujejo že od leta 2006 v okviru predmetov s področja jeklarstva – procesne metalurgije izdelave jekla. Tako lahko teoretično znanje, ki ga

The students from the Department of Metals and Metallurgy have been preparing for and participating in this competition since 2006 within the courses of steel industry – process metallurgy of steelmaking. With virtual steelmaking, future metallurgical engineers can test the theoretical knowledge obtained in class.

bodoči inženirji metalurgije dobijo med predavanji, preverijo pri virtualni izdelavi jekla. Poleg tega, da morajo upoštevati vse fizikalne in tehnološke zakonitosti, ki so nujne za proizvodnjo visokokvalitetnega jekla, je ključnega pomena ekonomika proizvodnje.

**Table 1:** Results of the regional competition in the Industry category (left) and the Student category (right)

**Preglednica 1:** Rezultati regijskega tekmovanja v kategoriji mladih inženirjev (levo) in študentov (desno)

Europe-CIS								
1	\$264.08	Paul Wiggins	Tata Steel	United Kingdom	\$263.61	Andraž Bradeško, Anže Tekavčič	University of Ljubljana	Slovenia
2	\$265.35	Róbert Hegeduš, Martin Kristiňák	U.S.Steel Košice	Slovak Republic	\$263.84	Lina Jerina	University of Ljubljana	Slovenia
3	\$265.38	Arghya Dey, Thomas Birchall	Tata Steel	United Kingdom	\$264.02	Matic Klug, Jure Voglar	University of Ljubljana	Slovenia
4	\$265.75	Benedict David Wesson	Tata Steel	United Kingdom	\$264.61	Mitja Zelenko	University of Ljubljana	Slovenia
5	\$266.20	Popia Gheorghe, Dinu Stanescu	Tenaris Silcotub	Romania	\$264.62	Janez Košir	University of Ljubljana	Slovenia
	\$266.20	Izaskun Alonso Oña, Diana Mier	Gerdau I+D Europa S.A.	Spain				
6	\$266.23	Dominik Sobiech, René Krieg	ThyssenKrupp Steel Europe	Germany	\$264.69	Andrej Resnik	University of Ljubljana	Slovenia
7	\$266.45	Daniel Kacir, Patrik Farkas	U.S.Steel Košice	Slovak Republic	\$264.87	Žiga Veber	University of Ljubljana	Slovenia
					\$264.87	Tomislav Goričan	University of Ljubljana	Slovenia
8	\$266.61	Robert Edward Shepherd, Jenny Rudnizki	ThyssenKrupp Steel Europe AG	Germany	\$264.93	Juho Moilanen	University of Oulu	Finland
9	\$266.64	Ondrej Tóth, Lukáš Galeštok	U.S.Steel Košice	Slovak Republic	\$264.98	Tomaž Klajnšek	University of Ljubljana	Slovenia
10	\$267.50	Rus Luminita Anca	Tenaris Silcotub	Romania	\$265.62	Žiga Laznik	University of Ljubljana	Slovenia

Besides having to obey all the laws of physics and technology necessary for the production of high quality steel, economic production is also a key element.

The two students even beat the competitors from the world biggest steel production companies (such as Tata Steel, 2011: 23,8 Mt – source: [www.worldsteel.org/statistics/top-producers.html](http://www.worldsteel.org/statistics/top-producers.html)). This success is proof of the high level of knowledge obtained by the students from the Department of Metals and Metallurgy of the Faculty of Natural Sciences and Engineering, University of Ljubljana. This knowledge helps Slovene steel producers to succeed on the global market. It is highly qualified engineers that enable them to produce high quality steel with high value added. The steel of Slovene producers (Štore Steel, Acroni Jesenice, Metal Ravne) is therefore greatly appreciated in the world. Due to the ability to adapt quickly to market demands, Slovenian steelworkers, with home-grown engineers, despite only 648,000 tonnes of annual production ([www.worldsteel.org/statistics/statistics archive/Steel production 2011](http://www.worldsteel.org/statistics/statistics%20archive/Steel%20production%202011)) defy the recession and provide jobs.

The success of the students resonated all over Slovenia, as the media covered the story. The two students were also received by the rector of the University of Ljubljana, professor Radovan Stanislav Pejovnik, PhD, and they received official congratulations from the President of the Republic of Slovenia and from the Minister of Education, Science and Sport.

You can read more about the competition and the remarkable success of Slovene students on: [www.worldsteel.org/media centre/press releases/worldsteel announces 7th steeluniversity Challenge World Champions](http://www.worldsteel.org/media%20centre/press%20releases/worldsteel%20announces%207th%20steeluniversity%20Challenge%20World%20Champions).

Uspeh (naša študenta sta premagala tudi tekmece iz največjih svetovnih proizvajalcev jekla, npr. Tata Steel, 2011: 23,8 mio. ton – vir: [www.worldsteel.org/statistics/top producers](http://www.worldsteel.org/statistics/top-producers)) je dokaz visokega nivoja znanja, ki ga dobijo študenti na Oddelku za materiale in metalurgijo Naravoslovnotehniške fakultete Univerze v Ljubljani. Znanje slovenskim proizvajalcem jekla omogoča, da se z visokokvalitetnimi jekli uveljavljajo in so prepoznavni na svetovnem trgu. Prav strokovno visoko usposobljeni inženirji jim omogočajo proizvodnjo plemenitih jekel z visoko dodano vrednostjo. Jekla slovenskih proizvajalcev (Štore Steel, Acroni Jesenice in Metal Ravne) so v svetu zato zelo cenjena. Zaradi sposobnosti hitrega prilagajanja zahtevam trga lahko slovenski jeklarji z doma vzgojenimi inženirji kljub samo 648 000 tonam letne proizvodnje ([www.worldsteel.org/statistics/statistics archive/Steel production 2011](http://www.worldsteel.org/statistics/statistics%20archive/Steel%20production%202011)) kljubujejo recesiji in zagotavljajo delovna mesta.

Uspeh je imel lep odmev tudi v Sloveniji, saj je več medijev poročalo o uspehu študentov. Sprejel ju je tudi rektor Univerze v Ljubljani prof. dr. Radovan Stanislav Pejovnik, uradne čestitke pa sta prejela tudi od predsednika Republike Slovenije in ministra za izobraževanje, znanost in šport Republike Slovenije.

Več o tekmovanju in izrednem uspehu slovenskih študentov lahko preberete na spletni strani: [www.worldsteel.org/media centre/press releases/worldsteel announces 7th steeluniversity Challenge World Champions](http://www.worldsteel.org/media%20centre/press%20releases/worldsteel%20announces%207th%20steeluniversity%20Challenge%20World%20Champions).

# Instructions to Authors

## Navodila avtorjem

RMZ – MATERIALS & GEOENVIRONMENT (RMZ – Materiali in geokolje) is a periodical publication with four issues per year (established in 1952 and renamed to RMZ – M&G in 1998). The main topics are Mining and Geotechnology, Metallurgy and Materials, Geology and Geoenvironment.

RMZ – M&G publishes original scientific articles, review papers, preliminary notes and professional papers in English. Only professional papers will exceptionally be published in Slovene. In addition, evaluations of other publications (books, monographs, etc.), in memoriam, presentation of a scientific or a professional event, short communications, professional remarks and reviews published in RMZ – M&G can be written in English or Slovene. These contributions should be short and clear.

Authors are responsible for the originality of the presented data, ideas and conclusions, as well as for the correct citation of the data adopted from other sources. The publication in RMZ – M&G obligates the authors not to publish the article anywhere else in the same form.

RMZ – MATERIALS AND GEOENVIRONMENT (RMZ – Materiali in geokolje), kratica RMZ – M&G je revija (ustanovljena kot zbornik 1952 in preimenovana v revijo RMZ – M&G 1998), ki izhaja vsako leto v štirih zvezkih. V reviji objavljamo prispevke s področja rudarstva, geotehnologije, materialov, metalurgije, geologije in geokolja.

RMZ – M&G objavlja izvirne znanstvene, pregledne in strokovne članke ter predhodne objave samo v angleškem jeziku. Strokovni članki so lahko izjemoma napisani v slovenskem jeziku. Kot dodatek so zaželeni recenzije drugih publikacij (knjig, monografij ...), nekrologi In memoriam, predstavitev znanstvenih in strokovnih dogodkov, kratke objave in strokovne replike na članke objavljene v RMZ – M&G v slovenskem ali angleškem jeziku. Prispevki naj bodo kratki in jasni.

Avtorji so odgovorni za izvirnost podatkov, idej in sklepov v predloženem prispevku oziroma za pravilno citiranje privzetih podatkov. Z objavo v RMZ – M&G se tudi obvežejo, da ne bodo nikjer drugje objavili enakega prispevka.

### Specification of the Contributions

Optimal number of pages is 7 to 15; longer articles should be discussed with the Editor-in-Chief prior to submission. All contributions should be written using the ISO 80000.

- Original scientific papers represent unpublished results of original research.
- Review papers summarize previously published scientific, research and/or expertise articles on a new scientific level and can contain other cited sources which are not mainly the result of the author(s).
- Preliminary notes represent preliminary research findings, which should be published rapidly (up to 7 pages).
- Professional papers are the result of technological research achievements, application research results and information on achievements in practice and industry.

### Vrste prispevkov

Optimalno število strani je 7–15, za daljše članke je potrebno soglasje glavnega urednika. Vsi prispevki naj bodo napisani v skladu z ISO 80000.

- Izvirni znanstveni članki opisujejo še neobjavljene rezultate lastnih raziskav.
- Pregledni članki povzemajo že objavljene znanstvene, raziskovalne ali strokovne dosežke na novem znanstvenem nivoju in lahko vsebujejo tudi druge (citirane) vire, ki niso večinsko rezultat dela avtorjev.
- Predhodna objava povzema izsledke raziskave, ki je v teku in zahteva hitro objavo obsega do sedem (7) strani.
- Strokovni članki vsebujejo rezultate tehnoloških dosežkov, razvojnih projektov in druge informacije iz prakse in industrije.

- Publication notes contain the author's opinion on newly published books, monographs, textbooks, etc. (up to 2 pages). A figure of the cover page is expected, as well as a short citation of basic data.
- In memoriam (up to 2 pages), a photo is expected.
- Discussion of papers (Comments) where only professional disagreements of the articles published in previous issues of RMZ – M&G can be discussed. Normally the source author(s) reply to the remarks in the same issue.
- Event notes in which descriptions of a scientific or a professional event are given (up to 2 pages).
- Recenzije publikacij zajemajo ocene novih knjig, monografij, učbenikov, razstav ... (do dve (2) strani; zaželena slika naslovnice in kratka navedba osnovnih podatkov).
- In memoriam obsega do dve (2) strani, zaželena je slika.
- Strokovne pripombe na objavljene članke ne smejo presežati ene (1) strani in opozarjajo izključno na strokovne nedoslednosti objavljenih člankov v prejšnjih številkah RMZ – M&G. Praviloma že v isti številki avtorji prvotnega članka napišejo odgovor na pripombe.
- Poljudni članki, ki povzemajo znanstvene in strokovne dogodke zavzemajo do dve (2) strani.

## Review Process

All manuscripts will be supervised shall undergo a review process. The reviewers evaluate the manuscripts and can ask the authors to change particular segments, and propose to the Editor-in-Chief the acceptability of the submitted articles. Authors are requested to identify three reviewers and may also exclude specific individuals from reviewing their manuscript. The Editor-in-Chief has the right to choose other reviewers. The name of the reviewer remains anonymous. The technical corrections will also be done and the authors can be asked to correct the missing items. The final decision on the publication of the manuscript is made by the Editor-in-Chief.

## Form of the Manuscript

The contribution should be submitted via e-mail as well as on a USB flash drive or CD.

The original file of the Template is available on RMZ – Materials and Geoenvironment Home page address: [www.rmz-mg.com](http://www.rmz-mg.com).

The contribution should be submitted in Microsoft Word. The electronic version should be simple, without complex formatting, hyphenation, and underlining. For highlighting, only bold and italic types should be used.

## Composition of the Manuscript

### *Title*

The title of the article should be precise, informative and not longer than 100 characters. The author should also indicate the short version of the title. The title should be written in English as well as in Slovene.

## Recenzentski postopek

Vsi prispevki bodo predloženi v recenzijo. Recenzent oceni primernost prispevka za objavo in lahko predlaga kot pogoj za objavo dopolnilo k prispevku. Recenzenta izbere uredništvo med strokovnjaki, ki so dejavni na sorodnih področjih, kot jih obravnava prispevek. Avtorji morajo predlagati tri recenzente. Pravico imajo predlagati ime recenzenta, za katerega ne želijo, da bi recenziral njihov prispevek. Uredništvo si pridržuje pravico, da izbere druge recenzente. Recenzent ostane anonimni. Prispevki bodo tudi tehnično ocenjeni in avtorji so dolžni popraviti pomanjkljivosti. Končno odločitev za objavo da glavni urednik.

## Oblika prispevka

Prispevek lahko posredujete preko e-pošte ter na USB mediju ali CD-ju.

Predloga za pisanje članka se nahaja na spletni strani: [www.rmz-mg.com](http://www.rmz-mg.com).

Besedilo naj bo podano v urejevalniku besedil Word. Digitalni zapis naj bo povsem enostaven, brez zapletenega oblikovanja, deljenja besed, podčrtavanja. Avtor naj označi le krepko in kurzivno poudarjanje.

## Zgradba prispevka

### *Naslov*

Naslov članka naj bo natančen in informativen in naj ne presega 100 znakov. Avtor naj navede tudi skrajšan naslov članka. Naslov članka je podan v angleškem in slovenskem jeziku.

### **Information on the Authors**

Information on the authors should include the first and last name of the authors, the address of the institution and the e-mail address of the leading author.

### **Abstract**

The abstract presenting the purpose of the article and the main results and conclusions should contain no more than 180 words. It should be written in Slovene and English.

### **Key words**

A list of up to 5 key words (3 to 5) that will be useful for indexing or searching. They should be written in Slovene and English.

### **Introduction**

### **Materials and methods**

### **Results and discussion**

### **Conclusions**

### **Acknowledgements**

### **References**

The sources should be cited in the same order as they appear in the article. They should be numbered with numbers in square brackets. Sources should be cited according to the SIST ISO 690:1996 standards.

[1] Trček, B. (2001): *Solute transport monitoring in the unsaturated zone of the karst aquifer by natural tracers*. Ph. D. Thesis. Ljubljana: University of Ljubljana 2001; 125 p.

[2] Higashitani, K., Iseri, H., Okuhara, K., Hatade, S. (1995): Magnetic Effects on Zeta Potential and Diffusivity of Nonmagnetic Particles. *Journal of Colloid and Interface Science*, 172, pp. 383–388.

Citing Electronic Sources:

CASREACT – Chemical reactions database [online]. Chemical Abstracts Service, 2000, renewed 2/15/2000 [cited 2/25/2000]. Available on: <<http://www.cas.org/casreact.html>>.

Scientific articles, review papers, preliminary notes and professional papers are published in English. Only professional papers will exceptionally be published in Slovene.

### **Podatki o avtorjih**

Podatki o avtorjih naj vsebujejo imena in priimke avtorjev, naslov pripadajoče inštitucije ter elektronski naslov vodilnega avtorja.

### **Izvleček**

Izvleček namena članka ter ključnih rezultatov z ugotovitvami naj obsega največ 180 besed. Izvleček je podan v angleškem in slovenskem jeziku.

### **Ključne besede**

Seznam največ 5 ključnih besed (3–5) za pomoč pri indeksiranju ali iskanju. Ključne besede so podane v angleškem in slovenskem jeziku.

### **Uvod**

### **Materiali in metode**

### **Rezultati in razprava**

### **Sklepi**

### **Zahvala**

### **Viri**

Uporabljane literaturne vire navajajte po vrstnem redu, kot se pojavljajo v prispevku. Označite jih s številkami v oglatem oklepaju. Literatura naj se navaja v skladu s standardom SIST ISO 690:1996.

[1] Trček, B. (2001): *Solute transport monitoring in the unsaturated zone of the karst aquifer by natural tracers*. doktorska disertacija. Ljubljana: Univerza v Ljubljani 2001; 125 str.

[2] Higashitani, K., Iseri, H., Okuhara, K., Hatade, S. (1995): Magnetic Effects on Zeta Potential and Diffusivity of Nonmagnetic Particles. *Journal of Colloid and Interface Science*, 172, str. 383–388.

Citiranje spletnih strani:

CASREACT – Chemical reactions database [online]. Chemical Abstracts Service, 2000, obnovljeno 15. 2. 2000 [citirano 25. 2. 2000]. Dostopno na svetovnem spletu: <<http://www.cas.org/casreact.html>>.

Znanstveni, pregledni in strokovni članki ter predhodne objave se objavijo v angleškem jeziku. Izjemoma se strokovni članek objavi v slovenskem jeziku.

## Annexes

Annexes are images, spreadsheets, tables, and mathematical and chemical formulas.

Annexes should be included in the text at the appropriate place, and they should also be submitted as a separate document, i.e. separated from the text in the article.

Annexes should be originals, made in an electronic form (Microsoft Excel, Adobe Illustrator, Inkscape, AutoCad, etc.) and in .eps, .tif or .jpg format with a resolution of at least 300 dpi.

The width of the annex should be at least 152 mm. They should be named the same as in the article (Figure 1, Table 1).

The text in the annexes should be written in typeface Arial Regular (6 pt).

The title of the image (also schemes, charts and graphs) should be indicated in the description of the image.

When formatting spreadsheets and tables in text editors, tabs, and not spaces, should be used to separate columns. Each formula should have its number written in round brackets on its right side.

References of the annexes in the text should be as follows: "Figure 1..." and not "as shown below:". This is due to the fact that for technical reasons the annex cannot always be placed at the exact specific place in the article.

## Manuscript Submission

Contributions should be sent to the following e-mail address: rmz-mg@ntf.uni-lj.si.

In case of submission on CD or USB flash drive, contributions can be sent by registered mail to the address of the editorial board:

RMZ – Materials and Geoenvironment, Aškerčeva 12, 1000 Ljubljana, Slovenia.

The contributions can also be handed in at the reception of the Faculty of Natural Sciences and Engineering (ground floor), Aškerčeva 12, 1000 Ljubljana, Slovenia with the heading "for RMZ – M&G".

The electronic medium should clearly be marked with the name of the leading author, the beginning of the title and the date of the submission to the Editorial Office of RMZ – M&G.

## Priloge

K prilogam prištevamo slikovno gradivo, preglednice in tabele ter matematične in kemijske formule.

Priloge naj bodo vključene v besedilu, kjer se jim odredi okvirno mesto. Hkrati jih je potrebno priložiti tudi kot samostojno datoteko, ločeno od besedila v članku.

Priloge morajo biti izvirne, narejene v računalniški obliki (Microsoft Excel, Adobe Illustrator, Inkscape, AutoCad ...) in shranjene kot .eps, .tif ali .jpg v ločljivosti vsaj 300 dpi. Širina priloge naj bo najmanj 152 mm. Datoteke je potrebno poimenovati, tako kot so poimenovane v besedilu (Slika 1, Preglednica 1).

Za besedilo v prilogi naj bo uporabljena pisava Arial navadna različica (6 pt).

Naslov slikovnega gradiva, sem prištevamo tudi sheme, grafikone in diagrame, naj bo podan v opisu slike.

Pri urejevanju preglednic/tabel, v urejevalniku besedila, se za ločevanje stolpcev uporabijo tabulatorji in ne presledki.

Vsaka formula naj ima zaporedno številko zapisano v okroglem oklepaju na desni strani.

V besedilu se je potrebno sklicevati na prilogo na način: „Slika 1 ...“, in ne „...“ kot je spodaj prikazano:“ saj zaradi tehničnih razlogov priloge ni vedno mogoče postaviti na točno določeno mesto v članku.

## Oddaja članka

Prispevke lahko pošljete po elektronski pošti na naslov rmz-mg@ntf.uni-lj.si.

V primeru oddaje prispevka na CD- ali USB-mediju le-te pošljite priporočeno na naslov uredništva:

RMZ – Materials and Geoenvironment, Aškerčeva 12, 1000 Ljubljana, Slovenija

ali jih oddajte na:

recepции Naravoslovnotehniške fakultete (pritličje), Aškerčeva 12, 1000 Ljubljana, Slovenija s pripisom „za RMZ – M&G“.

Elektronski mediji morajo biti jasno označeni z imenom vsaj prvega avtorja, začetkom naslova in datumom izročitve uredništvu RMZ – M&G.

**Information on RMZ – M&G**

- Editor-in-Chief  
Assoc. Prof. Dr. Peter Fajfar  
Telephone: +386 1 200 04 51  
E-mail address: peter.fajfar@omm.ntf.uni-lj.si
  
- Secretary  
Ines Langerholc, Bachelor in Business Administration  
Telephone: +386 1 470 46 08  
E-mail address: ines.langerholc@omm.ntf.uni-lj.si

These instructions are valid from July 2013.

**Informacije o RMZ – M&G**

- urednik  
izr. prof. dr. Peter Fajfar  
Telefon: +386 1 200 04 51  
E-poštni naslov: peter.fajfar@omm.ntf.uni-lj.si
  
- tajnica  
Ines Langerholc, dipl. poslov. adm.  
Telefon: +386 1 470 46 08  
E-poštni naslov: ines.langerholc@omm.ntf.uni-lj.si

Navodila veljajo od julija 2013.



